Design, Synthesis and Characterization of Polyethylene-Based Macromolecular Architectures by Combining Polyhomologation with Powerful Linking Chemistry

Dissertation by

Nazeeha Alkayal

In Partial Fulfillment of the Requirements

For the Degree of

Doctor of Philosophy of Science

King Abdullah University of Science and Technology

Thuwal, Kingdom of Saudi Arabia

The dissertation of Nazeeha Alkayal is approved by the examination committee.

Committee Chairperson [Prof. Nikos Hadjichristidis]

Committee Member [Prof. Suzana Nunes]

Committee Member [Prof. Valentin Rodionov]

Committee Member [Prof. Apostolos Avgeropoulos]

ABSTRACT

Design, Synthesis and Characterization of Polyethylene-Based Macromolecular Architectures by Combining Polyhomologation with Powerful Linking Chemistry

Nazeeha Alkayal

Polyhomologation is a powerful method to prepare polyethylene-based materials with controlled molecular weight, topology and composition. This dissertation focuses on the discovery of new synthetic routes to prepare polyethylene-based macromolecular architectures by combining polyhomologation with highly orthogonal and efficient linking reactions such as Diels Alder, copper-catalyzed azide-alkyne cycloaddition (CuAAC), and Glaser. Taking advantage of functionalized polyhomologation initiators, as well as of the efficient coupling chemistry, we were able to synthesize various types of polymethylene (polyethylene)-based materials with complex architectures including linear co/terpolymers, graft terpolymers, and tadpole copolymers.

In the first project, a facile synthetic route towards well-defined polymethylene-based co/terpolymers, by combining the anthracene/maleimide Diels–Alder reaction with polyhomologation, is presented. For the synthesis of diblock copolymers the following approach was applied: (a) synthesis of α-anthracene-ω-hydroxy-polymethylene by polyhomologation using tri (9 anthracene-methyl propyl ether) borane as the initiator, (b) synthesis of furan-protected-maleimide-terminated poly(ε-caprolactone) or polyethylene glycol and (c) Diels–Alder reaction between anthracene and maleimide-terminated polymers. In the case of triblock terpolymers, the α-anthracene-ω-hydroxy

polymethylene was used as a macroinitiator for the ring-opening polymerization of D, L-lactide to afford an anthracene-terminated PM-*b*-PLA copolymer, followed by the Diels–Alder reaction with furan-protected maleimide-terminated poly (ε-caprolactone) or polyethylene glycol to give the triblock terpolymers. The synthetic methodology is general and potentially applicable to a range of polymers.

The coupling reaction applied in the second project of this dissertation was copper-catalyzed "click" cycloaddition of azides and alkynes (CuAAC). Novel well-defined polyethylene-based graft terpolymers were synthesized via the "grafting onto" strategy by combining nitroxide-mediated radical polymerization (NMP), polyhomologation and copper(I)-catalyzed azide–alkyne cycloaddition (CuAAC). Three steps were involved in this approach: (a) synthesis of alkyne-terminated polyethylene-*b*-poly(ε-caprolactone) (PE-*b*-PCL-alkyne) block copolymers (branches) by esterification of PE-*b*-PCL-OH with 4-pentynoic acid; the PE-*b*-PCL-OH was obtained by polyhomologation of dimethylsulfoxonium methylide to afford PE-OH, followed by ring opening polymerization of ε-caprolactone using PE-OH as a macroinitiator (b) synthesis of random copolymers of styrene (St) and 4-chloromethylstyrene (4-CMS) with various CMS contents, by nitroxide-mediated radical copolymerization (NMP), and conversion of chloride to azide groups by reaction with sodium azide (NaN_3) (backbone) and (c) "click" linking reaction to afford the PE-based graft terpolymers. This method opens up new routes for the creation of polyethylene-based graft terpolymers by a combination of polyhomologation, NMP and CuAAC.

The third project deals with the synthesis of polyethylene-based tadpole copolymer (c-PE)-*b*-PSt. Cyclic polymers represent a class of understudied polymer architecture mainly due to the synthetic challenges. Within this dissertation, a new method was reported for the synthesis of cyclic polymers in exceptionally high purity and yield. The main approaches to synthesize macrocycles are based on the end-to-end ring-closure (coupling) of homo difunctional linear precursors under high dilution. Our process relies on the preparation of well-defined linear α, ω-dihydroxy polyethylene and a bromide group at the middle of the chain through polyhomologation of ylide using functionalized initiator, followed by ATRP of styrene monomer. The two hydroxyl groups were transformed into alkyne groups, via esterification reaction, followed by Glaser reaction between terminal alkynes to afford the tadpole-shaped copolymers with PE ring and PSt tail.

In Our PhD research, we also studied the self-assembly properties of the amphiphilic copolymers PM-*b*-PEG in aqueous solution by DLS, Cryo-TEM, and AFM. Furthermore, the critical micelle concentration (CMC) was estimated from the intensity of the pyrene emissions by the fluorescence technique.

All the findings presented in this dissertation are emphasizing the utility of polyhomologation for the synthesis of well-defined polyethylene-based complex macromolecular architectures, almost impossible through other kind of polymerization including the catalytic polymerization of ethylene.

ACKNOWLEDGEMENTS

In the beginning, praise and gratitude be to ALLAH almighty, without his gracious help, it would have been impossible to accomplish this work. Working with this dissertation has been very interesting and valuable experience to me and I have learned a lot. I want to express my thanks to the people who have been very helpful during my PhD.

First and foremost, I would like to thank my advisor Prof. Nikos Hadjichristidis for his patient guidance and mentorship in the last four years. It has been an honor for me to receive his generous guidance in research. I appreciate all his time, ideas and funding in my PhD pursuit. I would also like to thank my committee members, Prof. Suzana Nunes, Prof. Valentin Rodionov and Prof. Apostolos Avgeropoulos for their friendly guidance and strong support over my whole PhD research process

I would like to acknowledge all the members of professor Hadjichristidis group who have supported in my research. Also, I want to extend my thanks to the professor Tunca and his group for assistant and guidance. Lastly, I would like to thank my friends and my family for all their love and support. Thank you.

TABLE OF CONTENTS

LIST OF ABBREVIATIONS

AFM	Atomic force microscopy
ATRP	Atom transfer radical polymerization
$CDCl_3$	Deuterated chloroform
CMC	Critical micelle concentrations
Cp	Cyclopentadienyl
CuAAC	Copper (I)-catalyzed azide-alkyne cycloaddition
DA	Diels-Alder reaction
DA_{eff}	Diels Alder efficiency
DBU	1,8 diazabicyclo [5,4,0] undec-7-ene
DCC	N, N'-dicyclohexylcarbodIimide
DI	Deionized water
DLS	Dynamic light scattering
DMAP	4-(dimethyl amino) pyridine
DMF	Dimethylformamide
DMSO	Dimethyl sulfoxide
DSC	Differential scanning calorimetry
FTIR	Fourier transform infrared spectra
FTP	Freeze-pump-thaw
HDPE	High density polyethylene
HT-SEC	High-temperature-size exclusion chromatography
LDPE	Low density polyethylene
LLDPE	Linear low density polyethylene
MAO	Methylaluminoxane
NMR	Nuclear magnetic resonance spectroscopy
NMP	Nitroxide-mediated polymerization
PAA	Polyacrylic acid
PBuA	Poly (n–butyl acrylate)
PBd	polybutadiene
ε-PCL	ε-Polycaprolactone
PDI	Polydispersity index
PDMS	Polydimethylsiloxane
PE	Polyethylene (equivalent to PM)
PEG	Polyethylene glycol
PEO	Polyethylene oxide
PFST	2, 3, 4, 5, 6-Pentafluorostyrene
PIB	Polyisobutylene
PLA	Poly lactide
PM	Polymethylene (equivalent to PE)
PMMA	Poly (methyl methacrylate
PPM	Parts per million
PSt	Polystyrene

PTFE	Polytetrafluoroethylene
RAFT	Reversible addition-fragmentation chain transfer
ROMP	Ring-opening metathesis polymerization
ROP	Ring opening polymerization
SEM	Scanning electron microscope
TAO.2H_2O	Trimethylamine *N*-oxide dehydrate
TCB	1,2,4-Trichlorobenzene
TEM	Transmission electron microscopy
TFA	Trifluoroacetic acid
T_g	Glass transition temperature
T_m	Melting temperature
UCST	Upper critical solution temperature
UV-VIS	Ultraviolet–visible spectroscopy.

LIST OF FIGURES

LIST OF TABLES

LIST OF SCHEMES

Chapter 1: Polyhomologation

(Portions of this chapter are reproduced from *Macromol. Rapid Commun.* **2014***, 35,* 378)

1.1 Polyethylene

Polyethylene (PE), produced by polymerization of ethylene, is the most common industrial polymer with a production of 80 million tons annually.[1,2] During the polymerization, the chain is growing by two carbons at a time (C_2 polymerization). PE consists of a long carbon backbone with a pair of hydrogen atoms attached to each carbon (**Figure 1.1**). Due to high recyclability, good barrier properties, low cost and chemical resistance to different solvents, polyethylene-based materials are very important to modern life covering a wide spectrum of applications from commodity plastics (e.g., packaging, bottles) to precision processed biomaterials (e.g., artificial joint replacement and medical devices).[3,4]

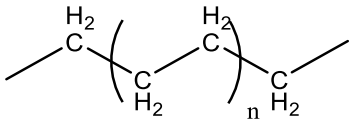

Figure 1.1 Polyethylene

1.1.1 Types of polyethylene products

The various types of PEs[5-7] differing in the number of branches (**Figure 1.2**) with a short explanation concerning the physical properties are given below:

a) *High-density polyethylene* (HDPE). HDPE is a linear polyethylene homopolymer with about five branches per 1000 backbone carbons and with 50-75 % crystallinity.

b) *Low-density polyethylene* (LDPE). LDPE is a branched polyethylene homopolymer with around 50 branches (randomly distributed along the chain) of ethyl and butyl groups per 1000 backbone carbons. The crystallinity of LDPE is lower than HDPE because of the weaker packing when the number of branches increases.

c) *Linear low-density polyethylene* (LLDPE). LLDPE is a copolymerization product of ethylene with another olefin (e. g. 1-butene or 1-hexene) with different physical properties than LDPE and HDPE.

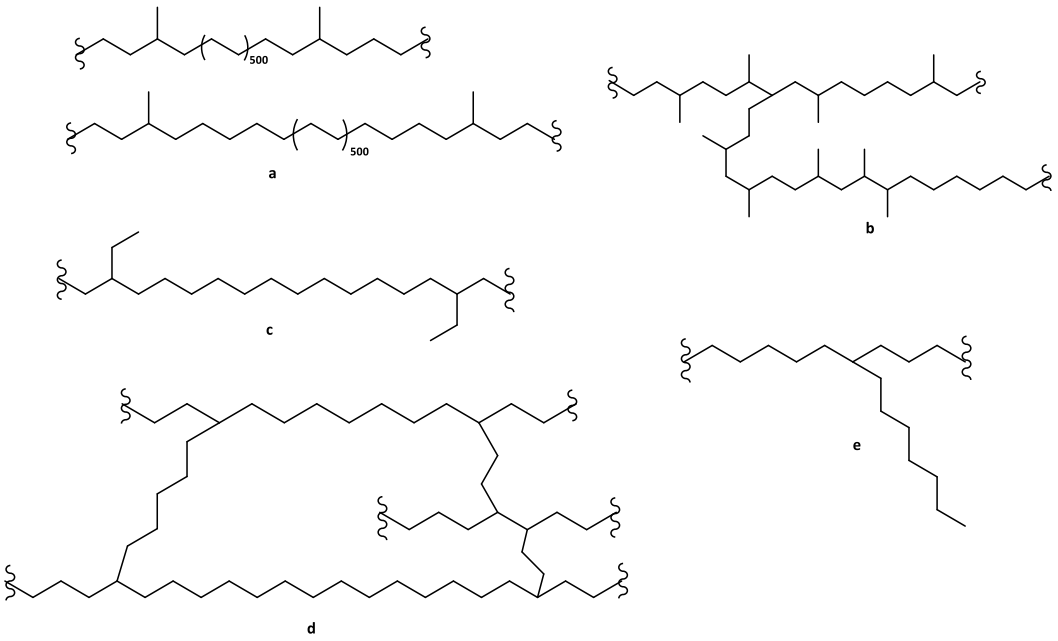

Figure 1.2 Different types of polyethylene: (a) high density polyethylene (HDPE), (b) low density polyethylene (LDPE), (c) linear low density polyethylene (LLDPE), (d) cross-linked polyethylene, (e) block and graft copolymers of polyethylene.

d) *Cross-linked polyethylene*. Cross-linked polyethylene consists of polyethylene chains connected to each other by a covalent bond. Cross-linked polyethylene is produced by irradiation[8] or reaction with peroxide of LDPE or HDPE shows decreased crystallinity, improved resistance to change temperature and increased density.

e) *Block and graft copolymers of polyethylene.* Copolymerization of polyethylene with different polar monomers such as vinyl chloride and acrylic acid can result in modified adhesive properties, elasticity, and solubility. Graft copolymers can be prepared by forming the initiator sites on the polymer backbone via ionization or irradiation.

1.1.2 Polymerization techniques of ethylene

The commercial polyethylenes are prepared by different polymerization techniques as follow:

Free radical polymerization

Polyethylene was firstly synthesized by the radical method in 1930.[9] This process needs high temperature and high pressure. As shown in **Scheme 1.1**, the radicals generated by the decomposition of peroxide or azo molecules.[10] Then, the growing chain is obtained by the reaction between radical and ethylene monomer. The termination step can occur by coupling between two radicals or disproportion process. This technique leads to LDPE or cross-linked PE depending on the intermolecular chain transfer.

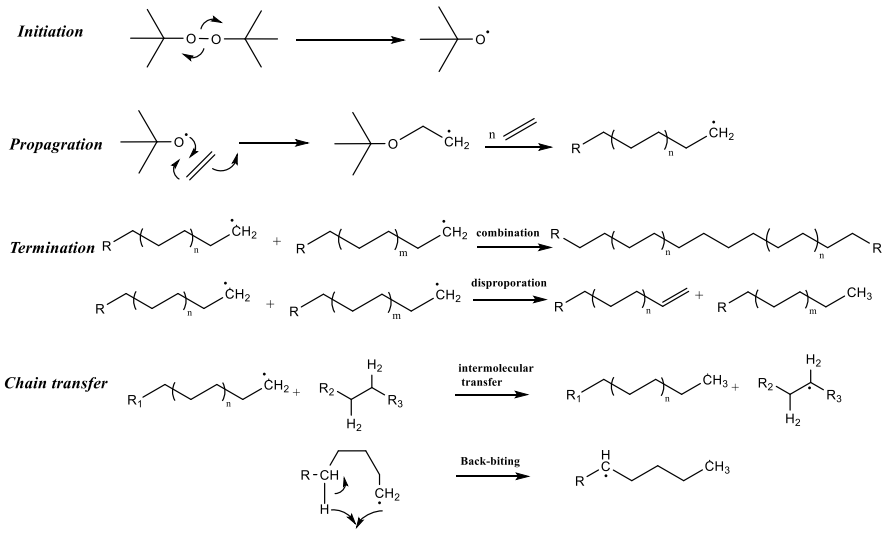

Scheme 1.1 Mechanism of radical polymerization of ethylene.

Ziegler-Natta catalysts

In 1950, Ziegler and Natta discovered catalysts to prepare polyethylene at room temperature.[11] A typical Ziegler-Natta catalyst is the complex of triethyl aluminum ($AlEt_3$) with titanium tetrachloride. The proposed mechanism is shown in **Scheme 1.2.** The reaction starts by the coordination of ethylene monomer to the metal-alkyl bond generating a long alkyl chain and an empty coordination site. Then, another molecule of ethylene coordinates to the metal and this cycle of catalyst continues. This polymerization can be terminated by β -hydride elimination to obtain PE with vinyl end group.[12] Ziegler-Natta method can be used to produce polyethylene consisting of few branches with high molecular weight and density (HDPE). Furthermore, LLDPE can be obtained by copolymerizing of ethylene with 1-butene using Ziegler-Natta catalyst.

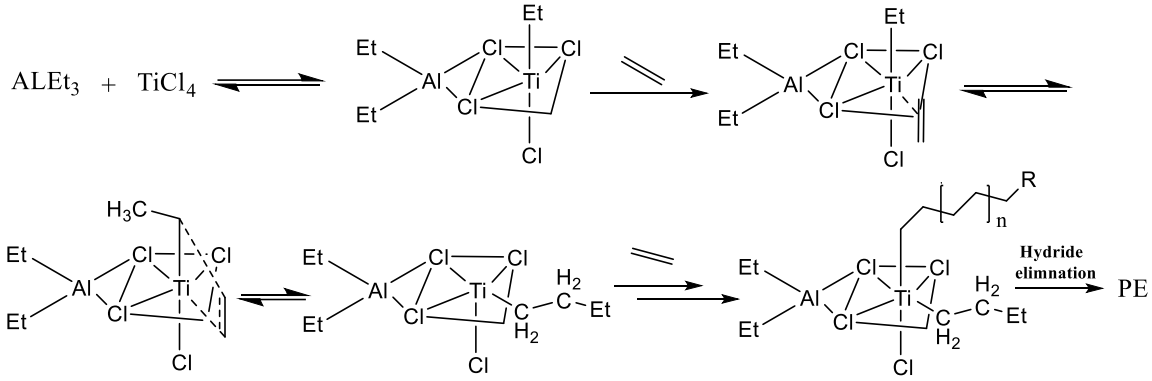

Scheme 1.2 Mechanism of Ziegler-Natta of ethylene polymerization.

Metallocene Catalysts

The metallocene catalysts (Cp_2Zr-alkyl groups) were introduced in 1970 by combining Cp, $ZrCl_2$ with methylaluminoxane (MAO). As shown in **Scheme 1.3**, the suggested mechanism is similar to that proposed for Ziegler-Natta system. The resulting

polyethylene from metallocene technique is HDPE with high molecular weight around 100 k and relatively low polydispersity (PDI= 2, the most probable).[13,14]

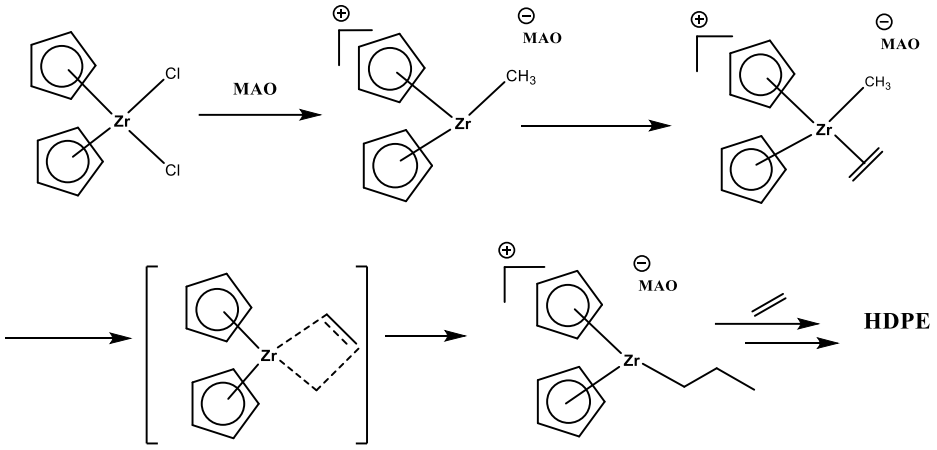

Scheme 1.3 Mechanism of metallocene polymerization of ethylene.

Despite the fact that the industrial methods for polymerizing ethylene can produce polymers in a large scale, they are not capable of controlling the molecular weight, polydispersity and macromolecular architectures. These challenges are being met later by the improvement of olefin polymerization catalysts and development of alternative approaches. For example, polyethylene with controlled molecular characteristics and a variety of different macromolecular architectures can be synthesized using anionic polymerization of butadiene (1,4 PBd) followed by hydrogenation reaction. Another approach for obtaining linear PE is hydrogenation of poly (cyclooctadiene) prepared from polymerization of cyclooctadiene via ROMP using Grubbs' catalysts.[15-20]

In this dissertation, a novel alternative method that produces a linear polymethylene without branches and controlled molecular weight and topology is described. This method called polyhomologation, a living polymerization of ylide, or C_1-

polymerization. Polymethylene is equivalent to polyethylene but in the case of polymethylene the polymer constructs by one carbon at a time.[21]

1.2 A Living polymerization of ylides.

The first polymethylene was prepared from the thermal decomposition of diazomethane in 1948 (**Scheme 1.4**).[22] The results from this kind of polymerization were high molecular weight polymers with very high polydispersity.

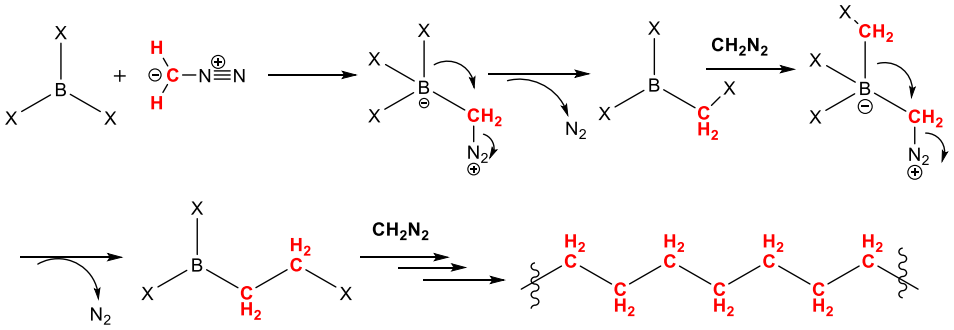

Scheme 1.4 C_1 polymerization of diazomethane to yield Polymethylene.

In 1997, Shea and coworkers [23–27] discovered an efficient method to prepare linear polyethylene. Their work drew from the homologation reaction of an organoborane with dimethylsulfoxonium methylide (**1**) (**Scheme 1.5**).[28] The reaction of a stoichiometric amount of tri-*n*-heptylborane and methylide (**1**) followed by oxidation give three byproducts: a non-homologated, a homologated and a double-homologated. From the formation of the nonanol which is the doubly homologated product, Shea and coworkers inspired to use a large excess of ylide to produce long hydrocarbon chains.

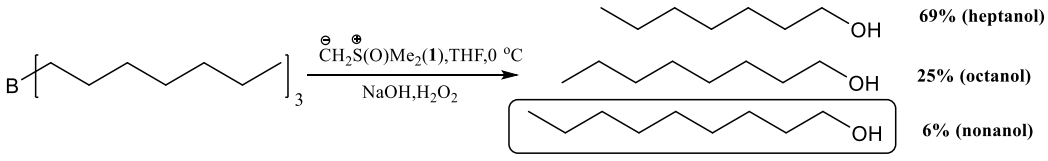

Scheme 1.5 Homologation reaction of organoborane and dimethylsulfoxonium methylide (**1**)

Living polymerization of ylide employs monomers (*i.e.* non-olefins), like dimethylsulfoxonium methylide (**1**) as the carbon source and trialkylboranes as the initiator/catalyst (**Scheme 1.6**).[29] This reaction involves elongation of the chain by a methylene group at a time. Polyhomologation is considered as living polymerization technique that enables to control molecular weight, and the degree of polymerization (DP) can be calculated by this formula DP=[ylide]/([borane]×3).

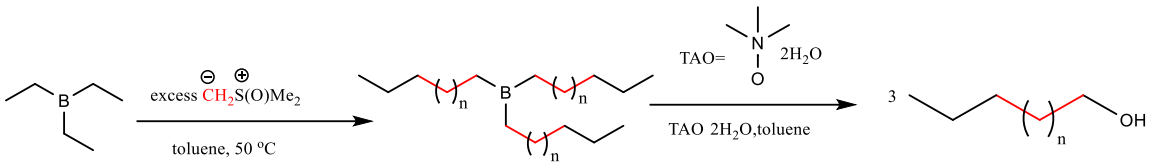

Scheme 1.6 Polyhomologation of ylide initiated by trialkylborane

1.2.1 Monomer

The most common monomer dimethylsulfoxonium methylide (**1**) is synthesized according to **Scheme 1.7**. Trimethylsulfoxonium iodide is converted to trimethylsulfoxonium chloride because the chloride salt has a higher stability and solubility to the reaction solvent (THF). The ylide is then produced by the deprotonation reaction of the chloride salt to afford a homogeneous ylide solution in toluene after filtration (elimination of NaCl). The concentration of ylide can be calculated by titration with a standard solution of HCl, and can be stored under argon at -20 °C for three weeks.[30]

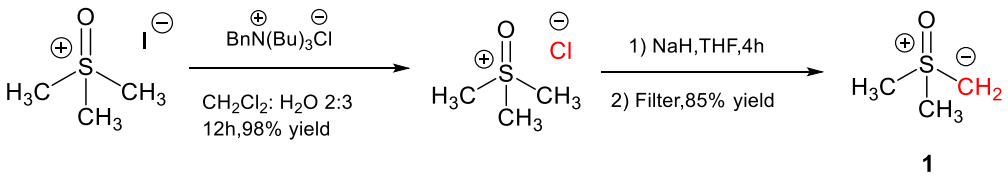

Scheme 1.7 Synthesis of dimethylsulfoxonium methylide (**1**).

1.3 Polyhomologation mechanism

Scheme 1.8 shows the proposed mechanism for polyhomologation reaction. The Lewis acidic trialkylborane is attacked by the nucleophilic ylide **1** to give the borate complex followed by 1,2-migration of one of the three alkyl arms and methylene insertion. Then, the polyhomologated borane is obtained followed by elimination of dimethyl sulfoxide (DMSO) molecules and meanwhile regenerating the alkylborane which participates in a new cycle. Under the assumption that there is no difference in migratory rate between the three polymer chains, repetitive homologation occurs at all three alkyl groups in the presence of excess ylide, giving rise to a tris(polymethylene)borane. The reaction proceeds until the whole ylide is consumed. Then, use of oxidation-hydrolysis TAO·2H_2O affords α-hydroxypolymethylene.[29]

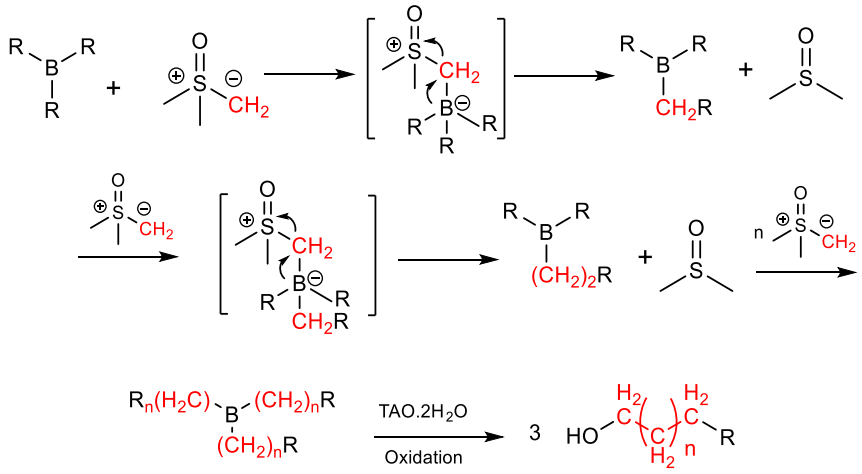

Scheme 1.8 Mechanism of polyhomologation reaction.

The polyhomologation mechanism was confirmed by ^{11}B NMR. The ^{11}B NMR (**Figure 1.3** a) of trialkylborane shows a peak at 87 ppm at 40 ^{o}C. Then, one equivalent of ylide (**1**) was added at –78 ^{o}C, the solution was warmed to –15 ^{o}C and analyzed by ^{11}B

NMR. The peak at 87 ppm disappeared and a new peak appeared at –13.4 ppm assigned to the zwitterionic complex (**Figure 1.3** b). Next, the solution was warmed to 40 °C and 1, 2 migration of one of the three-alkyl groups is expected to occur concurrently with elimination of DMSO molecule. The resonance peak shifted to 82 ppm (**Figure 1.3** c) assigned to the homologated trialkylborane.[29]

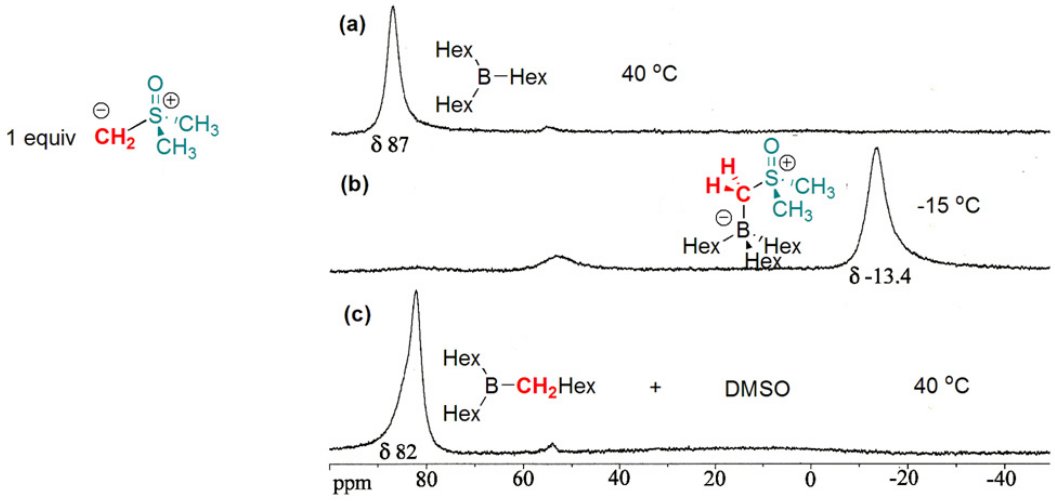

Figure 1.3 ^{11}B NMR of (a) tri-*n*-hexylborane at 40 °C; (b) tri-*n*-hexylborane·ylide complex at –15 °C; (c) trialkylboranes and DMSO product mixture at 40 °C in toluene.[29]

1.4 Telechelic polymers via polyhomologation

Polyhomologation is not only enabled for the excellent molecular weight control, but also for introducing different functional groups into the polymer chain. Functional polymethylene can be obtained either by use of a functional initiator or by subsequent termination reaction.[31-33]

1.4.1 Initiators

Functionalized polymers can directly obtain from a functional initiator. Hydroboration reaction between borane and vinyl group has been utilized to give functional initiator for polyhomologation producing functional polymethylene with low polydispersity. (**Scheme 1.9**).[34]

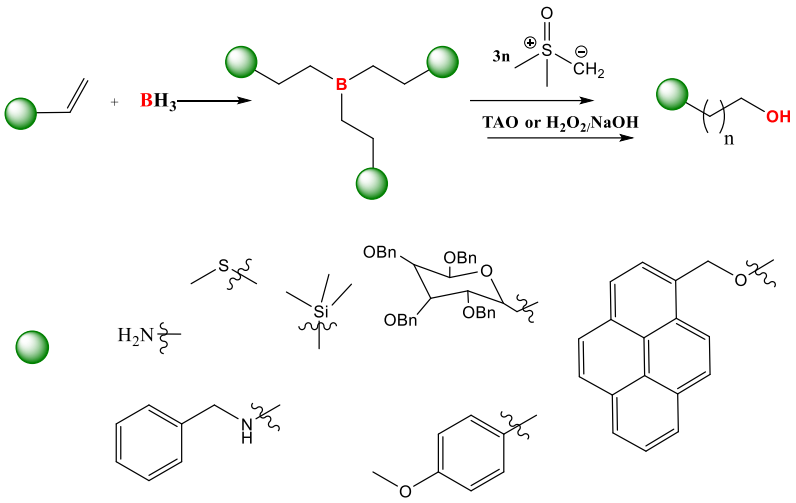

Scheme 1.9 Synthesis of α, ω-difunctional polymethylene.

This strategy also led to di- and triblock hydroxy-terminated block copolymers. For example, PEO-*b*-PM diblock and PM-*b*-PDMS-*b*-PM triblock copolymers (PEO: polyethylene oxide, PDMS: polydimethylsiloxane) were successfully synthesized.[35,36] As shown in **Scheme 1.10**, PEO was allylated with allyl bromide before reacting with BH_3. The resulting boron-linked PEO 3-arm star served as a macroinitiator for polyhomologation. After oxidation/hydrolysis, a hydroxyl-terminated PEO-*b*-PM diblock was obtained. In the case of PM-*b*-PDMS-*b*-PM triblock copolymers instead of BH_3, (thexyl)-BH_2 was used in

order to avoid gelation (**Scheme 1.11**). The thexyl group does not promote polyhomologation as reported.[37]

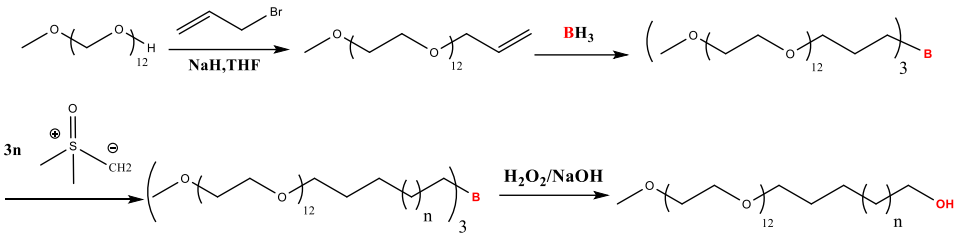

Scheme 1.10 Synthesis of PEO-*b*-PM diblock copolymer through a boron-macroinitiator.

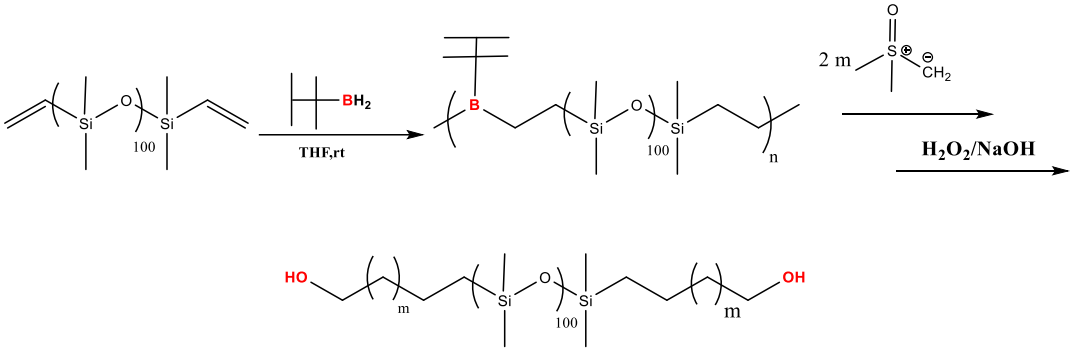

Scheme 1.11 Synthesis of PM-*b*-PDMS triblock copolymer.

The resulting boron-connected PDMS served as multifunctional macroinitiator for the polyhomologation of ylide, leading to a PM-*b*-PDMS-*b*-PM triblock copolymer. The NMR characterization of the resulting HO-PM-*b*-PDMS-*b*-PM-OH in $CDCl_3$ or toluene-d_8 solution revealed a microphase separation at room temperature; their signal being shielded at room temperature due to their aggregation (microcrystal). The PM blocks could be observed only at high temperature (80 ^{o}C) in ^{1}H NMR spectra. In toluene, the triblocks form nanoaggregates as visualized by atomic force microscopy (AFM) on a mica surface. A core–shell structure with a PM core and PDMS shell has been observed from

the AFM images (**Figures 1.4** and **1.5**). By slowly cooling a toluene solution of PM-*b*-PDMS-*b*–PM from 105 ºC to room temperature, crystal plates were obtained and visualized by transmission electron microscopy (TEM; **Figure 1.6**).

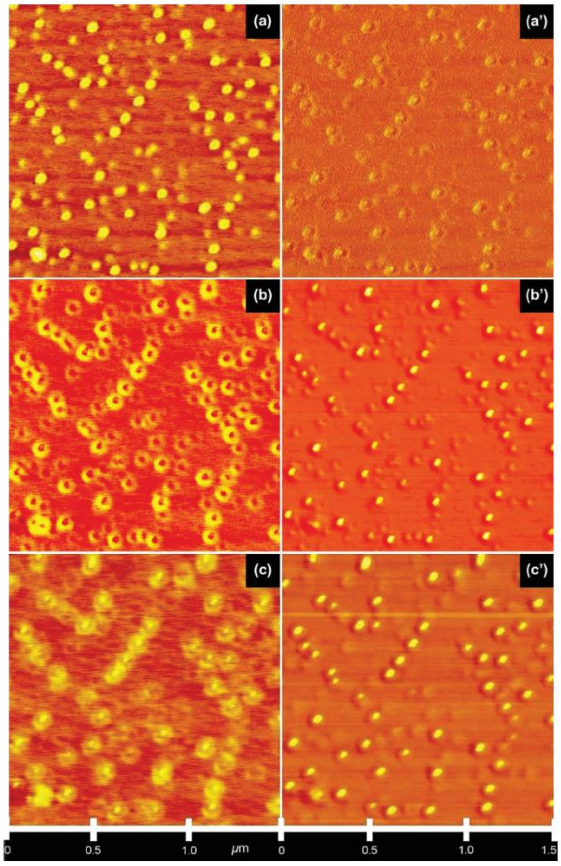

Figure 1.4 Topographic (left) and phase (right) atomic force microscopic (AFM) topographical height images of PM-*b*-PDMS-*b*-PM nanoaggregates produced on mica from toluene.[36]

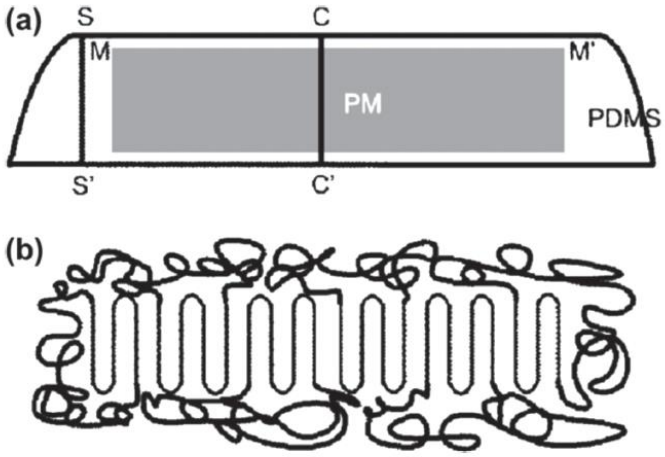

Figure 1.5 Schematic illustration of domain structures in PM-*b*-PDMS-*b*-PM nanodiscs deposited on mica surfaces (a) and possible chain packing in such nanodiscs in toluene (b).[36]

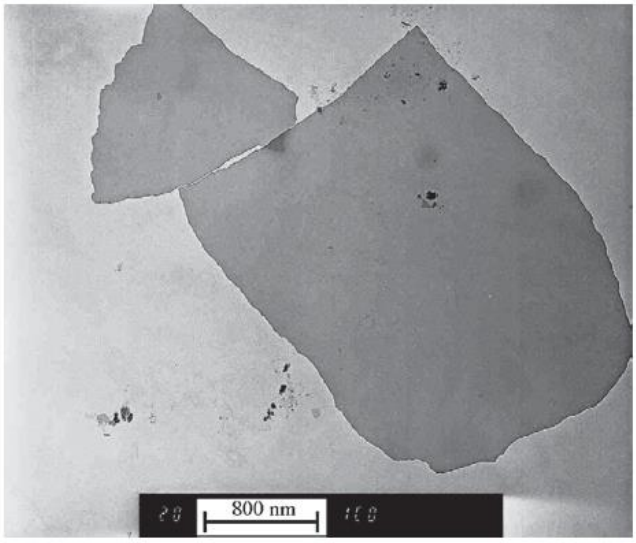

Figure 1.6 Crystal plates of PM-*b*-PDMS-*b*-PM triblock copolymers visualized by transmission electron microscopy (TEM).[36]

1.4.2 Termination reactions

Termination reactions of polyhomologated organoborane can be utilized to introduce functionality into polymer chains. There are different types of termination reactions for polyhomologation that can give different end groups such as halogens,[38,39] hydroxyl[40] or amine groups[41,42] (**Scheme 1.12**). The most common transformation

involves peroxide cleavage with TAO·2H_2O to give a hydroxyl-terminated linear polymethylene. Furthermore, in polyhomologated organoboranes, the replacement of the boron to carbon atom can be achieved through the so-called "stitching'' reaction. This reaction can create new pathways for synthesis of novel polyethylene-based materials with complex macromolecular architectures (star, cyclic etc.).[43,44]

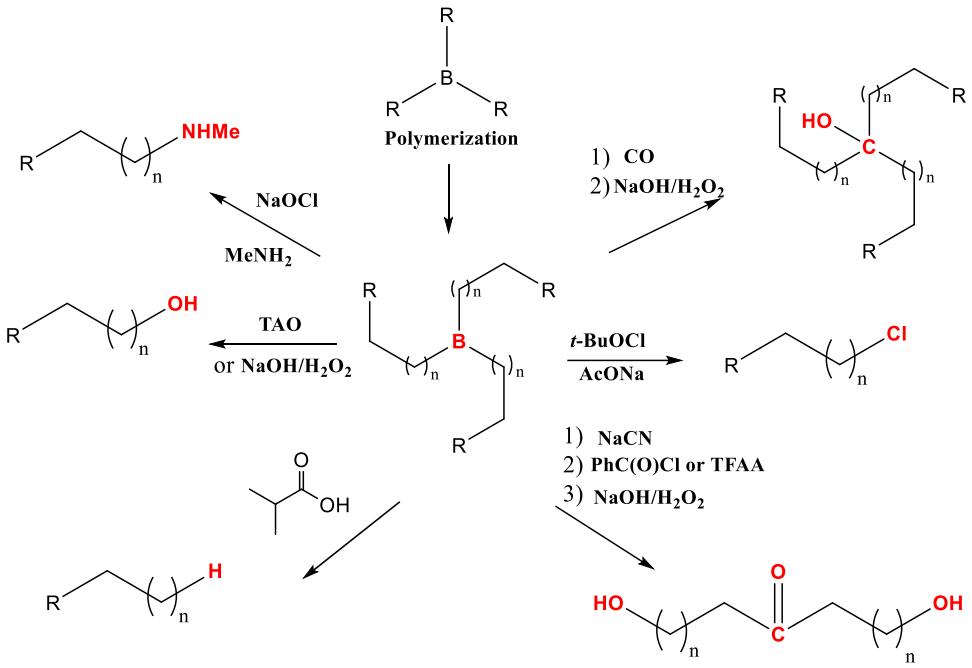

Scheme 1.12 Different types of termination reaction for polyhomologation

1.5 Combination of polyhomologation and controlled/living polymerization methods

By combining polyhomologation with controlled/ living polymerization methods, di and multiblock PM based copolymers have been synthesized. The combination of poly homologation with nitroxide-mediated polymerization (NMP), atom transfer radical polymerization (ATRP) and RAFT are described below. The key points of this strategy are the synthesis of the appropriate-functionalized initiators and the transformation of the functional end-groups into efficient initiators for controlled/living polymerizations. The

functionalized initiators were mainly synthesized by hydroboration of vinyl groups with boranes.

1.5.1 Combination of polyhomologation and nitroxide-mediated radical polymerization

Using the hydroboration/polyhomologation strategy and NMP, a PSt-*b*-PM (PSt: polystyrene) diblock copolymer was prepared (**Scheme 1.13**).[45,46] Styrene was first polymerized, using a hydroxyl-containing initiator, by NMP giving rise to a hydroxyl-terminated PSt. The hydroxyl group was then transformed to allyl group by coupling with allyl bromide. The resulting allyl-terminated PSt was employed to construct boron-linked star-like macroinitiator for polyhomologation, by hydroboration with BH_3 $S(CH_3)_2$. To facilitate characterization and hydroboration, short-PSt blocks (DP=10, 20) were prepared.

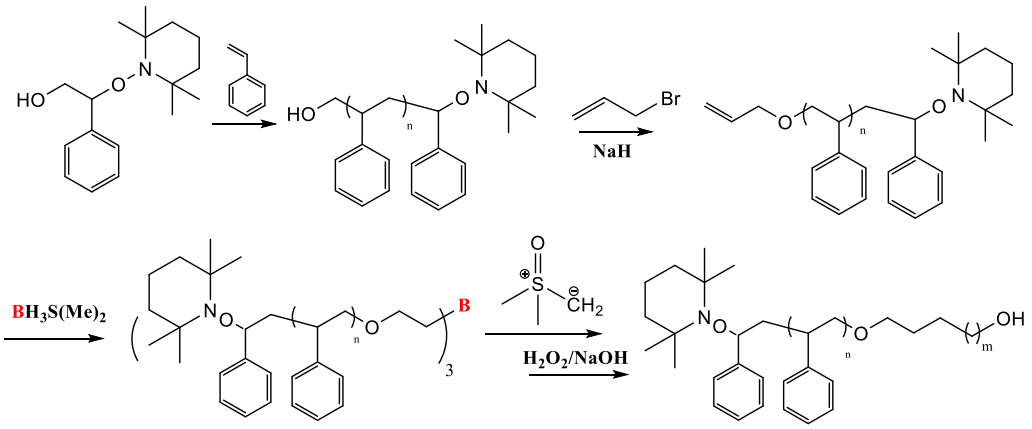

Scheme 1.13 Synthesis of PSt-*b*-PM block copolymer by NMP and polyhomologation**.**

The allyl-terminated PSt was used in excess to afford quantitative hydroboration and avoid the formation of PM homopolymer, since BH_3 $S(CH_3)_2$ can act as an initiator for polyhomologation. After polyhomologation and oxidation/hydrolysis, PSt-*b*-PM diblock copolymers were obtained with narrow polydispersities (PDI= 1.03). However, the

molecular weight of the PM block, determined by NMR at high temperature, was higher than the theoretical one. The stability of the (2, 2, 6, 6-tetramethyl-piperidin-1-yl) oxyl (TEMPO) group in the conditions of polyhomologation has been confirmed by preparation of a TEMPO-functionalized PM homopolymer by allylation, followed by hydroboration and polyhomologation. The melting point (T_m) of the PM block varied from 95.6 to 121.0 ^oC, depending on its length; the glass transition temperature (T_g) of the PSt block varied as well from 62.7 to 67.1 ^oC. PM-*b*-PSt was used as an efficient compatibilizer for PE/PSt blends where the miscibility between PSt and PE phases could be significantly improved (**Figure 1.7**). [46]

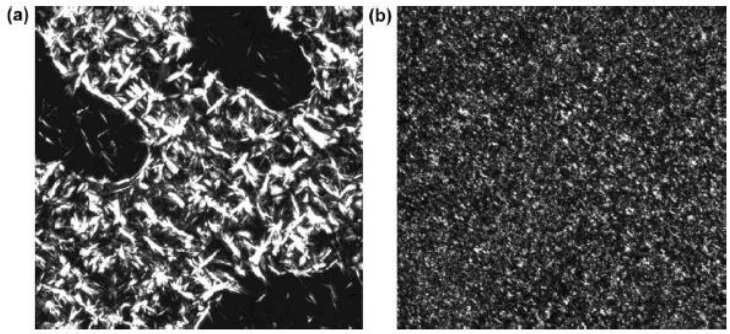

Figure 1.7 Polarized optical images of a) PE/PSt=50/50, b) PSt/PM-*b*-PSt/PE=50/8/50.[46]

1.5.2 Combination of polyhomologation and atom transfer radical polymerization

ATRP has been employed to synthesize different PM based blocks copolymers, such as PM-*b*-PMMA [PMMA: poly (methyl methacrylate)], PM-*b*-PBuA [PBuA: poly (n–butyl acrylate)], and PM-*b*-PSt, by using a PM–Br macroinitiator.[47,48] The latter was synthesized by reaction of α-bromoisobutyric acid with a vinyl-terminated PE, prepared by catalytic polymerization of ethylene (phenoxyimine zirconium complex). The terminal vinyl group could be transformed into hydroxy group, its reaction with 2-bromoisobutyryl

bromide, could afford an efficient ATRP initiator for the polymerization of the second block (PMMA, PBuA, PSt). The relatively high polydispersity of the PE block (≈1.70) was mirrored in the final copolymers.

In the case of polyhomologation, the hydroxyl-terminated PM was formed by breaking the boron-linked star-PM intermediate with H_2O_2/NaOH or trimethylamine *N*-oxide dihydrate (TAO.2H_2O). The terminal hydroxyl groups could be modified to bromide group to afford a PM-macroinitiator for the ATRP of methyl methacrylate and styrene (**Scheme 1.14**).[49–52] The high temperature required for ATRP is beneficial for the dissolution of PM block giving a homogeneous solution. Several PM–Br macroinitiators with molecular weight 1900 to 15000 have been used to prepare PM-*b*-PSt block copolymers with molecular weight from 5000 to 41800 g·mol^{-1}, and PDI ranging from 1.10 to 1.23.

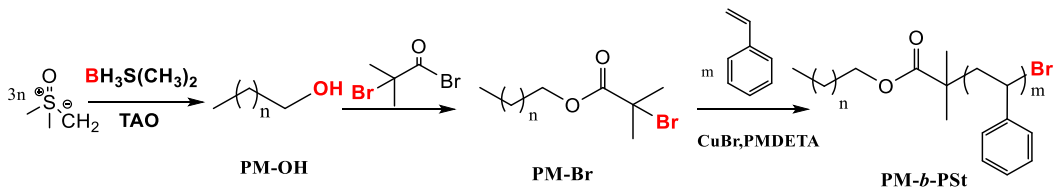

Scheme 1.14 Combination of polyhomologation with ATRP to synthesize PM-*b*-PSt copolymer.

The macroinitiator PM–Br was also employed to copolymerize of pentafluorostyrene and styrene leading to the following copolymer of PM-*b*-P (St-*co*-PFSt) (PFSt: 2, 3, 4, 5, 6-pentafluorostyrene) (**Scheme 1.15**).[52] A series of target block copolymers were obtained with molecular weight varying from 3500 to 12800 g·mol^{-1} and with narrow polydispersities (PDI < 1.07).

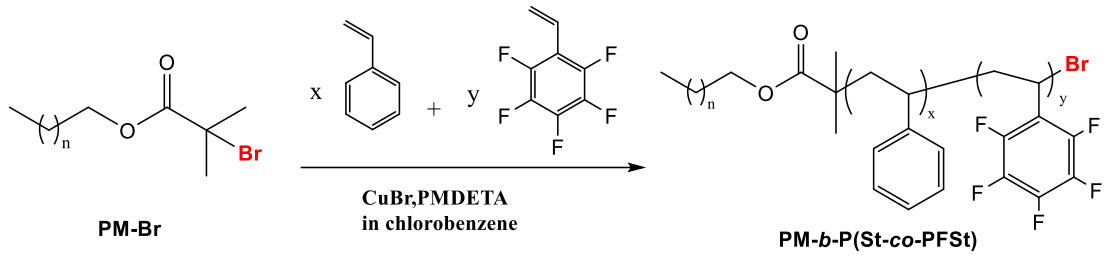

Scheme 1.15 Synthesis of PM-*b*-P(St-*co*-PFST) by ATRP using a PM-Br macroinitiator from polyhomologation.

A honeycomb-like porous film was prepared from a solution of PM-*b*-P (St-*co*-PFSt) using the breath-figure method. The resulting porous film showed higher water contact angle of 111° than the 95° found on the film prepared by spin-coating (**Figure 1.8** a, b). Comparison between films prepared from PM-*b*-PSt diblock copolymer under similar conditions, shows that the presence of PPFSt improved hydrophobicity of the film since the water contact angle was increased to 111° from 103° (**Figure 1.8** b, c).

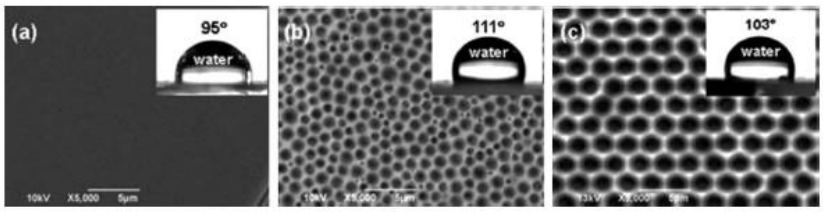

Figure 1.8 Scanning electron microscope(SEM) images and the water-droplet contact angles of copolymer films. a) PM-*b*-P(St-*co*-PFSt) ($M_{n,\ PM\text{-}b\text{-}P(St\text{-}co\text{-}PFSt)}$ = 9670 g·mol^{-1}, DP_{PM}= 50) flat film fabricated by spin-coating; b) PM-*b*-P(St-*co*-PFSt) ($M_{n,\ PM\text{-}b\text{-}P(St\text{-}co\text{-}PFSt)}$= 9670 g·mol^{-1},$DP_{PM}$= 50) porous film fabricated in 3 wt % CS_2 solution at 21 °C with relative humidity of 95 %; c) PM-*b*-PSt ($M_{n,\ PM\text{-}b\text{-}PSt}$= 9300 g·mol^{-1},$DP_{PM}$= 50) porous film fabricated on the same condition with (b).[52]

By using ATRP with PMDETA/CuBr as a catalyst system, a series of PM-*b*-PMMA has been synthesized with molecular weights, ranging from 3980 to 10100 g·mol^{-1} and PDI less than 1.22, as well as PM-*b*-P*n*BuA copolymers whose molecular weights ranged

from 7400 to 10230 g·mol^{-1} and with PDI less than 1.18 (**Scheme 1.16**).[53] The content of PM was found to be in the range of 49 % to 72.6 % in PM-*b*-PMMA and 48.9 % to 82.4 % in PM-*b*-P*n*BuA.

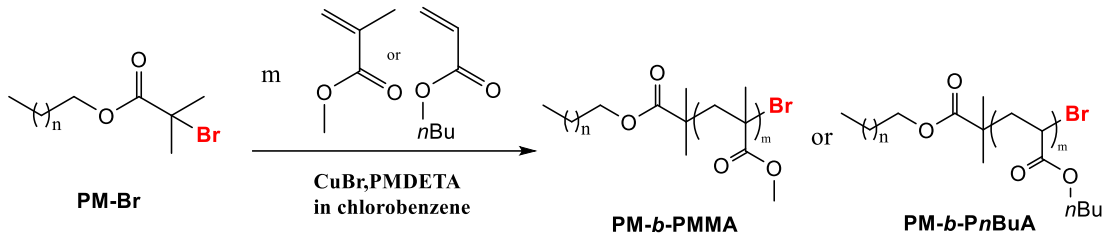

Scheme 1.16 Synthesis of PM-*b*-PMMA and PM-*b*-P*n*BuA by ATRP using a PM-Br macroninitator from polyhomologation.

The presence of PMMA and P*n*BuA decreases the T_m of PM–Br precursor and the enthalpy of fusion. These T_ms of PM-*b*-PMMA varied from 82.2 to 89.5 ^{o}C, and in PM-*b*-P*n*BuA from 95.2 to 96.6 ^{o}C. The diameter of the aggregates of PM-*b*-PMMA in dilute toluene solution was found to be 368 nm. The PM-*b*-PMMA diblock copolymer has been employed as compatibilizer of low-density polyethylene (LDPE)/PMMA blends bringing about a significant decrease of the domain sizes and compatibilization of the two polymers. An amphiphilic diblock copolymer of PM-*b*-PAA (PAA: polyacrylic acid) was also synthesized in a similar way. A PM–Br macroinitiator was employed to initiate ATRP of *tert* -butylacrylate that produced a PM-*b*-PAA diblock copolymer after hydrolysis of the *tert*-butyl ester group in the presence of trifluoroacetic acid (TFA) (**Scheme 1.17**).[54,55] Two PM–Br macroinitiators, with molecular weight of 1300 and 3300 g·mol^{-1}, PDI of 1.11 and 1.04, respectively, were employed for the ATRP of *tert*-butylacrylate leading to two series

of narrowly dispersed PM-*b*-PAA copolymers (PDI less than 1.09) with molecular weight ranging from 9600 to 15800 g·mol^{-1}, and 8800 to 13100 g·mol^{-1}, respectively.

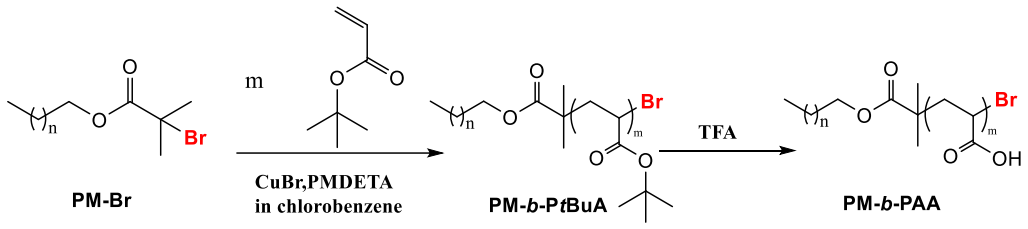

Scheme 1.17 Synthesis of an amphiphilic diblock copolymer of PM-*b*-PAA by ATRP using a pre-synthesized PM-Br macroinitiator from polyhomologation.

Recently, a novel strategy was developed to prepare polyethylene-based 3-miktoarm star copolymers PE_2-*b*-PSt, $(PE\text{-}b\text{-}PSt)_2$-*b*-PSt and terpolymers $(PE\text{-}b\text{-}PMMA)_2$-*b*-(PSt-*b*-PMMA) by combining polyhomologation, ATRP and boron chemistry as shown in **Scheme 1.18**. 1,4-Pentadiene-3-yl 2-bromo-2-methylpropanoate was hydroborated with thexylborane to obtain a multi heterofunctional initiator with two initiating sites for polyhomologation and one for ATRP.[56]

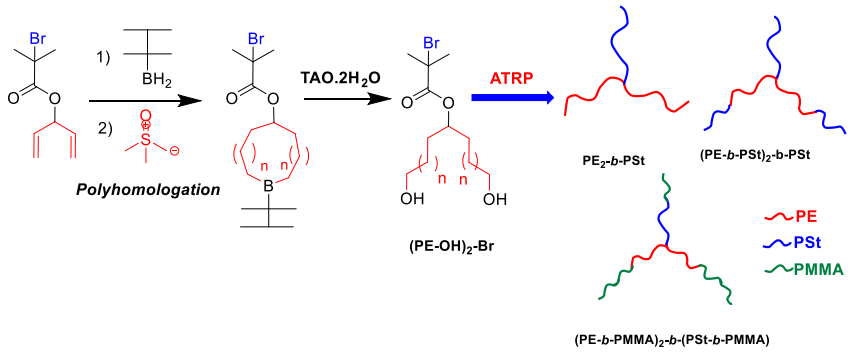

Scheme 1.18 Synthetic route to prepare PE_2-*b*-PSt, $(PE\text{-}b\text{-}PSt)_2$-*b*-PSt and $(PE\text{-}b\text{-}PMMA)_2$-*b*-(PSt-*b*-PMMA).

1.5.3 Combination of polyhomologation and reversible addition-fragmentation chain-transfer (RAFT) polymerization

A hydroxyl-terminated PM was synthesized by polyhomologation and transformed into a RAFT transfer-agent by esterification of S-1-dodecyl-S'-(a, a'-dimethyl-a''-acetate) trithiocarbonate, which was then used to initiate the controlled/ living polymerization of a monomer.[57] This macromolecular chain transfer agent was used to derive a series of PM-*b*–PSt (M_n= 55500–34000 g·mol^{-1}; PDI= 1.12–1.25) diblock copolymers (**Scheme 1.19**). The resulting PSt-*b*-PM diblock copolymers were used to fabricate microfibers and microspheres by electrospinning process. It was concluded that the morphology strongly depends on the concentration (**Figure 1.9**).

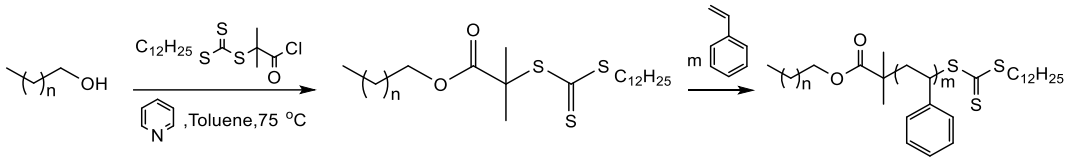

Scheme 1.19 Synthesis of PM-*b*-PSt copolymer by combining polyhomologation and RAFT.

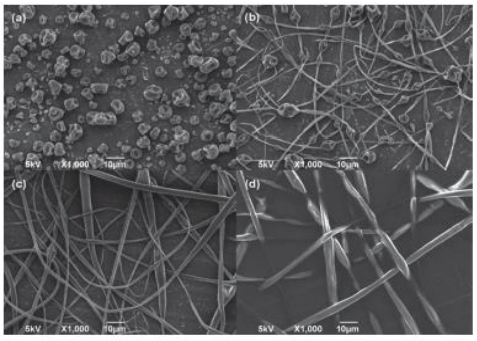

Figure 1.9 SEM images of electrospun PM-*b*-PSt microspheres, microspheres-on-stirring, and microfibers obtained from PM-*b*-PSt solution on DMf-$CHCl_3$ with different polymer concentrations ($M_{n,\ PM}$=1400 g·mol^{-1}, $M_{n,\ PM\text{-}b\text{-}PSt}$=27000 g.mol-1): a)5 %, b) 10 %, c)15 %, and d) 20 % w/w, respectively.[57]

1.6 Combination of polyhomologation and ring-opening polymerization

A hydroxyl-terminated PM has served also as macroinitiator for the ring-opening polymerization of cyclic ester monomers such as ε-caprolactone and lactide leading to the corresponding PM-based copolymers. PM-*b*–PCL (PCL: polycaprolactone) has been successfully synthesized by sequential polymerization and ring-opening polymerization (**Scheme 1.20**).[58] The ring-opening polymerization of ε-caprolactone required high temperature (80 °C), which is suitable for the dissolution of the PM initiator, resulting in a homogeneous solution. Two PM macroinitiators with molecular weight of 1700 and 5400 $g{\cdot}mol^{-1}$ were successfully employed to initiate the ring-opening polymerization of ε-caprolactone in the presence of $Sn(Oct)_2$ as catalyst.

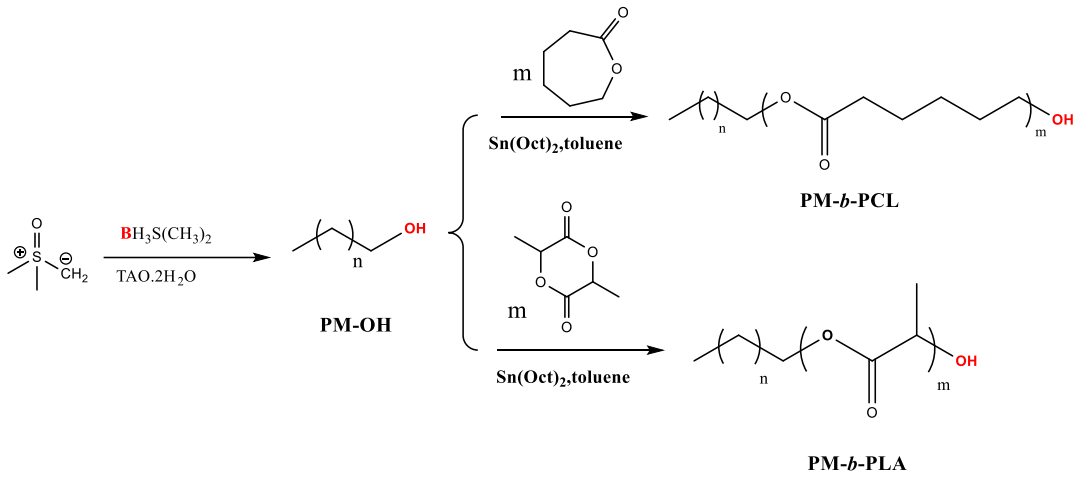

Scheme 1.20 Synthesis of PM-*b*-PCL and PM-*b*-PLA diblock copolymers by sequential polyhomologation and ring opening polymerization.

The resulting PM-*b*-PCL block copolymers with molecular weight up to 17400 $g{\cdot}mol^{-1}$ exhibited low PDIs (typically less than 1.2) with a content in PCL ranging from 51.7 % to 87.0 %. The synthesized PM-*b*-PCL served as a good compatibilizer for blending PM

and PCL (**Figure 1.10**). A honeycomb-like porous film has been prepared in the breath-figure method. Under the same condition, the lactide has also been polymerized leading to PM-*b*-PLA [PLA: poly (lactic acid)].[59]

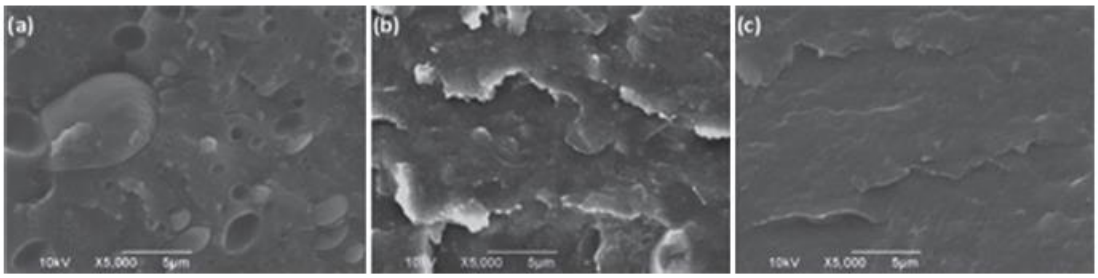

Figure 1.10 SEM images of polymer blends: a) binary with LDPE/PCL=70/30 (weight ratio); b) and c) ternary b; ends with LDPE/PCL (PM-*b*-PCL) = 70/30/10 (weight ratio), respectively.[58]

A triblock copolymer PM-*b*-PCL-*b*-PAA has been synthesized by sequential polyhomologation, ring-opening polymerization, and ATRP (**Scheme 1.21**).[60] From a PM-OH with a molecular weight of 1100 $g{\cdot}mol^{-1}$, ε–caprolactone was polymerized in the presence of $Sn(Oct)_2$. The resulting hydroxyl-terminated PM-*b*-PCL was brominated with 2-bromoisobutyryl bromide and used to initiate the polymerization of *tert* -butylacrylate with PMDETA/CuBr catalyst system, which produces a PM-*b*-PCL-*b*-PAA triblock copolymer after hydrolysis by TFA (M_n, PM= 1100 $g{\cdot}mol^{-1}$, M_n, PCL= 8900 $g{\cdot}mol^{-1}$, M_n, PAA= 3900 $g{\cdot}mol^{-1}$). The triblock terpolymers were successfully used for the fabrication of porous film.

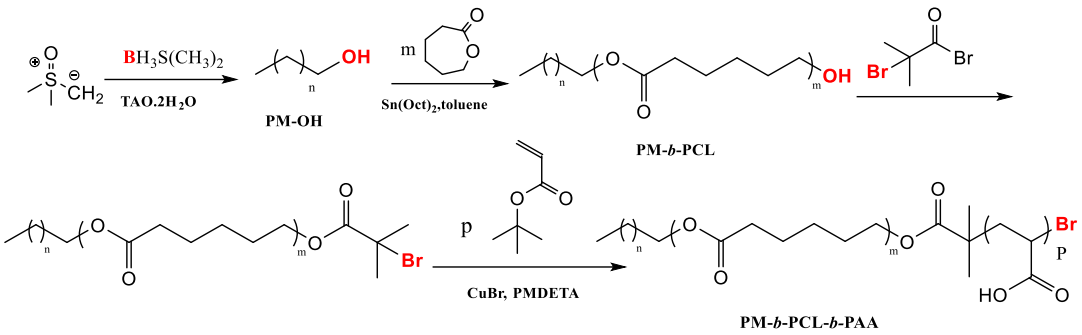

Scheme 1.21 Synthesis of PM-*b*-PCL-*b*-PAA triblock terpolymers via sequential polyhomologation, ring-opening polymerization and ATRP.

1.7 Combination of polyhomologation and living anionic polymerization

Recently, a novel one-pot method to synthesize PM-based block copolymers was developed by combining anionic polymerization and polyhomologation through BF_3 OEt_2 used as a "bridge molecule". [61] The synthetic approach involved the following steps: (a) synthesis of a 3-arm star polymer (trimacromolecular organoborane, macroinitiator) by reacting living polymeric anions with BF_3 OEt_2, (b) *in situ* polyhomologation of dimethylsulfoxonium methylide, from this macroinitiator to produce a 3-arm star block copolymer, and (c) the oxidation/ hydrolysis by $TAO.2H_2O$ to afford the PM-based block copolymer. For example, the synthesis of PBd-*b*-PM (PBd: polybutadiene) and PSt-*b*-PM are shown in **Scheme 1.22**. Both of the two diblock copolymers exhibited narrow polydispersities (PDI < 1.14). However, the molecular weights of PM block calculated from NMR characterization were higher than expected, indicating a low efficiency (≈30 %) of the linking reaction (living polymers with BF_3OEt_2). The peaks in HT-SEC traces shifted to the high-molecular-weight domain (low retention volume) and exhibited low polydispersity after polyhomologation, indicating the successful growth of the PM block (**Figure 1.11**). The thermal response of the resulting PM-based copolymers has been

quantitatively studied by an upper critical solution temperature (UCST) measurement and ^{1}H NMR. In the case of PBd-*b*-PM, a phase transition in toluene was found at 40–55 °C with the formation of a cloudy solution turning clear and transparent. The phase transition was also confirmed by NMR characterization at different temperatures, confirming that the PM block can only be seen at high temperature (higher than UCST) (**Figure 1.12**).

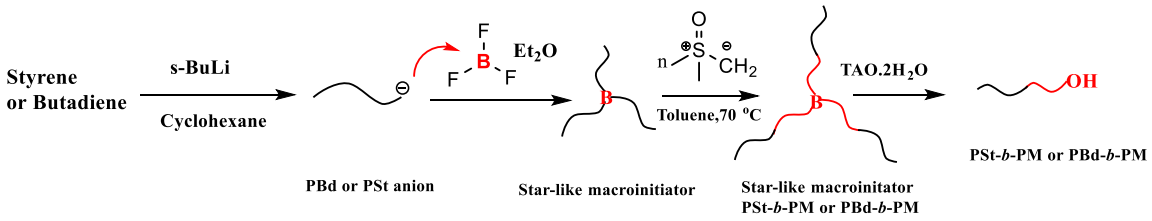

Scheme 1.22 One pot synthesis of PM-based block copolymers by combining anionic polymerization and polyhomologation

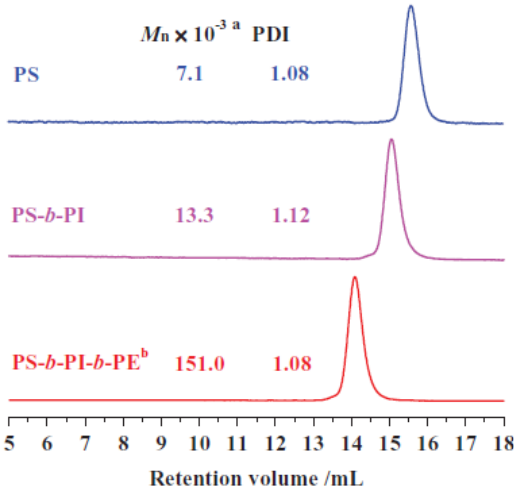

Figure 1.11 HT-SEC traces of PSt-*b*-PI-*b*-PM triblock using trichlorobenzene as eluent at 150 °C.[61]

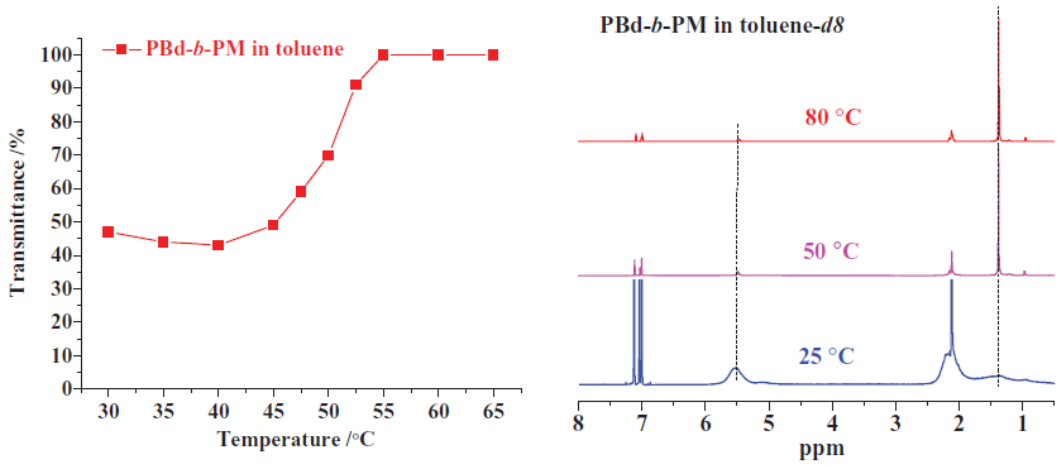

Figure 1.12 Thermal responses of PBd-*b*-PM solution in toluene revealed by UCST and ^{1}H NMR measurements at different temperatures.[61]

1.8 Combination of polyhomologation and ROMP

Recently, Hadjichristidis and coworkers synthesized novel well-defined polyethylene-based random, block, and bilayered molecular cobrushes through the macromonomer strategy "grafting through" by combining polyhomologation and ROMP (**Scheme 1.23**). Norbornyl-terminated polyethylene was synthesized via esterification of PE-OH with 5-norbornene-2-carboxylic acid using DCC and DMAP. Then, the ROMP of the obtained macromonomer was carried out using Grubbs catalyst to prepare PE-based cobrush. Using this strategy, series of PM-based cobrushes have been synthesized with different segments and molecular weights, ranging from 58000 to 170000 g·mol^{-1} and PDI less than 1.18.[62,63]

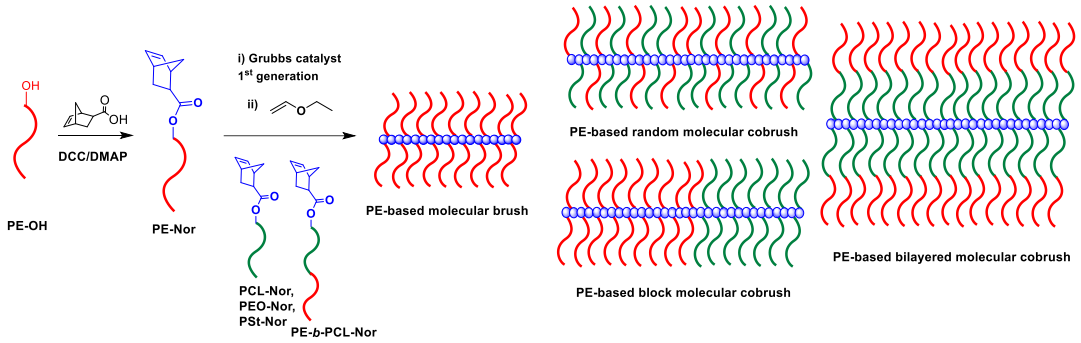

Scheme 1.23 Synthesis of PM-based cobrushes by combining polyhomologation and ROMP.

1.9 Combination of polyhomologation and living cationic polymerization

Using the hydroboration/polyhomologation strategy and living cationic polymerization, it has been possible to prepare a PIB-*b*-PM (PIB: polyisobutylene) diblock copolymer (**Scheme 1.24**). Allyl-terminated PIBs were firstly synthesized using living cationic polymerization. Then, the resulting allyl-terminated PIB was employed to construct boron-linked star-like macroinitiator for polyhomologation, by hydroboration with BH_3. THF. Then, polyhomologation took place by addition of ylide followed by oxidation using TAO.2H_2O to obtain PIB-*b*-PM.[64]

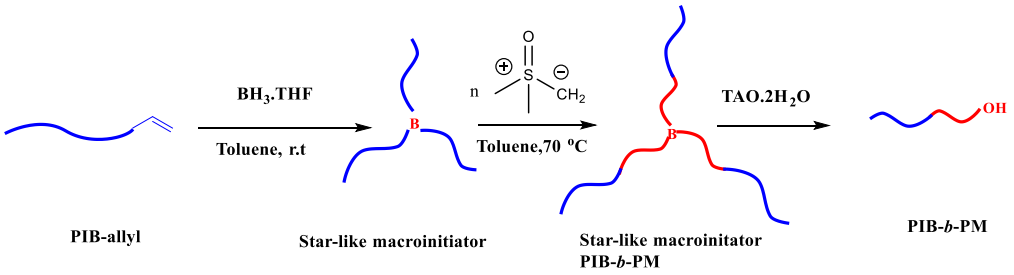

Scheme 1.24 Synthesis of PIB-*b*-PM diblock copolymer by combining polyhomologation and living cationic polymerization.

1.10 Aim of this dissertation

Due to the fact that physical properties of synthetic macromolecules depend on primary factors such as molecular weight, structure and PDI, synthesis of well-defined

polyethylene-based macromolecular architectures has been a challenge for researchers Polyhomologation technique can fulfill the criteria of accurate control of molecular weight, functionality over chain ends and polydispersity. Consequently, the basic goal of this study was to design and develop new facile strategies to synthesize polymethylene (polyethylene)-based different polymer topologies by combining polyhomologation and high efficient linking reactions such as Diels Alder, CuAAC and Glaser coupling. A sub-goal of this work was to utilize part of newly designed structures to explore and fundamentally understand the properties and morphology of self-assembled micelle systems.

We are planning in order to achieve the aim of this dissertation to:

1- Investigate the polyhomologation, as a viable method to synthesize new polyethylene-based macromolecular architectures such as linear co/ter polymers, graft and tadpole polymers.

2- Design, prepare and characterize functional polyethylene with functional groups such as anthracene and alkyne group synthesized via the modification of hydroxyl end group in polyethylene or design specific organoborane initiators.

3- Achieve polyethylene-based macromolecular architectures by using different polymerization techniques, such as nitroxide-mediated radical polymerization (NMP), ring-opening polymerization (ROP) and atom transfer radical polymerization (ATRP) have been combined with polyhomologation.

4- Investigate the self-assembly behavior of polyethylene-based copolymer in aqueous solution and study the morphology.

5- Study and confirm molecular characteristic of all intermediates and final products by using ^{1}H-NMR spectroscopy, SEC measurements, IR spectroscopy, DSC measurements, DLS, UV, TEM, AFM, Fluorescence spectroscopy.

1.11 Outline of this dissertation

This dissertation is divided into five chapters. The first chapter presents introductory information of polyethylene and polyhomologation. The combination of polyhomologation and different techniques such as controlled radical, ROP, ROMP and anionic polymerization are presented in Chapter 1. Chapters 2 to 5 are based on journal papers that have been published or will submit for publication. Chapter 2 describes a facile synthetic route to prepare linear polyethylene based block co/ter polymers by combining polyhomologation with Diels Alder reaction. The anthracene functionality is incorporated into the polyethylene chains as the end group via hydroboration reaction. Polymer chain length and molecular weight distribution were well controlled via polyhomologation. Chapter 3 presents the synthesis of polyethylene-based graft terpolymers via "grafting onto" method by combining NMP, polyhomologation and CuAAC ‘’click’’ reaction. Chapter 4 introduces a novel method to synthesize polyethylene–based tadpole structure by combining ATRP, polyhomologation and Glaser coupling. In Chapter 5, a series of amphiphilic polymers PM-*b*-PEG were used to study the self-assembly behavior of the micelles in aqueous solution and provides some insights to the impact and future directions of the related research work.

1.12 References

(1) Qiao, J.; Guo, M.; Wang, L.; Liu, D.; Zhang, X.; Yu, L.; Song, W.; Liu, Y. *Polym. Chem.* **2011**, *2*, 1611.
(2) Piringer, O. G.; Brandsch, J. Chatacteristics of Plastic Materials. In *Plastic Packaging: Interactions with Food and Pharmaceuticals,* 2nd ed.; Piringer, O. G., Baner, A. L., Eds.; VCH: New York, 2008.
(3) Peacock, A. J.; Handbook of Polyethylene: Structure, Properties, and Applications, CRC Press, New York, 2000.
(4) Chung, T. C. M.; *Macromolecules* **2013**, *46*, 6671.
(5) Whiteley, K. S. In *Ullman's Encyclopedia of Industrial Chemistry-,* 5th ed.; Schulz, G., Ed.: New York, 1992.
(6) Peacock, A. J. *Handbook of Polyethylene,* Marcel Dekker, Inc.: New York, 2000.
(7) Sirota, A. G. *Polyolefins, Modification of Structure and Properties,* keter Press: Jerusalem, 1971.
(8) Seymour, R. B.; Cheng, T. *Advances in Polyolefins, the World's Most Widely Used Polymers,* Plenum Press: New York, 1987.
(9) Kissen, Y. Y. In *Kirk-Othmer Encyclopedia of Chemical Technology,* 4th ed.; Howe-Grant, M., Ed.; Wiley-Interscience: New York, 1996.
(10) Allcock, H. R.; Lampe, F. W. *Contemporary Polymer Chemistry,* Prentice-Hall, Inc.: New Jersey, 1981.
(11) Boor, J. *Ziegler-Natta Catalysts and Polymerizations;* Academic Press: New York, 1979.
(12) Fink, G.; Muelhaupt, R.; Brintzinger, H. H. *Ziegler Catalysts: Recent Scientific Innovations and Technological Improvement',* Springer-Verlag: Berlin, 1995.
(13) Jordan, R. F. *Adv. Organomet. Chem.* **1991**, *32,* 325.
(14) Alt, H. G.; Koeppl, A. *Chem. Rev.* **2000,** *100,* 1205.
(15) Hadjichristidis, N.; Pitsikalis, M.; Pispas, S.; Iatrou, H. *Chem. Rev.* **2001**, *101*, 3747.
(16) Luo, J.; Shea, K. J. in Complex Macromolecular Architectures: Synthesis, Characterization, and Self-Assembly; Hadjichristidis, N.; Hirao, A.; Tezuka, Y.; Du Prez, F. Eds; John Wiley & Sons, Singapore, 2011.
(17) Hadjichristidis, N.; Xenidou, M.; Iatrou, H.; Pitsikalis, M.; Poulos, Y.; Avgeropoulos, A.; Sioula, S.; Paraskeva, S.; Velis, G.; Lohse, D. J.; Schulz, D. N.; Fetters, L. J.; Wright, P. J.; Mendelson, R. A.; Garcia-Franco, C. A.; Sun, T.; Ruff, C. J. *Macromolecules* **2000**, *33*, 2424.
(18) Rachapudy, H.; Smith, G. G.; Raju, V. R.; Graessley, W. W. *J. Polym. Sci., Polym. Phys. Ed.* **1979**, *17*, 1211.
(19) Bielawski, C. W.; Grubbs, R. H. *Angew. Chem.* **2000**, *112*, 3025.

(20) Bielawski, C. W.; Grubbs, R. H. in Controlled and Living Polymerizations: From Mechanisms to Applications; Muller, A. H. E.; K. Matyjaszewski, K. Eds; Wiley-VCH, Weinheim, Germany, 2009.
(21) Shea, K. J.; Walker, J. W.; Zhu, H.; Paz, M.; Greaves, J. *J. Am. Chem. Soc.* **1997**, *119*, 9049.
(22) Meerwein, H. *Angew. Chem.* **1948**, *60*, 78.
(23) Shea, K. J. *Chem. Eur. J.* **2000**, *6*, 1113.
(24) Shea, K. J. *Chem. Eur. J.* **2000**, *6*, 1113.
(25) Jellema, E.; Jongerius, A. L.; Reek, J. N.; Bruin, B. de *Chem. Soc. Rev.* **2010**, *39*, 1706
(26) Wagner, C. E.; Rodriguez, A. A.; Shea, K. J. *Macromolecules* **2005**, *38*, 7286.
(27) Zhou, X. Z.; Shea, K. J. *J. Am. Chem. Soc.* **2000**, *122*, 11515.
(28) (a) Tufariello, J.; Lee, L. *J. Am.Chem. Soc.* **1966,** *88,* 4757. (b) Tufariello, J.; Wojtkowski, P.; Lee, L. *J. Chem. Soc., Chem. Commun.* **1967,** 505. (c) Tufariello, J.; Lee, L.; Wotjkowski, P. *J. Am. Chem. Soc.* **1967,** *89,* 6804.
(29) Busch, B. B.; Paz, M. M.; Shea, K. J.; Staiger, C. L.; Stoddard, J. M.; Walker, J. R.; Zhou, X. Z.; Zhu, H. D. *J. Am. Chem. Soc.* **2002,** *124,* 3636.
(30) Corey, E. J.; Chaykovsky, M. *J. Am. Chem. Soc.*, **1965**, *87*, 1353.
(31) Busch, B. B.; Shea, K. J. *Abstr. Pap. Am. Chem. Soc.* **1997,** *214,* 6.
(32) Shea, K. J.; Busch, B. B.; Paz, M. M. *Angew. Chem. Int. Ed.* **1998,** *37,*1391.
(33) Sulc, R.; Zhou, X. Z.; Shea, K. J. *Macromolecules* **2006,** *39,* 4948.
(34) Busch, B. B.; Staiger, C. L.; Stoddard, J. M.; Shea, K. J. *Macromolecules* **2002**, *35*, 8330.
(35) Shea, K. L.; Staiger, C. L.; Lee, S. Y. *Macromolecules* **1999**, *32*, 3157.
(36) Wang, J.; Horton, J. H.; Liu, G.; Lee, S. Y; Shea, K. J. *Polymer* **2007**, *48*, 4123.
(37) Shea, K. J.; Lee, S. Y.; Busch, B. B. *J. Org. Chem.* **1998**, *63*, 5746.
(38) Jigajinni, V. B.; Paget, W. E.; Smith, K. *J. Chem. Res., Synop.* **1981**, 376.
(39) Nelson, D. J.; Soundararajan, R. *J. Org. Chem.* **1988,** *53,* 5664.
(40) Shea, K. J.; Wagner, C. W. *Org. Lett.* **2001,** 3063.
(41) Kabalka, G. W.; Wang, Z. *J. Organomet. Chem.* **1989,** *8,* 1093.
(42) Brown, H. C; Midland, M. M.; Levy, A. B.; Suzuki, A.; Sono, S.; Itoh, M. *Tetrahedron* **1987,** *43,* 4079.
(43) Brown, H. C. *Organic Syntheses via Boranes*; Wiley: New York, **1975**.
(44) Wagner, C. E.; Kim, J.-S.; Shea, K. J. *J. Am. Chem. Soc.* **2003**, *125,* 12179.
(45) Zhou, X.; Shea, K. J. *Macromolecules* **2001**, *34*, 3111.
(46) Luo, J.; Shea, K. J. *Acc. Chem. Res.* **2010**, *43*, 1420.
(47) Inoue, Y.; Matyjaszewski, K. *J. Polym. Sci., Part A: Polym. Chem.* **2004**, *42*, 496.

(48) Zhao, L.; Chen, J.; Shi, L.; Chen, W.; Li, G.; Wang, Y.; Ma, Z. *Acta Chim. Sin.* **2011**, *69*, 591.
(49) Chen, J.; Cui, K.; Zhang, S.; Xie, P.; Zhao, Q.; Huang, J.; Shi, L.; Li, G.; Ma, Z. *Macromol. Rapid Commun.* **2009**, *30*, 532.
(50) Chen, J.; Zhao, Q.; Lu, H.; Huang, J.; Li, G.; Cao, S.; Ma, Z. *J. Polym. Sci., Part A: Polym. Chem.* **2010**, *48*, 1894.
(51) Li, J.; Zhao, Q.; Chen, J.; Li, L.; Huang, J.; Ma, Z.; Zhong, Y. *Polym. Chem.* **2010**, *1*, 164.
(52) Xue, Y.; Lu, H.; Zhao, Q.; Huang, J.; Xu, S.; Cao, S.; Ma, Z. *Polym. Chem.* **2013**, *4*, 307
(53) Chen, J.; Zhao, Q.; Shi, L.; Huang, J.; Li, G.; Zhang, S.; Ma, Z. *J. Polym. Sci., Part A: Polym. Chem.* **2009**, *47*, 5671.
(54) Lu, H.; Xue, Y.; Zhao, Q.; Huang, J.; Xu, S.; Cao, S.; Ma, Z. *J. Polym. Sci., Part A: Polym. Chem.* **2012**, *50*, 3641.
(55) Lv, H.; Xu, S.; Zhao, Q.; Huang, J.; Cao, S.; Ma, Z. *Acta Chim. Sin.* **2011**, *69*, 1126.
(56) Zhang, Z.; Altaher, M.; Zhang, H.; Wang, D.; Hadjichristidis, N. *MacromoleculeS* **2016**, *49*, 2630
(57) Wang, X.; Gao, J.; Zhao, Q.; Huang, J.; Mao, G.; Wu, W.; Ning, Y.; Ma, Z. *J. Polym. Sci., Part A: Polym. Chem.* **2013**, *51*, 2892.
(58) Li, Q.; Zhang, G.; Chen, J.; Zhao, Q.; Lu, H.; Huang, J.; Wei, L.; Dagosto, F.; Boisson, C.; Ma, Z. *J. Polym. Sci., Part A: Polym. Chem.* **2011**, *49*, 511.
(59) Li, Q.; Zhang, G.; Huang, J.; Zhao, Q.; Wei, L.; He, Z.; Ma, Z. *Acta Chim. Sin.* **2011**, *69*, 497.
(60) Yuan, C.; Lu, H.; Li, Q.; Yang, S.; Zhao, Q.; Huang, J.; Wei, L.; Ma, Z. *J. Polym. Sci., Part A: Polym. Chem.* **2012**, *50*, 2398.
(61) Zhang, H.; Alkayal, N.; Gnanou, Y.; Hadjichristidis, N. *Chem. Commun.* **2013**, *49*, 8952.
(62) Zhang, H.; Gnanou, Y.; Hadjichristidis, N. *Polym. Chem.* **2014**, *5*, 6431.
(63) Zhang, H.; Zhang, Z.; Gnanou, Y; Hadjichristidis, N. *Macromolecules* **2015**, *48*, 3556-3562.
(64) Zhang, H.; Banerjee, S.; Faust, R.; Hadjichristidis, N. *Polym. Chem*. **2016**, *7*, 1217.

Chapter 2. Well-Defined Polymethylene-Based Block co/ter-Polymers by Combining Anthracene/Maleimide Diels-Alder Reaction with Polyhomologation

(This chapter is reproduced from *Polym. Chem.,* **2015***, 6,* 4921.)

2.1 Introduction

The Diels-Alder (DA) reaction consists of [4+2] cycloaddition between a diene and a dienophile (**Scheme 2.1**), and it is still one of the most useful and important reactions in modern organic chemistry.[1,2] Recently, due to its broad practicability and orthogonality, DA reaction became an important linking method in polymer chemistry too.[3,4] It has been successfully applied for the synthesis of polymers, mainly styrenic and (meth) acrylic, with different macromolecular architectures, e.g. homo- and miktoarm stars [5,6], combs [7,8], cyclic [9], dendritic [10], etc.[11,12]

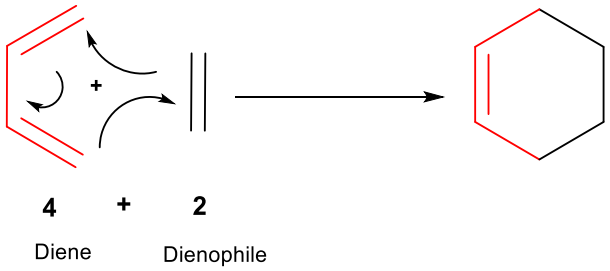

Scheme 2.1 General mechanisms of Diels Alder reaction

On the other hand, alkylborane-initiated polymerization of dimethyl sulfoxonium methylide recently developed by Shea, [13-15] leads to perfectly linear polymethylene, PM (or polyethylene, PE). The general reaction scheme involves the formation of an organo boron zwitterionic complex between the dimethylsulfoxonium methylide and the trialkylborane which breaks down by intramolecular 1, 2-migration. As a consequence,

the methylene group is randomly inserted one by one (C_1 polymerization or polyhomologation) into the three branches of the trialkylborane leading to a 3-arm star having boron as junction point. The resulting star is subsequently oxidized/hydrolyzed to give OH-end-capped linear PMs.

By combining polyhomologation and anthracene/furan-protected maleimide Diels-Alder reaction, we were able to synthesize well-defined PM-based diblock copolymers of PM with poly(ε-caprolactone) (PCL) or polyethylene glycol (PEG) as well as triblock terpolymers of polylactide with PM and either PCL or PEG. This method is a general one opening new horizons for the synthesis of well-defined PE-based polymeric materials with different macromolecular architectures. Due to their amphiphilic nature these copolymers are perfect candidates for many industrial applications in compatibilization, dyeing, printing, adhesion, etc.[16-32]

2.2 Experimental section

2.2.1 Materials

Sodium hydride (60% dispersion in mineral oil, Acros) was washed with petroleum ether (40-60 ^{o}C) before use. Methanol (99%, Fisher), acetonitrile (99%, Fisher), diethyl ether (99%, Aldrich), dichloromethane (>99%, Fisher), and hexane (99%, Fisher) were used as received. Tetrahydrofuran (99%, Fisher) and toluene (99.7%, Fluka) were freshly distilled over sodium and benzophenone. 1,8 diazabicyclo [5,4,0] undec-7-ene (DBU) (99%, Fluka), ε-caprolactone (99%, Alfa Aesar), allyl bromide (97%, Aldrich), and ethanol amine (99.5%, Aldrich) were distilled from CaH_2. D, L-lactide (99%, Across); exo-3,6-epoxy-1,2,3,6-tetrahydrophathalic anhydride (99%, Aldrich) was purified by crystallization in

toluene. 9-anthracenemethanol (97%, Alfa Aesar) was purified by crystallization in ethyl acetate. Calcium hydride (CaH_2) (95%, Aldrich), trimethylsulfoxonium iodide (98%, Alfa Aesar), *t*-BuP_2 (2.0 M in THF, Aldrich), benzyltri-n-butylammonium chloride (98%, Alfa Aesar), trimethylamine N-oxide dihydrate (TAO) (>99%, Fluka), succinic anhydride (99%, Aldrich), 4-(dimethyl amino) pyridine (DMAP) (99%, Aldrich), N, N'-dicyclohexylcarbod - iimide (DCC) (99%, Aldrich), polyethylene glycol methyl ether (PEG) (M_n= 4000 $g \cdot mol^{-1}$, DP_n= 91, Aldrich), and BH_3.THF (1M in THF, Aldrich) were used as received.

2.2.2 Instrumentation

High-temperature-size exclusion chromatography (HT-SEC) measurements were performed on a Viscotek HT-SEC module 350 with two PL gel 10 µm MIXED-B columns using 1,2,4-trichloro benzene as eluent at a flow rate of 0.8 mL/min at 150 ^oC. ^1H NMR spectra were recorded on a Bruker AVANCE III-600 spectrometer. SEC chromatograms at 35 ^oC were recorded on a Viscotek TDA 305 instrument with a column of PLgel 10 µm MIXED-C (only used for PS3B) or two columns of Styragel HR2 THF (7.8×300 mm) and Styragel HR4 THF (7.8×300 mm). THF was the eluent at a flow rate of 1 $mL \cdot min^{-1}$. The system was calibrated by PST standards. Differential scanning calorimetry (DSC) characterization was performed on a Mettler Toledo DSC1/TC100 system in an inert nitrogen atmosphere. The second heating curve was used to determine the melting temperature (T_m), glass transition temperature (T_g), and degree of crystallinity. UV-VIS measurements were performed on an Evolution 600 instrument with a manual temperature controller.

2.2.3 Nomenclature

To simplify the identification of compounds, the following convention was applied: As a prefix, Ant- was assigned to the anthracene and the subscript number means the degree of polymerization. A suffix was added to identify the functionality at the end of the polymer chain: -MI, for mailemide-terminated polymers and -OH for hydroxyl-terminated polymer.

2.2.4 Synthetics procedures

2.2.4.1 Synthesis of 9-Anthracenemethyl allyl ether [33]

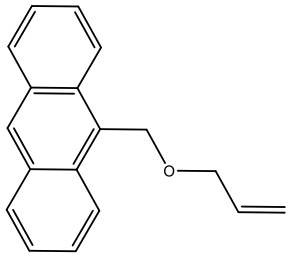

In three neck flask, sodium hydride (1.72 g, 72 mmol) and 9-anthracen methanol (5 g, 24 mmol) in dry THF (50 mL) was mixed and heated under reflux at 70 $^{\circ}$C for 1h. The solution was cooled and allyl bromide (6.22 mL, 72 mmol) was slowly added. After heating under reflux for 24 h, the mixture was cooled and the product was extracted by washing with water and diethyl ether. The residue was chromatographed on silica using mixture of (3:7) of dichloromethane and hexane as the elution. (3.5 g, 70 % yield), ^{1}H NMR 600 MHz ($CDCl_3$) δ 4.2 (2H, d), 5.3-5.5 (4H, m), 6.06 (1H, m), 7.28-8.49 (9H, m, aromatic), GC-MS m/z 248 (M^+).

2.2.4.2 Synthesis of dimethylsulfoxonium chloride[34]

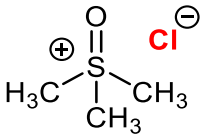

In 2L flask trimethylsulfoxonium iodide (85.6 g, 389 mmol) and benzyltributyl ammonium chloride (130.2 g, 417.4 mmol) were added to the mixture of CH_2Cl_2 (650 mL) and H_2O (840 mL) and stirred for two days in the dark. Then, the aqueous layer was extracted and treated with CH_2Cl_2 (2×80 mL), and evaporated in vacuum. Then, the obtained product was recrystallized using a mixture from MeOH: toluene (95:5), then filtered and dried in a vacuum oven at 40 ^oC (24.6 g, 98.4 % yield).

2.2.4.3 Synthesis of dimethylsulfoxonium methylide.[34]

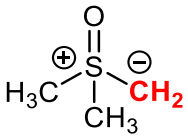

In a three-necked flask connected to a condenser and an argon/vacuum line, 6.8 g of NaH was introduced followed by the addition of 20 g of trimethylsulfoxonium chloride and 200 mL of THF. The entire operation was performed under argon flow. The mixture was heated and refluxed at 70 ^oC until cessation of the gas (4-6 h). After 6 h, the THF was removed under vacuum followed by adding dry toluene. The solution was filtered by dry celite-545 aid (2-3 cm). The flask and filtration cake was washed with 200 mL fresh

toluene. A clear solution with a light yellow color was obtained, which was titrated with a standard HCl aqueous solution (0.73 mmol/mL).

2.2.4.4 Synthesis of furan-protected-maleimide-terminated poly (ε-caprolactone) (PCL_{50}-MI)

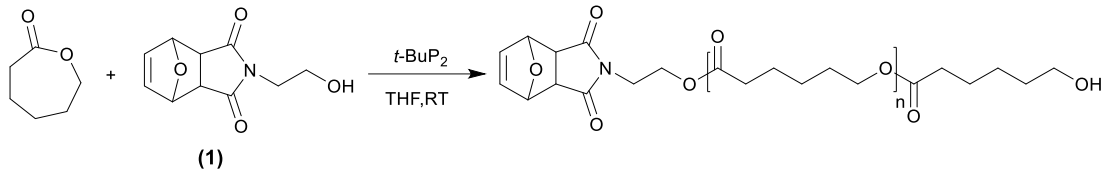

In a 100 mL Schlenk flask, 0.056 g of (**1**), was synthesized as reported in the literature,[35] was added to the reactor and 0.13 mL of *t*-BuP_2 in THF was injected. 6 mL of dry THF and 3 mL of ε-CL monomer were added into the flask. The mixture was kept under stirring for three days followed by quenching with acetic acid. The obtained product was precipitated in cold methanol and dried in a vacuum oven at 40 ^{o}C (1.9 g, 63 % yield, $M_{n,\ NMR}$= 5700 g·mol^{-1}, PDI= 1.10). The values for the ^{1}H NMR (600 MHz, $CDCl_3$) included results: 6.58 ppm (s, 2H, vinyl protons), 5.27 ppm (s, 2H, -C*H*O, bridge-head protons), 4.27 ppm (t, 2H, NCH_2CH_2OC=O), 4.02 ppm (t, CH_2OC=O of polycaprolactone), 3.77-3.64 ppm (m, 4H, NCH_2CH_2OC=O and CH_2OH), 2.85 ppm (s, 2H, C*H*-C*H*, bridge protons), 2.33 ppm (t, C=OCH_2 of polycaprolactone), and 1.63-1.35 ppm (m, CH_2 of PCL).

2.2.4.5 Synthesis of furan-protected-maleimide-terminated polyethylene glycol (PEG_{100}-MI)[36]

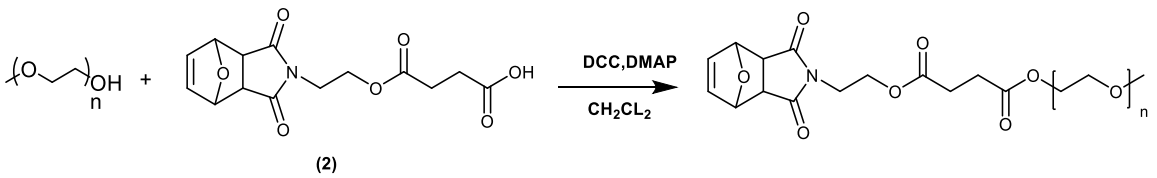

In 250 mL round bottom flask, mPEG (M_n = 4000) (5 g, 1.25 mmol) was dissolved in 20 mL of dry CH_2Cl_2. Maliemide adduct acid (**2**) (1.3 g, 3.75 mmol), was synthesized as reported in the literature,[36] and DMAP (0.15 g, 1.25 mmol) were added into the reaction flask. Then, DCC (0.77 g, 3.75 mmol) was dissolved in 3 mL of CH_2Cl_2 and slowly added to the reaction mixture. After stirring overnight at room temperature, the solution was filtered and the solvent was removed. The residue was precipitated in hexane and dried under a vacuum oven to give a white solid. (4.8 g, 96 % Yield) ^{1}H-NMR (600 MHz, $CDCl_3$) included results: δ= 6.5 (s, 2H, vinyl protons), 5.2 (s, 2H, C*H*CH =CHC*H*, bridge-head protons), 4.2 (m, 4H, NCH_2CH_2OC =O and C =OOCH_2CH_2), 3.9–3.5 (m, OCH_2CH_2, repeating unit of PEG and NCH_2CH_2OC =O), 3.4 (s, 3H, OCH_3, end group of PEG), 2.8 (s, 2H, CH_2NC =OC*H*-C*H*, bridge protons), 2.6 (m, 4H, OC =OCH_2CH_2C =OO). The DP_n of PEG (Aldrich, nominal DP_n = 91) checked by ^{1}H NMR found to be 100. This more accurate DP_n was used to calculate the molecular weight of diblock copolymers and triblock terpolymers.

2.2.4.6 Synthesis of the initiator tri (9-anthracene-methyl propyl ether) borane

1.5 mL (1.5 mmol) of a THF solution of BH_3.THF (1.0 M) was added over 5 min to a toluene solution (3.5 mL, 1.5 g, 6.04 mmol) of 9-anthracene-methyl allyl ether at 0 ^{o}C. The reaction was allowed to reach room temperature over 2 h. The final concentration of the initiator solution in toluene was 0.3 M.

2.2.4.7 Synthesis of anthracene-terminated polymethylene (ant-PM-OH)

(0.95 mL, 0.3 M, 0.29 mmol) of the initiator tri (anthracene-methyl propyl ether) borane was added to the methylide solution (80 mL, 0.75 M, 60 mmol) at 50 ^{o}C. After consumption of methylide, 0.29 g of TAO was added to the solution. Then, the solution

was stirred for 2 h and precipitated in methanol. Finally, the purified polymer was dried in vacuum oven at 50 ^{o}C (0.9 g, 100 % yield, $M_{n,\,NMR}$=1600 g·mol^{-1}, PDI=1.20). ^{1}H NMR (600 MHz, toluene-d_8, 80 ^{o}C) included results: 8.40 ppm (s, ^{1}H, ArH of anthracene), 8.18 ppm (d, 2H, ArH of anthracene), 7.77 ppm (d, 2 H, ArH of anthracene), 7.35–7.28 ppm (m, ArH of anthracene), 5.34 ppm (s, 2H, *O*-*CH*$_2$-anthracene), 3.56 ppm (t, 2H, *CH*$_2$-*O*-*CH*$_2$-anthracene), 1.36 ppm (m, -*CH*$_2$- of PM), and 3.38 ppm (m, 2H, *CH*$_2$-*OH*, end-group of PM).

2.2.4.8 Synthesis of PM$_{100}$-*b*-PEG$_{100}$ and PM$_{100}$-*b*-PCL$_{50}$ copolymers

Ant-PM$_{100}$-OH (0.1 g, 0.062 mmol, $M_{n,\,NMR}$=1600 g·mol^{-1}, 1 equiv.) and PEG$_{100}$-MI (0.18 g, 0.041 mmol, $M_{n,\,NMR}$=4500 g·mol^{-1}, 1.5 equiv.) were dissolved in 25 mL of toluene under Ar. The mixture was refluxed at 110 ^{o}C and kept in the dark for 48 h. The solvent was then evaporated until dryness, the product was dissolved in THF, precipitated in hexane, and dried in vacuum oven at 40 ^{o}C overnight (0.24 g, 70 % yield, $M_{n,\,NMR}$=5600 g·mol^{-1}, PDI=1.14). ^{1}H NMR (600 MHz, toluene-d_8, 80 ^{o}C) included results: 3.54 ppm (m, 4H, *CH*$_2$*CH*$_2$*O* of PEG), 1.40 ppm (m, -*CH*$_2$- of PM).

The Diels-Alder reaction of ant-PM$_{100}$-OH and MI-PCL$_{50}$ targeting PM$_{100}$-*b*-PCL$_{50}$ was performed similarly to that described for the synthesis of PM$_{100}$-*b*-PEG$_{100}$. Toluene was evaporated until dryness; the product was dissolved in THF, precipitated in methanol, and dried in a vacuum oven at 40 ^{o}C overnight (0.20, 50 % yield, $M_{n,\,NMR}$= 6900 g·mol^{-1}, PDI= 1.51). ^{1}H NMR (600 MHz, toluene-d_8, 80 ^{o}C) included results: 4.02 ppm (t, *CH*$_2$*O*- of polycaprolactone), 2.23 ppm (t, *C*=*OCH*$_2$), 1.61-1.26 ppm (m, *CH*$_2$ of polycaprolactone) and 1.40 ppm (m, -*CH*$_2$- of PM).

2.2.4.9 Synthesis of anthracene-terminated block copolymer (ant-PM_{100}-*b*-PLA_{20})

The macroinitiator ant-PM_{100}-OH (0.27 g, 0.173 mmol, $M_{n,\,NMR}$ = 1600 g·mol^{-1}) and D, L-lactide (0.5 g, 3.46 mmol) were dissolved in 15 mL of dry toluene at 90 ^{o}C in a Schlenk flask equipped with a stirring bar under dry Ar. After the polymer was completely dissolved, the catalyst solution (0.02 mL DBU, 0.173 mmol in 1 mL toluene) was added to perform ROP under argon at 90 ^{o}C. After 21 h, the solvent was evaporated; the polymer was precipitated/washed with methanol several times, and dried overnight at 40 ^{o}C in vacuum oven. (0.68 g, 89 % yield, $M_{n,\,NMR}$ = 4500 g·mol^{-1}, PDI= 1.56). ^{1}H NMR results of PM_{100}-*b*-PLA_{20} (600 MHz, toluene-d_8, 80 ^{o}C) include 8.40 ppm (s, ^{1}H, *ArH* of anthracene), 8.18 ppm (d, 2H, *ArH* of anthracene), 7.77 ppm (d, 2H, *ArH* of anthracene), 7.35–7.28 ppm (m, *ArH* of anthracene), 5.34 ppm (s, 2H, *O-CH*$_2$-anthracene), 5.11 ppm (m, 2 CHC=O of LA), 3.56 ppm (t, 2H, *CH*$_2$-*O*-*CH*$_2$-anthracene), 3.40 ppm (m, *2CH3CHC=O* of LA), and 1.42 ppm (m, *CH*$_2$ of PM).

2.2.4.10 Synthesis of PLA_{20}-*b*-PM_{100}-*b*-PEG_{100} and PLA_{20}-*b*-PM_{100}-*b*-PCL_{50} terpolymers via the Diels-Alder reaction

Ant-PM_{100}-*b*-PLA_{20} (0.2 g, 0.044 mmol, $M_{n,\,NMR}$=4500 g·mol^{-1}, 1 equiv) and PEG_{100}-MI (0.13 g, 0.029 mmol, $M_{n,\,NMR}$=4500 g·mol^{-1}, 1.5 equiv.) were dissolved in 25 mL of toluene under Ar. The mixture was refluxed at 110 ^{o}C and stored in the dark for 48 h. The solvent was then evaporated until dryness, the product was dissolved in THF, precipitated in hexane, and dried in a vacuum oven at 40 ^{o}C overnight (0.26 g, 72 % yield, $M_{n,\,NMR}$=8300 g·mol^{-1}, PDI=1.32). ^{1}H NMR (600 MHz, toluene-d_8, 80 ^{o}C) values include 5.17 ppm (m, 2 *CHC=O* of LA), 3.54 ppm (m, 4H, *CH*$_2$*CH*$_2$*O* of PEG), and 1.40 ppm (m, -*CH*$_2$- of PM).

The Diels-Alder reaction of ant-PM_{100}-*b*-PLA_{20} and PCL_{50}-MI targeting PLA_{20}-*b*-PM_{100}-*b*-PCL_{50} was performed similarly to the procedure described for the synthesis of PLA_{20}-*b*-PM_{100}-*b*-PEG_{100}. The solvent was evaporated until dryness, the product was dissolved in THF, precipitated in methanol, and dried in a vacuum oven at 40 ^{o}C overnight (0.25, 60 % yield, $M_{n,\,NMR}$=9500 g·mol^{-1}, PDI=1.64). ^{1}H NMR (600 MHz, toluene-d_8, 80 ^{o}C) values include 5.17 ppm (m, *2 CHC=O* of LA), 4.09 ppm (m, *CH_2OC=O* of PCL), 2.23 ppm (t, *C=OCH_2* of PCL), and 1.42 ppm (m, *CH_2* of PM).

2.3 Results and Discussion

2.3.1 Polymethylene (PM)-based diblock copolymers.

The basic reaction for synthesis of diblock copolymer is given in **Scheme 2.2**.

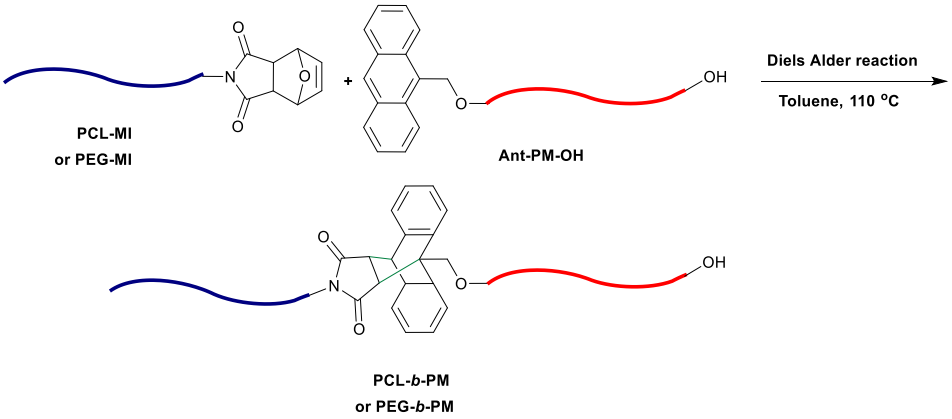

Scheme 2.2 Synthesis of polymethylene-based diblock copolymers via the Diels-Alder coupling.

The α-anthracene-ω-hydroxy polymethylene (ant-PM-OH) was prepared by polyhomologation of sulfoxonium methylide using tri (9-anthracene-methyl propyl ether) borane as the initiator (**Scheme 2.3**) at 50 ^{o}C for 1 h, followed by oxidation with TAO.

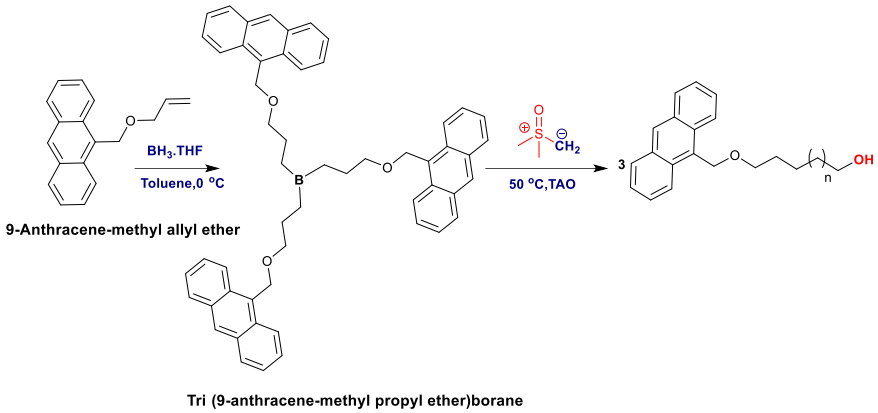

Scheme 2.3 Preparation of α-anthracene ω-hydroxy polymethylene.

The structure of ant-PM-OH was confirmed by ^{1}H NMR and UV-VIS spectroscopy. As shown in **Figure 2.1** all hydrogen atoms of the ant-PM-OH are present in the ^{1}H NMR spectrum, except that of the –OH group (extremely low concentration) and in **Figure 2.2** (upper line) the characteristic five-finger absorbance (350-400 nm) of anthracene is also present. The number-average molecular weight of ant-PM-OH was estimated from the ^{1}H NMR spectrum by comparing the integrated peak of polymethylene (-CH_2-) at 1.40 ppm with the peak of the end-CH_2-OH group at δ= 3.40 ppm, $M_{n,\,NMR}$ = [100 (DP$_n$ of PM) × [14 g·mol^{-1} (M_W of CH_2)] + 248 g·mol^{-1} (M_W of anthracene end-group)] = 1600 g·mol^{-1} close to the theoretical value (**Table 2.1**).

Table 2.1 Characteristic molecular weight data of PM-based copolymers

Entry	Polymer	PDI	$M_{n,\,NMR}$ g·mol^{-1}	$M_{n,\,theo.}$ g·mol^{-1}	DA $_{eff}^{g}$
1	Ant-PM$_{100}$-OH	1.20[a]	1600[b]	1200[c]	—
2	PM$_{100}$-*b*-PEG$_{100}$	1.14[d]	5600[e]	6600[f]	82%
3	PLA$_{20}$-*b*-PM$_{100}$-*b*-PEG$_{100}$	1.32[d]	8300[e]	9500[f]	85%
4	PM$_{100}$-*b*-PCL$_{50}$	1.51[a]	6900[e]	7300[f]	75%
5	PLA$_{20}$-*b*-PM$_{100}$-*b*-PCL$_{50}$	1.64[a]	9500[e]	10200[f]	82%

[a,e] High-temperature SEC, PSt standards. [b] $M_{n,\,NMR}$ of PM homopolymer =14 × DP$_n$ of PM (integrated value of -CH_2- at 1.40 ppm/ integrated value of -CH_2-OH at 3.40ppm). [c] $M_{n,\,theo.}$ of PM homopolymer

was calculated from the ratio of ylide to the initiator. [d] SEC in THF, PS standards, PEG is not stable in HT-SEC. [e] $M_{n,\ NMR}$ of co/terpolymers were calculated by taking into account the ratio of integrated values of PM signals to PCL or PEG signals. [f] $M_{n,\ theo}$= sum of $M_{n,\ NMR}$ of homopolymers. [g] $DA_{\ eff}$. %=[1-(A_t/A_0)] ×100 (A is absorbance at 367 nm).

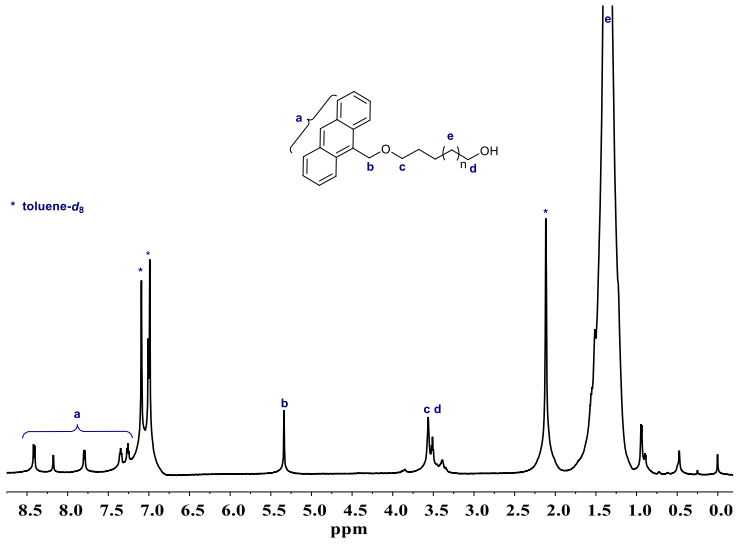

Figure 2.1 ^{1}H NMR spectrum of α-anthracene-ω-hydroxy polymethylene in toluene-d_8 at 80^{o}C (600 MHz)**.**

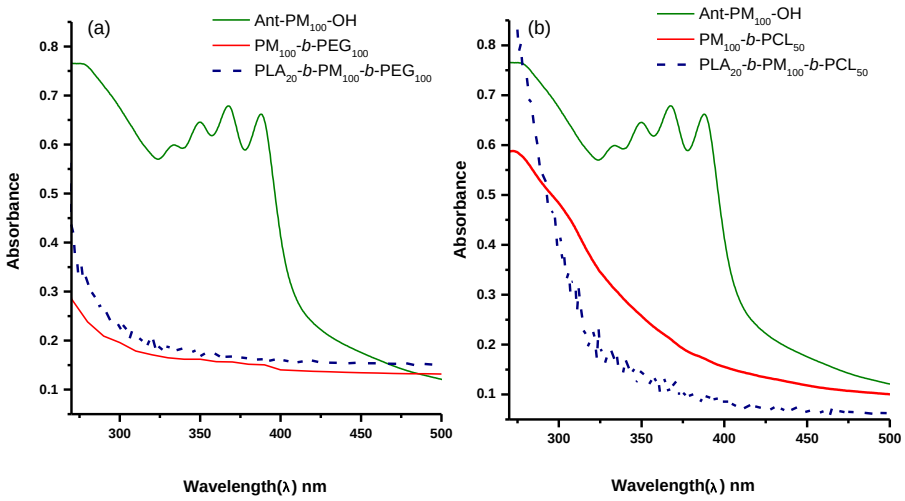

Figure 2.2. UV-VIS spectra of (a) ant-PM_{100}-OH (C_0= 6.2 x 10^{-5} M), PM_{100}-*b*-PEG_{100} (C= 1.5 X10^{-5} M), PLA_{20}-*b*-PM_{100}-*b*-PEG_{100} (C=1.11 x 10^{-5} M), (b) ant-PM_{100}-OH (C_0= 6.2X10^{-5} M), PM_{100}-*b*-PCL_{50} (C=1.36 X 10^{-5} M), and PLA_{20}-*b*-PM_{100}-*b*-PCL_{50} (C=1.03 X 10^{-5} M) in 1, 2-dichloroethane at 80 ^{o}C.

The HT-SEC trace of ant-PM-OH [**Figure 2.3 (A)**] shows a monomodal distribution (PDI= 1.20) with no tail in the lower molecular weight region or any shoulder in the higher molecular weight region. This evidences the successful initiation of the polyhomologation of ylide using this novel borane initiator (**Scheme 2.3**).

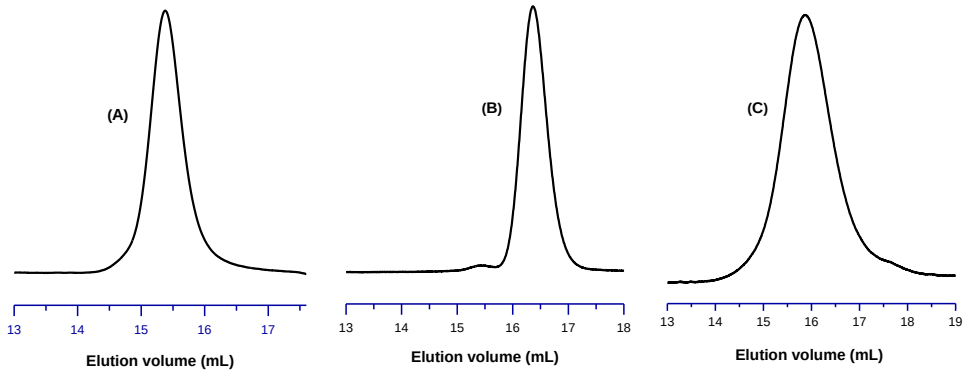

Figure 2.3 SEC traces of (A) ant-PM_{100}-OH from HT-SEC, (B) PEG_{100}-MI from THF-SEC and (C) diblock copolymer PM_{100}-*b*-PEG_{100} from THF-SEC.

The ant-PM_{100}-OH was reacted with furan-protected-maleimide-terminated PCL or PEG to afford PM_{100}-*b*-PEG_{100} and PM_{100}-*b*-PCL_{50} diblock copolymers. The Diels-Alder reaction was monitored by UV-VIS spectroscopy by following the disappearance of the characteristic five-finger absorbance of anthracene (**Figures 2.2**). The HT-SEC chromatograms of PM_{100}-*b*-PEG_{100} (**Figure 2.3(C)**) and PM_{100}-*b*-PCL_{50} copolymers (**Figure 2.4 (C)**) display a monomodal distribution of polymethylene-based diblock copolymers and clearly after the Diels-Alder reaction the chromatogram is shifted to the higher molecular weight region. Furthermore, the ^{1}HNMR spectra of PM_{100}-*b*-PEG_{100} (**Figure 2.5**) and PM_{100}-*b*-PCL_{50} copolymers (**Figure 2.6**) are clear proofs of the target structures of

diblock copolymers, demonstrating the successful performance of the Diels-Alder reaction.

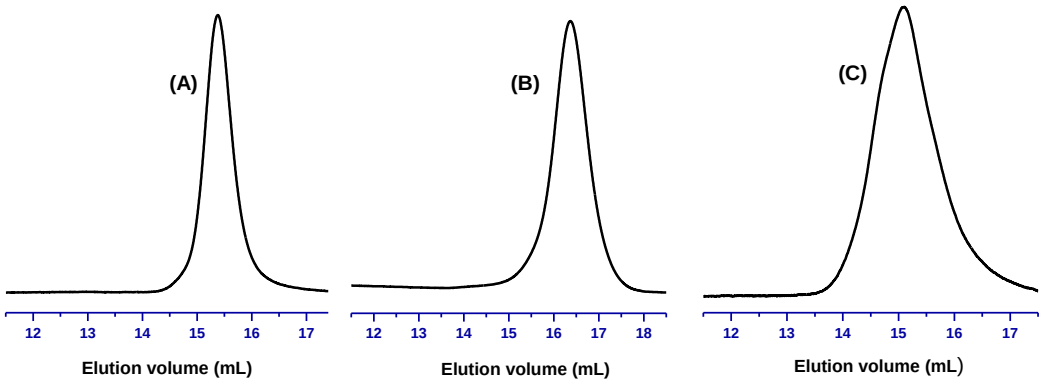

Figure 2.4 SEC chromatograms of (A) ant-PM_{100}-OH, (B) PCL_{50}-MI from THF-SEC and (C) diblock copolymer PM_{100}-*b*-PCL_{50} from HT-SEC.

Figure 2.5 shows the ^{1}HNMR spectrum of PM_{100}-*b*-PEG_{100}, all characteristic proton signals of polyethylene glycol (4H, -CH_2CH_2O-) and polymethylene (2H, -CH_2-) are present. The molecular weight of the PM_{100}-*b*-PEG_{100} copolymer was calculated from the ^{1}H NMR (**Figure 2.5**) by comparing the integrated signal at 1.40 ppm (2H, -CH_2-) with that at 3.54 ppm (4H, -OCH_2CH_2-), $M_{n,\,NMR}$= [100 (DP$_n$ of PEG) × 44 g·mol^{-1} (M_W of CH_2CH_2O)] + [86 (DP$_n$ of PM) × 14 g·mol^{-1}] = 5600 g·mol^{-1}, close to the theoretical value (**Table 2.1**).

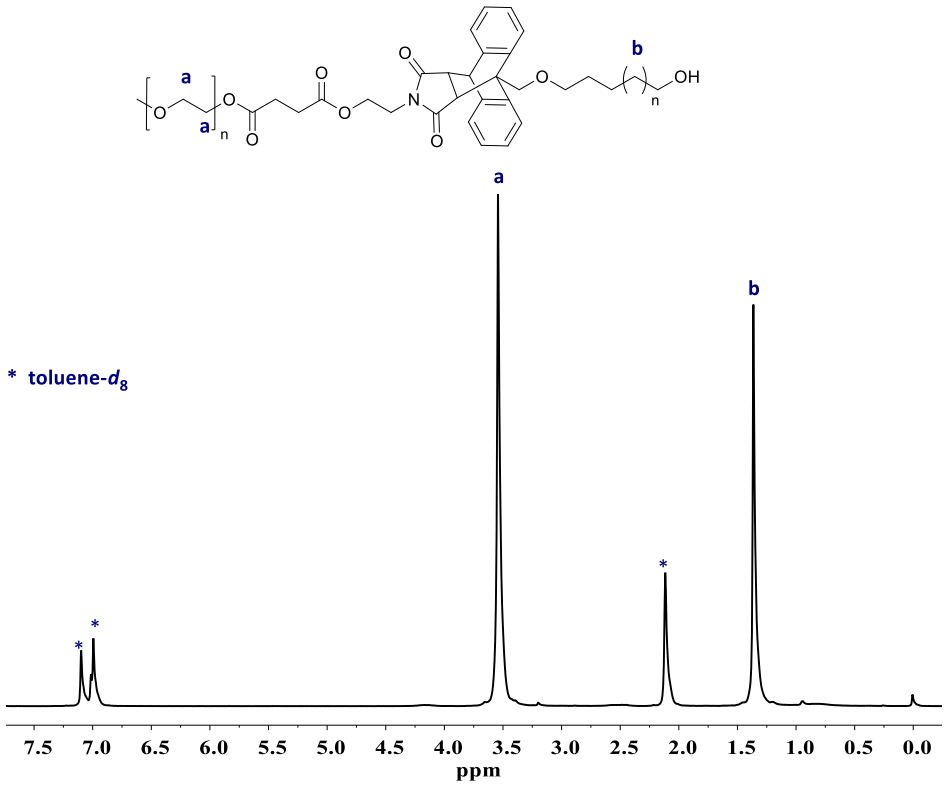

Figure 2.5 ^{1}H NMR spectrum of the diblock copolymer (PM_{100}-*b*-PEG_{100}) in toluene-d_8 at 80 ^{o}C (600 MHz).

The ^{1}H NMR spectrum (**Figure 2.6**) of the obtained diblock PM_{100}-*b*-PCl_{50} shows signals at δ = 1.40 ppm (polymethylene backbone) and at δ = 4.02, 3.56, 1.61-1.26 ppm (protons of poly (ε-caprolactone) PCL). The DP_n of homopolymer PCL, calculated by ^{1}H NMR (**Figure 2.7**) from the ratio of the integrated signal at 4.02 ppm (2H, -$OCH_2C=O$) and the integrated signal for the initiator at 6.58 ppm (2H, -*CH=CH*-) was 50. The molecular weight of the PM_{100}-*b*-PCL_{50} copolymer was calculated from the ^{1}H NMR spectrum (**Figure 2.6**) by comparing the integrated signal at 1.40 ppm with that at 4.02 ppm $M_{n,\,NMR}$ = [50 (DP_{PCL}) × 114.14 g·mol^{-1} (M_W of the repeating unit)] + (87 (DP_{PM} × 14 g·mol^{-1}) = 6900 g·mol^{-1} close to the theoretical value (**Table 2.1**).

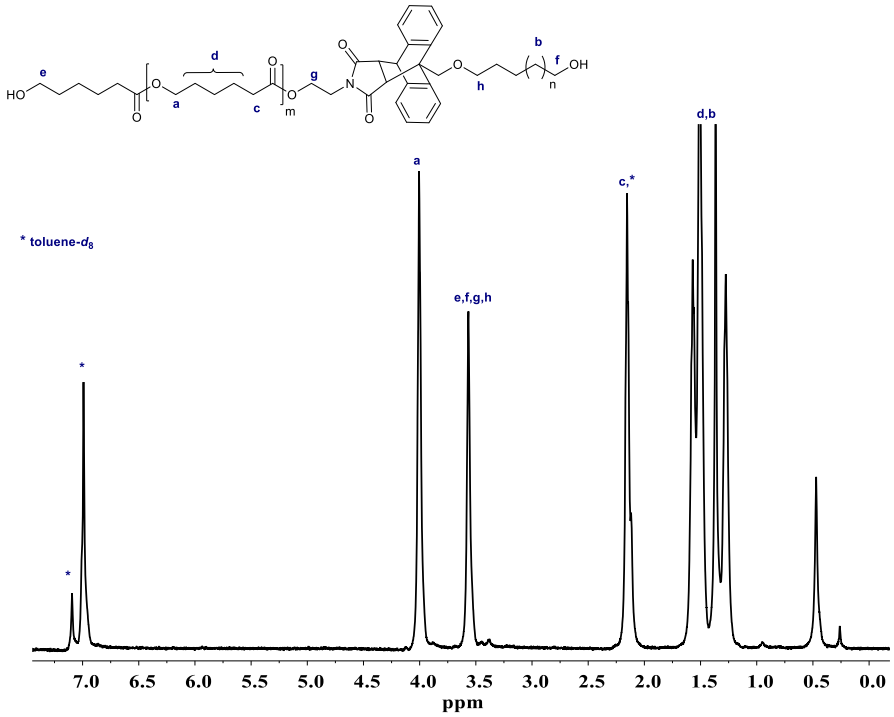

Figure 2.6 ^{1}H NMR spectrum of the diblock copolymer (PM_{100}-*b*-PCL_{50}) in toluene-d_8 at 80 ^oC (600 MHz).

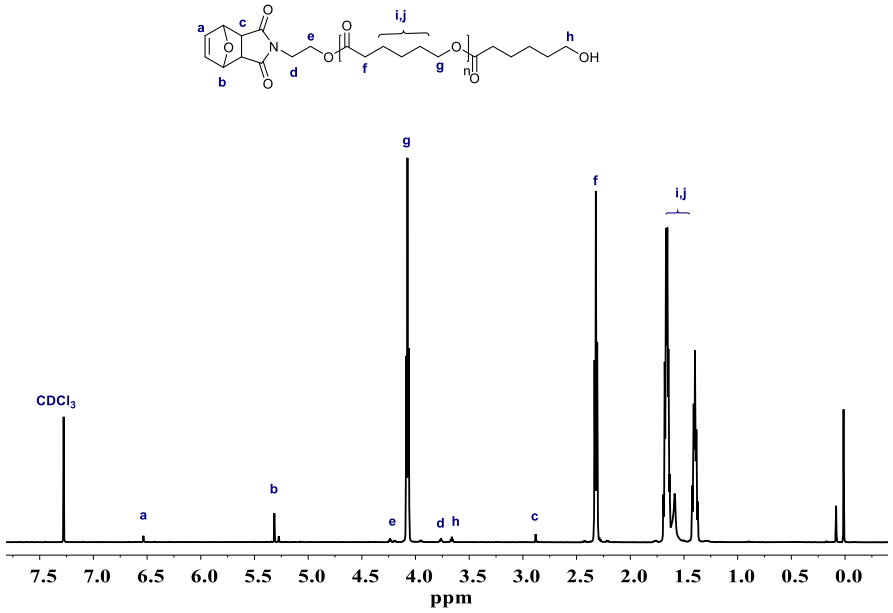

Figure 2.7. The ^{1}H NMR spectrum of furan- protected-maleimide-terminated poly (ε-caprolactone) (PCL_{50}–MI) in $CDCl_3$ (600 MHz).

2.3.2 Polymethylene (PM)-based triblock terpolymers

The basic reactions for synthesis of PM-based triblock terpolymers are given in **Scheme 2.4**.

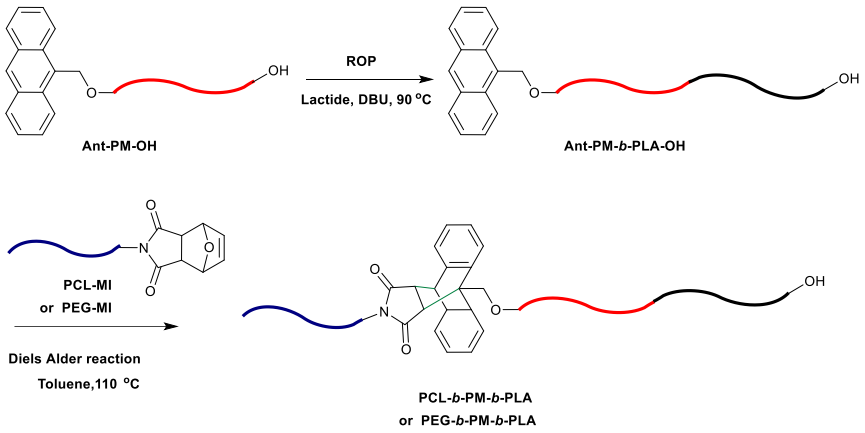

Scheme 2.4 Synthesis of polymethylene-based triblock terpolymers via the Diels-Alder coupling.

The ring opening polymerization (ROP) of D, L-lactide was initiated by ant-PM_{100}-OH with DBU as a catalyst in toluene at 90 °C to give the ant-PM_{100}-*b*-PLA_{20} copolymer. The ^1H NMR spectrum of this polymer shows the characteristic signals of anthracene, of polymethylene at 8.49 - 7.32 ppm, and the polylactide segments (**Figure 2.8**). The DP_n of the PLA, calculated from ^1H NMR by comparing the integrated signals of the main backbone of polylactide (2H, 2 -*CHC=O* of LA) at 5.11 ppm with the signal of the macroinitiator (2H, anthracene -CH_2-*O*-) at 5.34 ppm, was found to be 20. Consequently, the $M_{n,\,NMR}$ of the ant-PM_{100}-*b*-PLA_{20} is 4500 g·mol^{-1} [20 (DP_{PLA} from NMR) × 144.11 g·mol^{-1} + M_n of the macroinitiator ant-PM_{100}-OH (1600 g·mol^{-1})]. Moreover, the HT-SEC chromatogram (**Figure 2.9(A)**) shows a symmetrical shape meaning that the ant-PM-OH initiated system did not show any transesterification reaction.

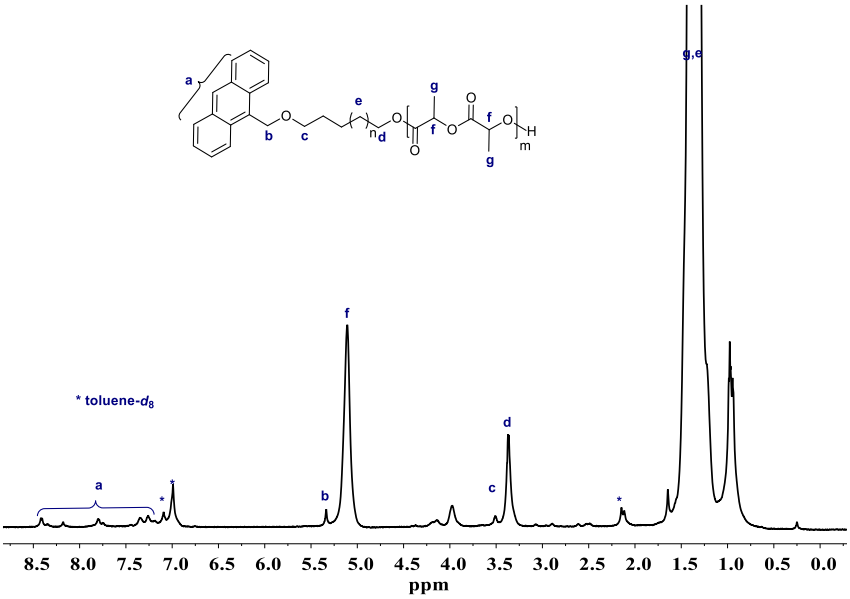

Figure 2.8 ^{1}H NMR spectrum of the diblock copolymer (ant-PM_{100}-*b*-PLA_{20}) in toluene-d_8 at 80 ^{o}C (600 MHz).

The (ant-PM_{100}-*b*-PLA_{20}-OH) copolymer was reacted with the furan-protected-maleimide-terminated linear homopolymer PCL and homopolymer PEG_{100}-MI to yield polymethylene-based triblock (PLA_{20}-*b*-PM_{100}-*b*-PCL_{50}) and (PLA_{20}-*b*-PM_{100}-*b*-PEG_{100}) terpolymers. The Diels-Alder adducts were monitored using UV-VIS spectroscopy by following the disappearance of the characteristic five-finger absorbance of anthracene from 300 to 400 nm (**Figure 2.2**); the Diels-Alder efficiency of terpolymers (DA $_{eff.}$ %) is given in **Table 2.1**.

The HT-SEC chromatograms of terpolymers (PLA_{20}-*b*-PM_{100}-*b*-PEG_{100}) in **Figure 2.9 (C)** and (PLA_{20}-*b*-PM_{100}-*b*-PCL_{50}) in **Figure 2.10 (c)** show monomodal distribution traces shifted to the higher molecular weight region indicating the success of the Diels-Alder reaction.

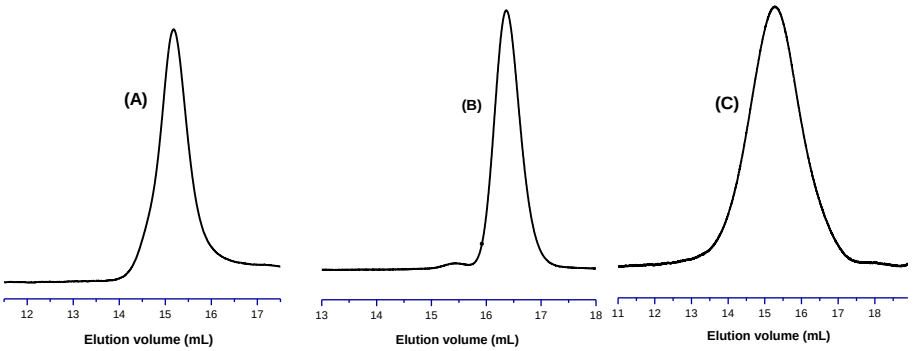

Figure 2.9 SEC traces of (A) ant-PM_{100}-*b*-PLA_{20}-OH from HT-SEC, (B) PEG_{100}-MI from THF-SEC and (C) the triblock terpolymer PLA_{20}-*b*-PM_{100}-*b*-PEG_{100} from THF-SEC.

Figure 2.11 displays the ^{1}H NMR spectrum of (PLA_{20}-*b*-PM_{100}-*b*-PEG_{100}) and all the characteristic proton signals of polymethylene (δ= 1.40 ppm), polyethylene glycol (δ= 3.54 ppm, and polylactide (δ= 5.11 ppm) segments are present. The molecular weight of the PLA_{20}-*b*-PM_{100}-*b*-PEG_{100} terpolymer was calculated from the ^{1}H NMR spectrum (**Figure 2.11**) by comparing the integrated signal at 1.40 ppm with that at 3.54 ppm. The $M_{n,\ NMR}$ of (PLA_{20}-*b*-PM_{100}-*b*-PEG_{100}) terpolymer = [100 (DP_{PEG}) × 44 g·mol^{-1})] + [(72 (DP_{PM}) × 14 g·mol^{-1}) + [20 (DP_{PLA}) × 144.11 g·mol^{-1})] = 8300 g·mol^{-1} close to the theoretical value (**Table 2.1**).

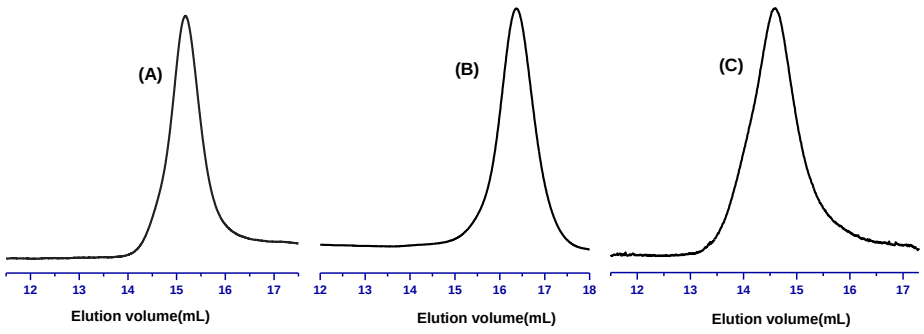

Figure 2.10 HT-SEC chromatograms of (A) ant-PM_{100}-*b*-PLA_{20}-OH, (B) PCL_{50}-MI from THF-SEC and (C) the triblock terpolymer PLA_{20}-*b*-PM_{100}-*b*-PCL_{50} from HT-SEC**.**

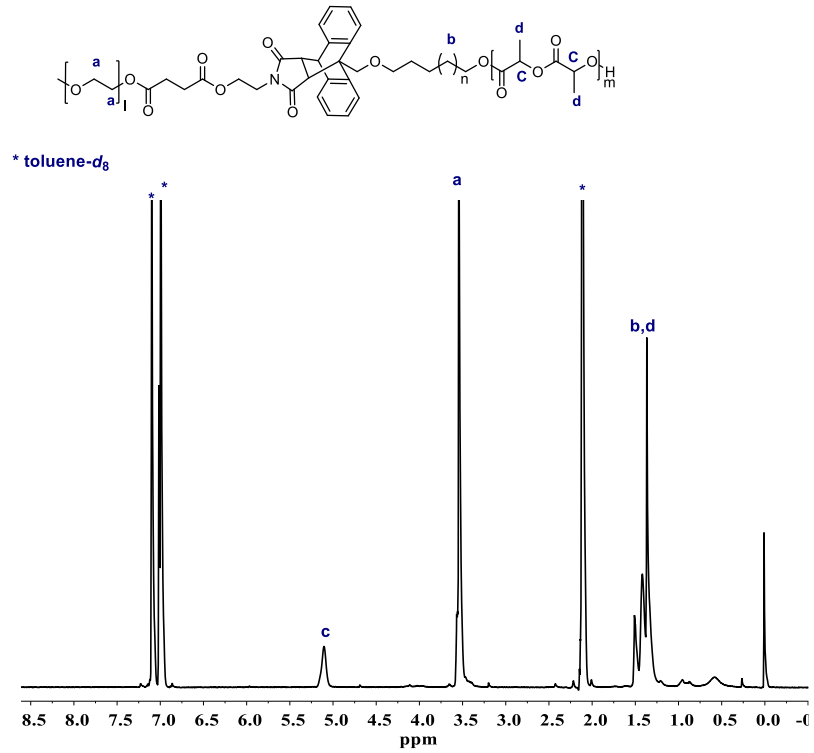

Figure 2.11 ^{1}H NMR spectrum of triblock terpolymer (PLA$_{20}$-*b*-PM$_{100}$-*b*-PEG$_{100}$) in toluene-d_8, 80 ^{o}C, (600MHz).

Similarly, the ^{1}H NMR spectrum (**Figure 2.12**) of (PLA$_{20}$-*b*-PM$_{100}$-*b*-PCL$_{50}$) clearly confirms the structure of the target triblock terpolymer by showing all characteristic signals for the three polymers PCL (δ = 4.02 ppm), PM (δ= 1.40 ppm), and PLA (δ= 5.11 ppm). The $M_{n,\,NMR}$ of the terpolymer = [50 (DP$_{PCL}$) × 114.14 g·mol^{-1}] + [53 (DP$_{PM}$) × 14 g·mol^{-1}] + [20 (DP$_{PLA}$) × 144.11 g·mol^{-1}] = 9500 g·mol^{-1} close to the theoretical value (**Table 2.1**).

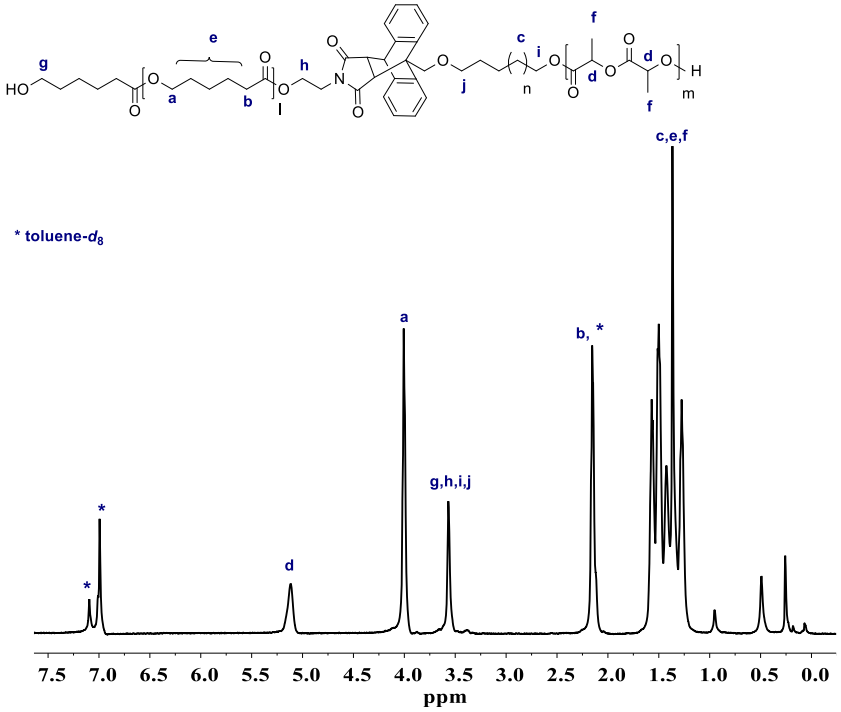

Figure 2.12 ^{1}H NMR spectrum of the triblock terpolymer (PLA_{20}-*b*-PM_{100}-*b*-PCL_{50}) in toluene-d_8 at 80 ^{o}C (600 MHz).

DSC traces of PLA_{20}-*b*-PM_{100}-*b*-PEG_{100} and PLA_{20}-*b*-PM_{100}-*b*-PCL_{50} as well as the corresponding diblock and monoblock precursors are shown in **Figure 2.13**. In all cases the melting point of PM (119-115 ^{o}C) is present and only in the case of the diblock copolymer the PCL or PEG melting point appears. It seems that in the case of triblock copolymer the PCL or PEG trace is absent, maybe due to the triblock structure. This is in accordance with the decrease in crystallinity of PM going from the monoblock to the triblock terpolymer.

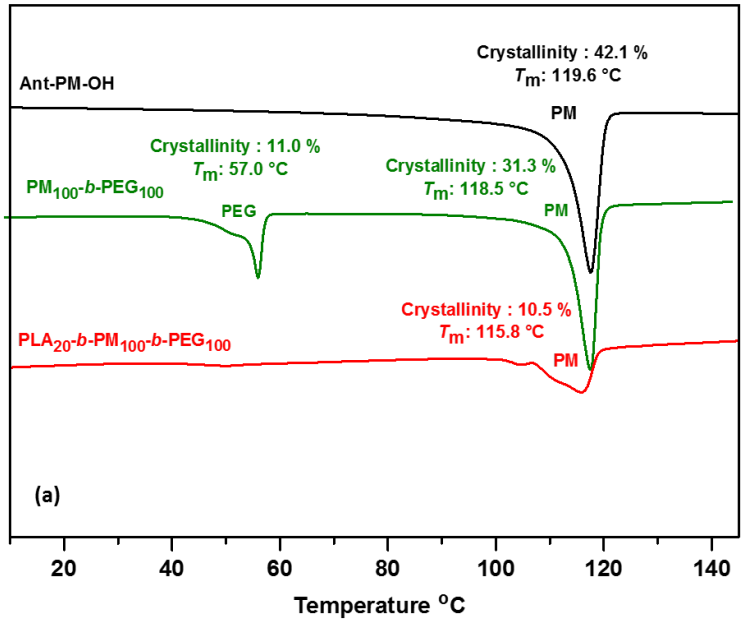

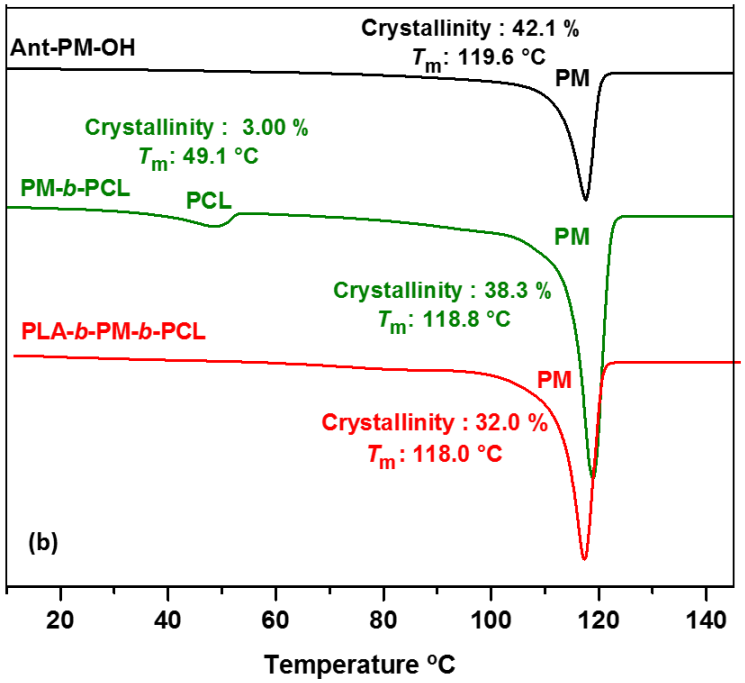

Figure 2.13. DSC curves of (a) ant-PM$_{100}$-OH, PM$_{100}$-*b*-PEG$_{100}$, and PLA$_{20}$-*b*-PM$_{100}$-*b*-PEG$_{100}$ (b) ant-PM$_{100}$-OH, PM$_{100}$-*b*-PCL$_{50}$, and PLA$_{20}$-*b*-PM$_{100}$-*b*-PCL$_{50}$ (N_2 atmosphere, 10 °C/ min, second heating cycle).

2.4. Conclusions

In this work, a simple and effective method for the synthesis of polymethylene-based di/triblock co/terpolymers by combining polyhomologation and furan-protected-maleimide/anthracene Diels-Alder coupling is presented. This method is a general one opening new horizons for the synthesis of well-defined PE-based polymeric materials with complex macromolecular architectures.

2.5. References

(1) Hizal, G.; Tunca, U.; Sanya, A. *J. Polym. Sci., Part A: Polym. Chem.* **2011**, *49*, 4103.
(2) Tasdelen, M. A. *Polym. Chem.* **2011**, *2*, 2133.
(3) Sinnwell, S.; Inglis, A. j.; Davis, T. P.; Stenzel, M. H.; Barner-Kowollik, C. *Chem. Commun.* **2008**, 2052.
(4) Inglis, A. J.; Sinnwell, S.; Stenzel, M. H.; Barner-Kowollik, C. *Angew. Chem. Int. Ed.* **2009**, *48*, 2411.
(5) Durmaz, H.; Karatas, F.; Tunca, U.; Hizal, G. *J. Polym. Sci., Part A: Polym. Chem.* **2006**, *44*, 499.
(6) Durmaz, H.; Dag, A.; Hizal, A.; Hizal, G.; Tunca, U. *J. Polym. Sci., Part A: Polym. Chem.* **2008**, *46*, 7091.
(7) Gacal, B.; Durmaz, H.; Tasdelen, M. A.; Hizal, G.; Tunca, U.; Yagci, Y.; Demirel, A. L. *Macromolecules* **2006**, *39*, 5330.
(8) Dag, A.; Sahin, H.; Durmaz, H.; Hizal, G.; Tunca, U. *J. Polym. Sci., Part A: Polym. Chem.* **2011**, *49*, 886.
(9) Durmaz, H.; Dag, A.; Hizal, G.; Tunca, U. *J. Polym. Sci., Part A: Polym. Chem*. **2010**, *48*, 5083.
(10) Tonga, M.; Cengiz, N.; Kose, M. M.; Dede, T.; Sanyal, A. *J. Polym. Sci., Part A: Polym. Chem.* **2010**, *48*, 410.
(11) Gungor, E.; Hizal, G.; Tunca, U. *J. Polym. Sci., Part A: Polym. Chem*. **2009**, *47*, 3409.
(12) Durmaz, H.; Colakoglu, B.; Tunca, U.; Hizal, G. *J. Polym. Sci., Part A: Polym. Chem*. **2006**, *44*, 1667.
(13) Busch, B. B.; Staiger, Ch. L.; Stoddard, J. M.; Shea, K. J. *Macromolecules* **2002**, *35*, 8330.
(14) Shea, K. J.; Walker, J. W.; Zhu, H.; Paz, M.; Greaves, J. *J. Am. Chem. Soc*. **1997**, *119*, 9049.
(15) Shea, K. J.; Busch, B. B.; Paz, M. *Angew. Chem. Int. Ed*. **1998**, *37*, 1391.
(16) Singh, R. P. *Prog. Polym. Sci*. **1992**, *17*, 251.
(17) Chung, T. C.; Dong, J. Y. *J. Am. Chem. Soc*. **2001**, *123*, 4871.
(18) Xu, G.; Chung, T. C. *J. Am. Chem. Soc*. **1999**, *121*, 6763.
(19) Lu, Y. Y.; Hu, Y. L.; Chung, T. C. *Polymer* **2005**, *46*, 10585.
(20) Kashiwa, N.; Matsugi, T.; Kojoh, S.; Kaneko, H.; Kawahara, N.; Matsuo, S.; Nobori, T.; Imuta, J. *J. Polym. Sci. Part A: Polym. Chem*. **2003**, *41*, 3657.
(21) Baez, J. E.; Hernandez, A. R.; Fernandez, A. M. *Polym. Adv. Technol*. **2010**, *21*, 55.
(22) Han, C. J.; Lee, M. S.; Byun, D. J.; Kim, S. Y. *Macromolecules* **2002**, *35*, 8923.
(23) Iha, R. K.; Wooley, K. L.; Nystrom, A. M.; Burke, D. J.; Kade, M. J.; Hawker, C. J. *Chem. Rev*. **2009**, *109*, 5620.

(24) Briquel, R.; Mazzolini, J.; Bris, T. L.; Boyron, O.; Boisson, F.; Delolme, F.; Agosto, F. D.; Boisson, C.; Spitz, R. *Angew. Chem. Int. Ed*. **2008**, *47*, 9311.
(25) Li, T.; Wang, W. J.; Liu, R.; Liang, W. H.; Zhao, G. F.; Li, Z. Y.; Wu, Q.; Zhu, F. M. *Macromolecules* **2009**, *42*, 3804.
(26) Zhou, X. Z.; Shea, K. J. *Macromolecules* **2001**, *34*, 3111.
(27) Chen, J. Z.; Cui, K.; Zhang, S. Y.; Xie, P.; Zhao, O. L.; Huang, J.; Shi, L. P.; Li, G. Y.; Ma, Z. *Macromol. Rapid Commun*. **2009**, *30*, 532.
(28) Shea, K. J.; C. L. Staiger, C. L.; and S. Y. Lee, S.Y. *Macromolecules* **1999**, *32*, 3157.
(29) Xue, Y.; Lu, H. C.; Zhao, Q. L.; Huang, J.; Xu, S. G.; Caoa, S. K.; Ma, Z. *Polym. Chem*. **2013**, *4*, 307.
(30) Zhang, H.; Alkayal, N.; Gnanou, Y.; Hadjichristidis, H. *Chem. Commun*. **2013**, *49*, 8952.
(31) Li, Q. Z.; Zhang, G. Y.; Chen, J. Z.; Zhao, Q. L.; Lu, H. C.; Huang, J.; Wei, L. H.; D'Agosto, F.; Boisson, C.; Ma, Z. *J. Polym. Sci., Part A: Polym. Chem.* **2011**, *49*, 511.
(32) Lu, H. C.; Xue, Y.; Zhao, Q. L.; Huang, J.; Xu, S. G.; Ma, Z. J. *Polym. Sci., Part A: Polym. Chem.* **2012**, *50*, 3641.
(33) Ciganek, E. *J. Org. Chem*. **1980**, *45,* 1497.
(34) Busch, B. B.; Paz, M. M.; Shea, K. J.; Staiger, C. L.; Stoddard, J. M.; Walker, J. R.; Zhou, X. Z.; Zhu, H. *J. Am. Chem. Soc.* **2002**, *124,* 3636.
(35) Mantovani, G.; Lecolley, F.; Tao, L.; Haddleton, D. M.; Clerx, J.; Cornelissen, J.; Velonia, K. *J. Am. Chem. Soc*. **2005**, *127*, 2966.
(36) Dag, A.; Durmaz, H.; Hizal, G.; Tunca, U.; *J. Polym. Sci. part A: Polym. Chem*. **2008**, *46*, 302.

Chapter 3 Well-Defined Polyethylene-Based Graft Terpolymers By Combining Nitroxide-Mediated Radical Polymerization, Polyhomologation and Azide/Alkyne "Click" Chemistry

(This chapter is reproduced from *Polym. Chem.,* **2016***, 7,* 2986.)

3.1 Introduction

In recent years, there has been increasing interest in graft copolymers because of their compact structure and potential applications.[1,2] Based on the nature of their backbone and side chains they can be used, among other, as compatibilizers, polymeric emulsifier and thermoplastic elastomer.[3,4] There are three general methods to obtain graft copolymers: (a) "grafting through" or "macromonomer strategy", where the macromonomers are copolymerized with conventional monomers;[5] (b) "grafting from", where the branches are produced by polymerization of monomers using backbone initiating sites;[6,7] and (c) "grafting onto", where the branches are attached to the backbone through highly efficient coupling reactions.[8-10]

Recently, a wide range of complex macromolecular architectures were prepared by post-polymerization modifications and ''click'' reactions.[11] The copper (I)-catalyzed azide-alkyne cycloaddition (CuAAC) is one of the most useful and widely employed coupling reactions in polymer chemistry since CuAAC is highly efficient, robust and orthogonal to most functional groups used in polymer synthesis.[12,13] Up to now, various well-defined graft copolymers have been synthesized *via* ''grafting onto'' by combination of CuAAC with ring opening polymerization (ROP),[14,15] atom transfer radical

polymerization (ATRP),[16-18] reversible addition-fragmentation chain transfer (RAFT)[19] and nitroxide-mediated radical polymerization (NMP).[20,21]

Polyethylene-based block copolymers with polystyrene (PSt), polycaprolactone (PCL) and polyacrylate, have attracted significant interest.[22,23] Despite the fact that several well-defined grafts have been synthesized, there are only a few reports so far dealing with polyethylene-based grafts due to the challenge of controlling the molecular weight and functionality of PE.[24-29] Recently, Shea developed a polymerization methodology leading to hydroxyl-terminated polyethylene (polyhomologation). The general reaction scheme involves the formation of an organoboron zwitterionic complex between the dimethylsulfoxonium methylide and the trialkyl borane that breaks down by intramolecular 1,2-migration. As a consequence, a methylene group is randomly inserted one by one into the three branches of the trialkyl borane to give a 3-arm star having boron junction point. The resulting star is subsequently oxidized/hydrolyzed to afford hydroxyl-end-capped linear PEs.[30-33] The hydroxyl-functionalized PE can be used directly as an initiator for (ROP)[34,35] of cyclic ethers/esters or indirectly, after chemical modification, for (ATRP),[36-39] (RAFT)[40] and ring-opening metathesis polymerization (ROMP).[41-43]

In this work, we report the synthesis of novel polyethylene-based graft terpolymers *via* the “grafting onto” strategy by combining NMP, polyhomologation and CuAAC “click” chemistry.

3.2 Experimental information

3.2.1 Materials

Styrene (St, 99%, Acros) and 4-chloromethyl styrene (4-CMS, 90%, Aldrich) were passed through basic alumina before use. ε-Caprolactone (99%, Alfa Aesar) was distilled over CaH_2.Sodium hydride (60% dispersion in mineral oil, Acros) was washed with hexane before use. DMF (99%, Fisher), methanol (99%, Fisher), dichloromethane (>99%, Fisher), hexane (99%, Fisher) were used as received. Tetrahydrofuran (99%, Fisher) and toluene (99.7%, Fluka) were distilled over Na and benzophenone. CuBr (98%, Aldrich) was purified by stirring with acetic acid and washing with methanol and then dried under vacuum. Calcium hydride (CaH_2, 95%, Aldrich), trimethylsulfoxonium iodide (98%, Alfa Aesar), benzyl tri-n-butylammonium chloride (98%, Alfa Aesar) and trimethylamine *N*-oxide dihydrate (TAO, >99%, Fluka), 2, 2, 6, 6-tetramethyl-1-piperidinyloxy (TEMPO, 98%, Aldrich), benzoyl peroxide (BPO, 75%, Aldrich), NaN_3 (99%, Fisher), *N*,*N*,*N*′,*N*′′,*N*′′-pentamethyldiethylenetriamine (PMDETA, 99%, Aldrich), 4-pentynoic acid (95%, Aldrich), triethyl borane (Et_3B, 95%, Aldrich), *N, N*- dimethylpyridin-4-amine (DMAP, 99%, Aldrich), *N*, *N*′-dicyclohexylcarbodiimide (DCC, 99%, Aldrich), *t*-BuP_2 (2.0 M in THF, Aldrich), Merrifield's resin (1% crosslinked chloromethylated PS, Aldrich) and 1-hexyne (97%, Aldrich) were used as received. Dimethylsulfoxonium methylide was prepared as described previously in Chapter 2.

3.2.2 Instrumentation

High-temperature-size exclusion chromatography (HT-SEC) measurements were carried out with the Agilent PL-SEC 220 having one PLgel 10 µm MIXED-B column. 1,2,4-

Trichlorobenzene (TCB) was used as eluent at a flow rate of 1.0 mL/min at 150 ^{o}C. The system was calibrated with PSt standards. SEC measurements at 35 ^{o}C were recorded on a Viscotek TDA 305 instrument equipped with one PLgel 10 µm mixed-C column (only used for $(PSt)_3B$) or two columns, Styragel HR2(7.8×300 mm) and Styragel HR4 (7.8×300 mm). THF was used as eluent at the flow rate of 1 mL/min. The system was calibrated with PSt standards. ^{1}H NMR spectra were recorded on a Bruker AVANCE III-600 spectrometer. Fourier transform infrared spectra (FTIR) were obtained with a Nicolet Magna 6700 FT spectrometer. Differential scanning calorimetry (DSC) was performed on a Mettler Toledo DSC1/TC100 system in an inert nitrogen atmosphere. The second heating curve was used to determine the glass transition temperature (T_g), melting temperature (T_m), and degree of crystallinity.

3.2.3 Synthetics procedure

3.2.3.1 Synthesis of hydroxyl terminated polyethylene (PE-OH)

Into a dried 100 mL round bottom flask equipped with a stirrer, a solution of dimethylsulfoxonium methylide in toluene (84 mL, 0.96 mmol/mL, 81 mmol) was introduced by syringe under argon and heated to 50 ^{o}C, followed by the addition of 0.26 mL of trie thyl borane (1 M, 0.26 mmol). After 15 min a sample of the reaction mixture was taken and added to water to measure the pH of the solution. Since the pH was neutral, meaning that all methylide monomer was consumed, TAO (0.28 g) was added to the solution under argon. After 3 hours the solvent was removed under reduced pressure and the polymer was precipitated in methanol and dried under vacuum. (1.2 g, 100 %

yield, $M_{n,\ NMR}$= 2030 g·mol^{-1}). ^{1}H NMR (600 MHz, toluene-d_8, 80 ^{o}C) included results: 3.38 ppm (t, 2H, CH_2-OH, end-group of PE), 1.36 ppm (m, 2H, -CH_2-, the backbone of PE).

3.2.3.2 Synthesis of OH-terminated polyethylene-*b*-polycaprolactone (PE-*b*-PCL-OH)

0.71 g of the macroinitiator PE-OH ($M_{n,\ NMR}$ = 2030 g.mol^{-1}, 0.35 mmol) was dissolved in 3 mL of hot toluene (80 ^{o}C) followed by addition of 4 mL of ε-caprolactone (35 mmol), and 0.1 mL of catalyst solution *t*-BuP_2 (2 M in THF, 0.35 mmol) to perform ROP under argon at 80 ^{o}C. The polymerization was kept at 80 ^{o}C for 15 h and quenched by acetic acid (0.5 mL). The obtained copolymer was precipitated in methanol and dried under vacuum (2.3 g, 47 % yield, $M_{n,\ NMR}$ = 4800 g·mol^{-1}). ^{1}H NMR (600 MHz, toluene-d_8, 80 ^{o}C) included results: 4.02 ppm (t, CH_2O- of PCL), 3.38 ppm (t, 2H, CH_2-OH, end-group of PCL) 2.23 ppm (t, C=OCH_2 of PCL), 1.61-1.26 ppm (m, CH_2 of PCL), 1.40 ppm (m, -CH_2- of the PE backbone).

3.2.3.3 Synthesis of alkyne-terminated polyethylene-*b*-polycaprolactone (PE-*b*-PCL-alkyne)

PE-*b*-PCL-alkyne was synthesized by reacting PE-*b*-PCL-OH with 4-pentynoic acid in the presence of DCC and DMAP. 2.2 g of PE-*b*-PCL-OH ($M_{n,\ NMR}$ = 4800 g·mol^{-1}, 0.45 mmol) was dissolved in 15 mL of freshly distilled toluene followed by addition of 4-pentynoic acid (0.45 g, 4.5 mmol), DCC (1.3 g, 4.5 mmol) and DMAP (0.1 g, 0.9 mmol). The reaction was kept under stirring at 80 ^{o}C for 24 h. The white solid formed during the esterification was removed by filtration. The filtrate was precipitated in methanol twice giving a white solid product. The resulted PE-*b*-PCL-alkyne (2.1 g, 95 % yield, $M_{n,\ NMR}$ =

4900 g·mol^{-1}) was characterized by HT-SEC, ^{1}H NMR and FTIR. ^{1}H NMR (600 MHz, toluene-d_8, 80 ^{o}C) included results: 4.02 ppm (t, CH_2O- of PCL), 2.30-2.25 ppm (alkyne-CH_2-CH_2-CO-O-). 2.20 ppm (t, C=OCH_2 of PCL), 1.61-1.26 ppm (m, CH_2 of PCL), 1.40 ppm (m, -CH_2- of PE backbone).

3.2.3.4 Copolymerization of St and 4-CMS to synthesize poly (styrene-*co*-chloro methyl styrene) (poly(St-*co*-4-CMS)) under NMP conditions

Poly(St-*co*-4-CMS) was prepared *via* NMP of styrene and 4-CMS at 125°C. In a 50 mL of Schleck tube, St (5.0 mL, 0.047 mmol), 4-CMS (2.84 mL, 0.200 mmol), TEMPO (0.127 g, 0.8 mmol), BPO (0.151 g, 0.620 mmol) were added, the reaction mixture was degassed by three FPT cycles. The tube was placed in a thermostatic oil bath at 125 ^{o}C for 17 h, the polymerization mixture was precipitated in methanol and dried for 24 h in a vacuum oven at 30°C (2.5 g, 32 % yield, $M_{n,\,NMR}$ = 9950 g·mol^{-1}). The random copolymer contains 25 CMS units, as determined by ^{1}H NMR in $CDCl_3$, and is labeled as poly (St-*co*-4-CMS)-25 in this text. Another copolymerization was carried out using the following monomers and initiator feed: St (5 mL, 0.047 mmol), CMS (6.6 mL, 0.047 mmol), TEMPO (0.22 g, 0.940 mmol) and BPO (0.19 g, 0.940 mmol) under same conditions. The copolymer was precipitated in methanol and dried for 24 h in a vacuum oven at 30 °C (5.0 g, 43 % yield, $M_{n,\,NMR}$ = 15400 g·mol^{-1}). This copolymer contains 55 4-CMS units, as analyzed by ^{1}H NMR, and is labeled poly(St-*co*-4-CMS)-55. A typical ^{1}H NMR spectrum of the copolymers (600 MHz, $CDCL_3$) shows the following peaks: 6.5-7.5 ppm (m, 9H, Ar*H* of PSt and P (4-CMS)), 4.5 ppm (s, 2H, Ph-*CH2*-Cl, P (4-CMS)), 2.2-0.6 ppm (m, 2H, aliphatic protons).

3.2.3.5 Synthesis of poly (styrene-*co*-azido methyl styrene) (poly (St-*co*-4-AMS))

1 g of poly (St-*co*-4-CMS)-25 or 1.5 g poly (St-*co*-4-CMS)-55 was dissolved in DMF (15 mL), followed by addition of sodium azide (0.61 g, 9.400 mmol). The mixture was stirred at room temperature overnight. The obtained polymers poly(St-*co*-4-AMS) were precipitated in methanol and dried in vacuum oven at 25 ^{o}C. The following results were obtained: poly(St-*co*-4-AMS)-25 (0.95 g, 95 % yield, $M_{n,\,NMR}$ = 10200 g·mol^{-1}) and poly(St-*co*-4-AMS)-55 (1.2 g, 80 % yield, $M_{n,\,NMR}$ = 15800 g·mol^{-1}) in this work. A typical ^{1}H NMR spectrum (600 MHz, $CDCL_3$) includes the following peaks: 6.5-7.5 ppm (m, 9H, Ar*H* of PSt and P (4-CMS)), 4.23ppm (s, 2H, Ph-CH_2-N_3, P (4-CMS)), and 2.2-0.6 ppm (m, 2H, aliphatic protons).

3.2.3.6 "Click" grafting of PE-*b*-PCL-alkyne chains onto the azide-containing polymeric backbone

Poly (St-*co*-4-AMS)-25 and poly (St-*co*-4-AMS)-55 were reacted with PE-*b*-PCL-alkyne in the presence of CuBr and PMDETA in toluene at 80 ^{o}C. Typical "click" grafting reactions are as follows. The azido-functionalized backbone poly(St-*co*-4-AMS)-25 (0.05 g, 0.0043 mmol, 1equiv of azide group), the ω-alkyne-functionalized branches PE-*b*-PCL-alkyne (0.4 g, 0.086 mmol, 20 equiv of alkyne group) and CuBr (0.012 g, 0.086 mmol) were added into a 100 mL Schlenk flask followed by addition of 6 ml of deoxygenated toluene. Then, deoxygenated PMDETA (15 µL, 0.086 mmol) was added with an argon-purged syringe. In another experiment, deoxygenated PMDETA (17 µL, 0.098 mmol) was introduced with an argon-purged syringe to the backbone solution poly(St-*co*-4-AMS)-55 (0.05 g, 0.0028 mmol, 1equiv of azide group), PE-*b*-PCL-alkyne (0.5 g, 0.098 mmol, 35

equiv of alkyne group) and CuBr (0.015 g, 0.098 mmol) in 6 mL dry toluene. The two mixtures were degassed by three freeze-thaw-purge (FTP) cycles and stirred under argon at 80 ^{o}C for 6h. The unreacted azide units were reacted with 1-hexyne until the FTIR absorption of azide group completely disappeared. The obtained graft terpolymer solutions were passed through neutral alumina columns to remove the copper, then precipitated in methanol and dried under vacuum at room temperature. The obtained graft terpolymers were washed with acetone to remove unreacted polystyrene and successfully treated with Merrifield's resin-azide to remove unreacted PE-*b*-PCL-alkyne. Graft terpolymers synthesized from the backbone with 25 units of azide groups (0.15 g, 33 % yield) are designated as PSt-*g*-(PCL-*b*-PE)-1 and those from 55 units (0.2 g, 40 % yield) as PSt-*g*-(PCL-*b*-PE)-2. A typical ^{1}H NMR spectrum (600 MHz, toluene-d_8, 80 ^{o}C) for graft terpolymers gives the following results: 7.50 ppm (s, 1H, C*H*=C triazole ring), 6.5-7.3 ppm (m, 9H, Ar*H* of PSt and P (4-CMS)), 5.14 ppm (s, 2H, Ph-CH_2-triazole), 4.02 ppm (t, CH_2O- of PCL), 3.86 ppm (t, 2H, -CH_2-OCO-, PCL-*b*-PE), 2.71 ppm (2H, -CH_2CH_2- triazole), 1.61-1.26 ppm (m, 2H, aliphatic protons CH_2 of PCL, PS and PE).

3.2.3.7 Synthesis of Merrifield's resin-azide[44]

Merrifield's resin (1 g, 1 mmol) was suspended in DMF (30 mL), and (2.6 g, 40 mmol) sodium azide was added to the mixture. The reaction mixture was stirred overnight at 80 ^{o}C, then filtered, washed with distilled water, methanol, and acetone to give Merrifield's resin with methyl-azido functionalities and dried in vacuum oven at 25 ^{o}C.

3.2.3.8 General procedure for the treatment of graft terpolymers with Merrifield's resin-azide to remove the unreacted PE–*b*-PCl–alkyne copolymer [44]

The crude graft terpolymers PSt-*g*-(PCL-*b*-PE) were dissolved in toluene in a Schlenk tube. 20 eq. of CuBr and PMDETA were added to the solution followed by addition of 0.1 g of Merrifield's resin-azide. The mixture was degassed by three freeze-pump-thaw (FTP) cycles and stirred under argon at 80 ^{o}C for 2 days. The obtained polymers were passed through a neutral alumina column to remove the copper and then precipitated in methanol and dried under vacuum at room temperature.

3.3 Results and discussion

3.3.1 Synthesis of PE-*b*-PCL-alkyne

The synthetic route for the alkyne-terminated PE-*b*-PCL-alkyne is illustrated in **Scheme 3.1.** Hydroxyl terminated polyethylene (PE-OH) was synthesized *via* polyhomologation of dimethylsulfoxonium methylide using triethylborane as the initiator followed by oxidation with TAO. The PE-OH was then used as a macroinitiator to polymerize *ε*-caprolactone in the presence of phosphazene base *t*-BuP_2 as a catalyst. Alkyne side groups were attached on the polymeric chain by esterification of the hydroxyl groups of PE-*b*-PCL-OH with 4-pentynoic acid. The molecular characteristics of PE-OH, PE-*b*-PCL-OH and PE-*b*-PCL-alkyne are listed in **Table 3.1**.

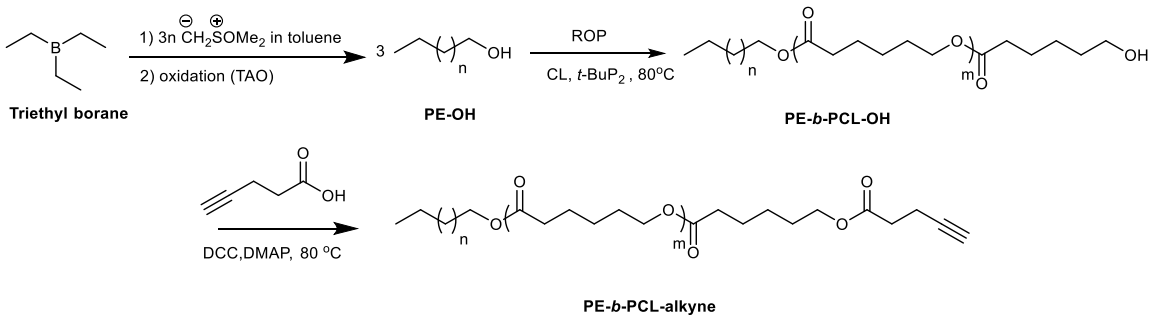

Scheme 3.1. Synthetic route for PE-*b*-PCL-alkyne copolymers.

Table 3.1 Molecular characteristics of PE-OH, PE-*b*-PCL-OH and PE-*b*-PCL-alkyne copolymers

No.	Polymers	$M_{n,SEC}$[a] (g·mol^{-1})	PDI [a]	$M_{n,NMR}$ (g·mol^{-1})
1	PE-OH	2150	1.12	2030[b]
2	PE-*b*-PCL-OH	3850	1.19	4800[c]
3	PE-*b*-PCL-alkyne	4000	1.16	4900[c]

[a] High- temperature SEC, PSt standards. [b] $M_{n,NMR}$ of PE homopolymer =14 × DP_n of PE (integrated value of -CH_2-at 1.40 ppm/ integrated value of -CH_2-OH at 3.40 ppm). [c] $M_{n,NMR}$ of copolymers were calculated from ratio of integrated values of signals at δ = 1.20-1.40 ppm to signal at δ = 4.02 ppm.

As revealed by the HT-SEC traces (**Figure 3.1**) PE-OH, PE-*b*-PCL-OH and PE-*b*-PCL-alkyne polymers showed monomodal and narrow distributions. The success of the different synthetic steps was confirmed by FTIR spectroscopy (**Figure 3.2**). After the ROP of *ε*-caprolactone by using PE-OH (**Figure 3.2** (a)) as the macroinitiator the characteristic absorption peak of the ester groups of PCL at 1730 cm^{-1} was appeared (**Figure 3.2** (b)). In the case of PE-*b*-CL-alkyne (**Figure 3.2** (c)), the broad band of hydroxyl group (3200-3600 cm^{-1}) disappeared and the characteristic absorption peaks of alkyne group appeared at 3300 cm^{-1}.

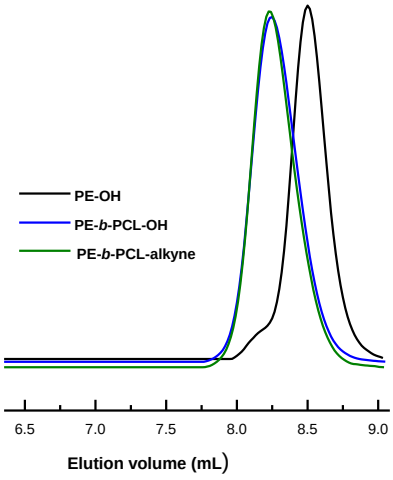

Figure 3.1 HT-SEC chromatograms of PE-OH, PE-*b*-PCL-OH and PE-*b*-PCL-alkyne in 1,2,4-trichlorobenzene at 150 °C.

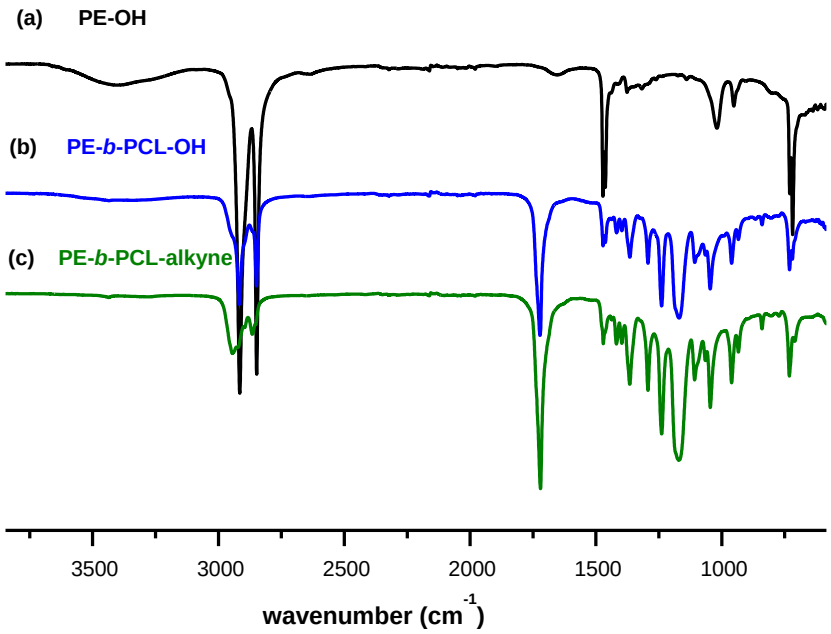

Figure 3.2 IR spectra of PE –OH, PE-*b*-PCL-OH and PE-*b*-PCL-alkyne.

The successful synthesis of PE-OH and PE-*b*-PCL-OH was also confirmed by ^{1}H NMR (**Figure 3.3** (a) and (b)), where all characteristic fingerprints of PE-OH and PCL are present. The ^{1}H NMR spectrum of the resulting product PE-*b*-PCL-alkyne (**Figure 3.3** (c)) revealed that the esterification of PE-*b*-PCL-OH proceeded practically quantitatively as confirmed by the presence of the new peaks at δ = 2.24-2.28 ppm corresponding to the two methylene groups close to alkyne end group (alkyne-CH_2-CH_2-CO-O-). The peak of the –OH at δ = 3.38 ppm of PE-*b*-PCL-OH (**Figure 3.3** (b)) completely disappeared and a new peak at δ = 3.90 ppm (**Figure 3.3** (c)) corresponding to the ester group, overlapped by the peak of PCL at δ = 4.00 ppm, appeared.

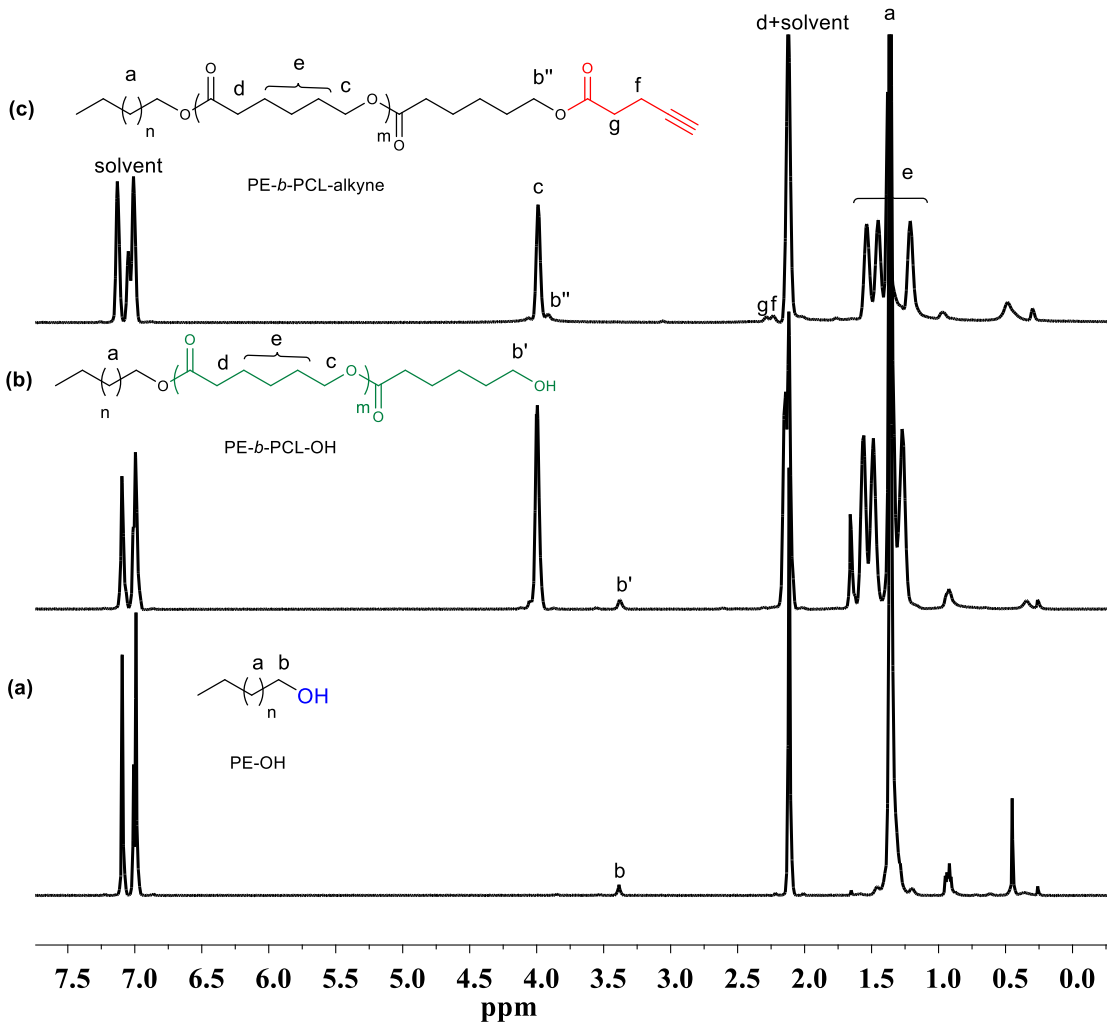

Figure 3.3 ^{1}H NMR spectra (a) PE-OH, (b) PE-*b*-PCL-OH and (C) PE-*b*-PCL-alkyne in toluene-d_8 at 80 ^{o}C (600 MHz).

The melting points were determined from the DSC traces (**Figure 3.4**) to be 110.59 ^{o}C (PE-OH) and 110.3 and 54.4 ^{o}C corresponding to the PE and PCL blocks of PE-*b*-PCL-OH.

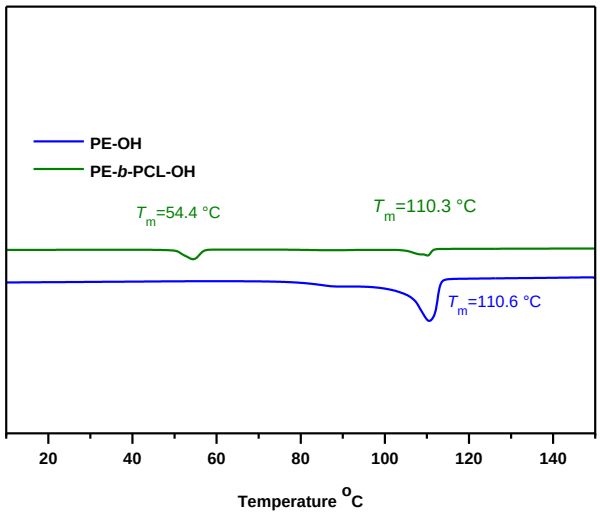

Figure 3.4 DSC traces of PE–OH and PE-*b*-PCL-OH (N_2 atmosphere, 10 ^{o}C/ min, second heating cycle).

3.3.2 Synthesis poly(St-*co*-4-CMS) and poly(St-*co*-4-AMS)

TEMPO-mediated copolymerization of styrene (St) and 4-chlormethylstyrene (4-CMS) was carried out in bulk in the presence of peroxide (BPO) as initiator at 125 ^{o}C (**Scheme 3.2**). Two of copolymers with different molecular weights and number of 4-CMS units were synthesized by the different molar ratio between monomer to TEMPO. A typical ^{1}H NMR spectrum of poly (St-*co*-4-CMS) is given in **Figure 3.5** (a). The characteristic signals at 6.30-7.50 ppm were assigned to aromatic protons of St and 4-CMS, peak at 4.50 ppm was attributed to the benzylic chloride (ph-CH_2-Cl) in 4-CMS unit and the signal at 0.90 ppm was assigned to the four methyl protons of TEMPO indicated the copolymers were end-capped with TEMPO. The composition of copolymers was determined using ^{1}H NMR and the mole fractions of St and 4-CMS were calculated from the ratio of the signal at 4.50 ppm to the total area between 6.30-7.50 ppm. The number average molecular weights ($M_{n,\ NMR}$) determined by ^{1}H NMR and the results are shown in **Table 3.2**.

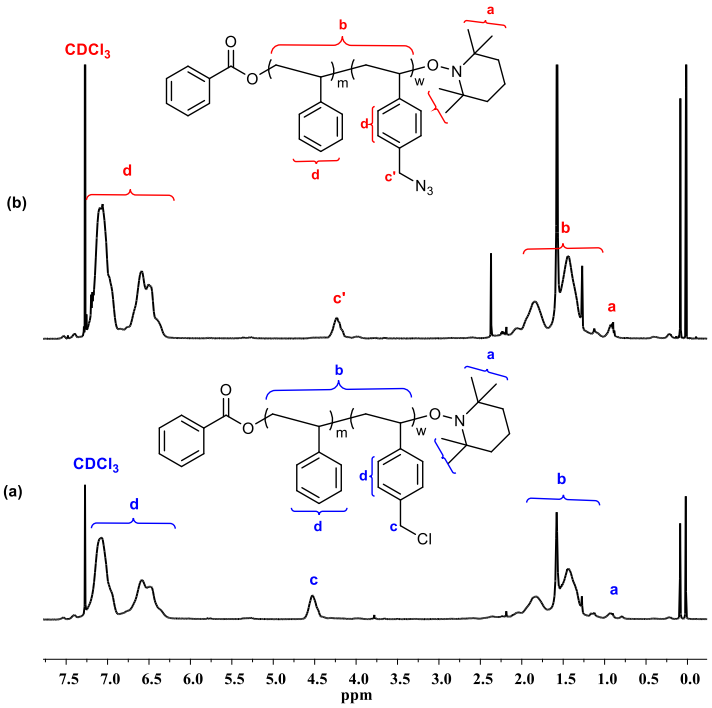

Figure 3.5 ^{1}H NMR spectra (a) poly (St-*co*-4-CMS) and (b) poly (St-*co*-4-AMS) in $CDCl_3$ (600 MHz).

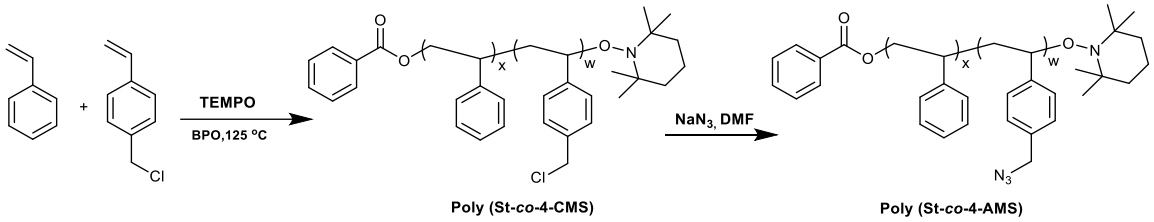

Scheme 3.2 Synthetic route to prepare poly(St-*co*-4-CMS) and poly(St-*co*-4-AMS)

Table 3.2 Molecular weights of the backbone polymers at various stages.

	Poly (St-*co*-4-CMS)			Poly (St-*co*-4-AMS)			
No.	**Feed ratio St/CMS[a]**	**$M_{n,\ SEC}$[b] ($g \cdot mol^{-1}$)**	**PDI[b]**	**$M_{n,\ NMR}$[c] ($g \cdot mol^{-1}$)**	**$M_{n,\ SEC}$[b] ($g \cdot mol^{-1}$)**	**PDI[b]**	**$M_{n,\ NMR}$[c] ($g \cdot mol^{-1}$)**
1	65/35	10600	1.15	9950	11600	1.13	10200
2	47/53	15900	1.32	15400	17900	1.29	15800

[a] Feed ratio of St and 4-CMS = $M_{n,\ SEC}$ x (composite of CMS or AMS were calculated from the ratio of the signal at 4.50 or 4.22 ppm to the total area between 6.30-7.50 ppm)/M_w of CMS. [b] SEC in THF as the eluent and PSt-based calibration. [c] $M_{n,\ NMR}$ of copolymers were calculated from the ratio of integrated values of signal at 0.9 ppm to the signals at 4.50 or 4.22 ppm and signal at 6.50 ppm.

The SEC-THF traces in **Figure 3.6** showing the monomodal distribution demonstrated the successful transformation of chlorides to azide groups and indicated that was no change of apparent molecular weight between poly (St-*co*-4-CMS) and poly (St-*co*-4-AMS). According to **Scheme 3.2**, the pendent chlorides of poly (St-*co*-4-CMS) can be converted into azide groups by reaction with the excess of NaN_3 in DMF overnight at room temperature to yield poly (St-*co*-4-AMS). ^1H NMR (**Figure 3.5**) proves that the substitution of the pendent chloride groups into azide groups is quantitative. The typical FTIR spectra of the starting copolymer and the product after reaction with NaN_3 are presented in **Figure 3.7**. A strong absorbance peak was observed at 2104 cm^{-1} related to the azide group.

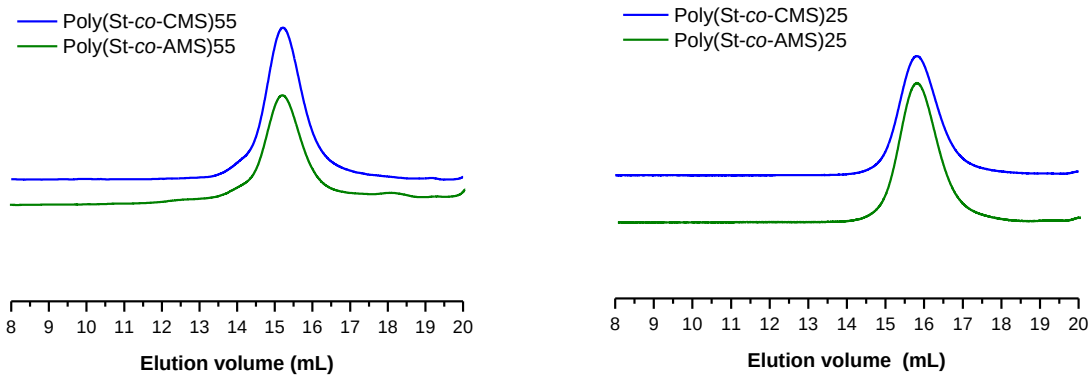

Figure 3.6 SEC-THF traces of (a) poly(St-*co*-4-CMS)-25, poly(St-*co*-4-AMS)-25 and (b) poly(St-*co*-4-CMS)-55, poly(St-*co*-4-AMS)-55 in THF at 35 ^oC.

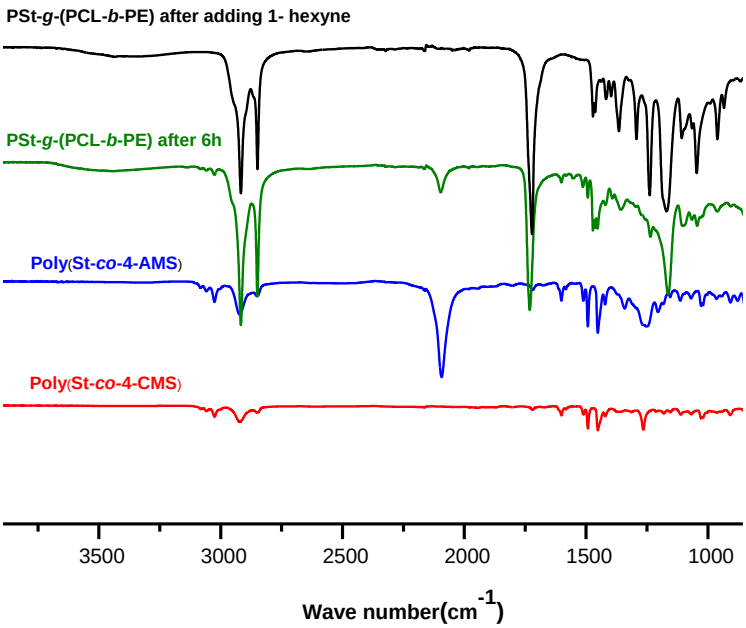

Figure 3.7 IR spectra of (a) poly(St-*co*-4-CMS), (b) poly(St-*co*-4-AMS), (c) PSt-*g*-(PCL-*b*-PE) before and (d) after adding 1-hexyne.

3.3.3 Synthesis of graft terpolymers PSt-*g*-(PCL-*b*-PE) by CuAAC ''click'' reaction

The graft terpolymers were synthesized by coupling the alkyne-terminal groups of PE-*b*-PCL-alkyne with the side azido-groups of the two backbones, poly (St-*co*-4-AMS)-25 and poly (St-*co*-4-AMS)-55, using the PMDETA/CuBr catalytic system in toluene at 80 $^{\circ}$C (**Scheme 3.3**). After 6 h, 1-hexyne was added to react with the unreacted azide group. The graft terpolymers were purified using Merrifield's resin–azide to remove unreacted PE-*b*-PCL-alkyne.

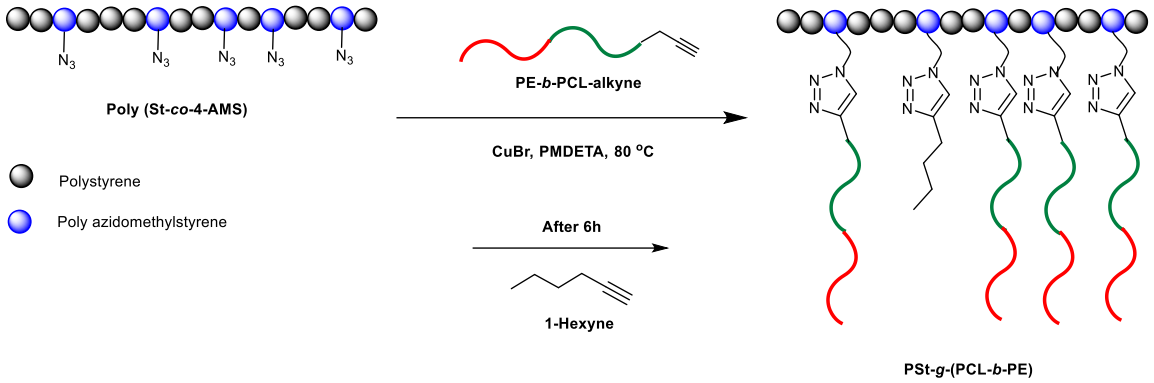

Scheme 3.3 Synthetic route for PSt-*g*-(PCL-*b*-PE) graft terpolymers *via* CuAAC.

As shown in **Figure 3.8**, the HT-SEC traces of graft terpolymers shifted to a higher molecular weight compared to that of precursor polymers, PE-*b*-PCL-alkyne and poly (St-*co*-4-AMS), indicating the successful synthesis of grafted terpolymers.

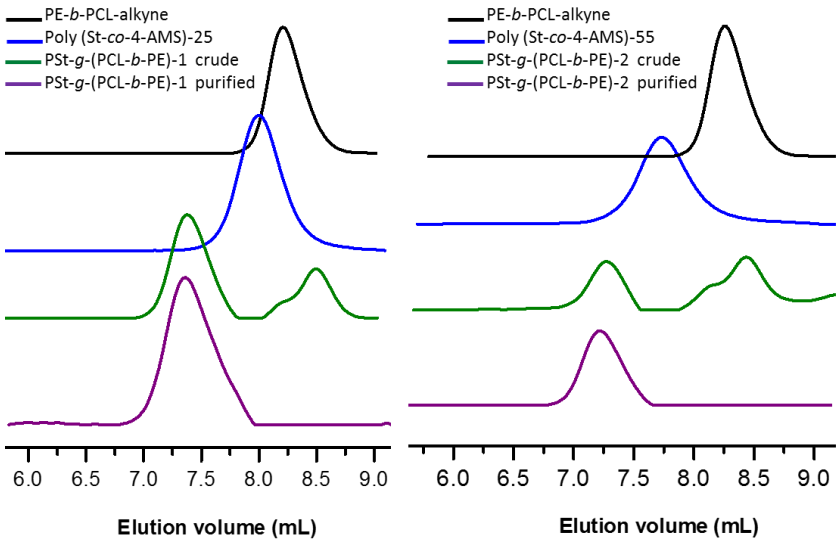

Figure 3.8 HT-SEC (TCB at 150 °C, PSt standard) traces of PSt-*g*-(PCL-*b*-PE)-1 and PSt-*g*-(PCL-*b*-PE)-2.

Another proof of the successful synthesis of the graft terpolymers comes from the ^{1}H NMR spectroscopy. As shown in **Figure 3.9**, the appearance of the new peaks at δ =

7.50 ppm is assigned to the proton of triazole ring and the peak at δ = 5.14 ppm to the methylene protons between phenyl and triazole rings. Furthermore, all fingerprints of PE, PCL and PSt are present in ^{1}H NMR spectrum and used to calculate the M_n of the graft terpolymers (**Table 3.3**). The efficiency of the CuAAC "click" reaction was calculated from ^{1}H NMR and it was found to be around 20 and 16 % for PSt-*g*-(PCL-*b*-PE)-1 and PSt-*g*-(PCL-*b*-PE)-2, respectively. Therefore, it is reasonable to postulate that the click reaction efficiency of the "grafting onto" method was affected by steric hindrance. Similar behavior was observed in other "grafting onto" cases.[16,20] The success of the "click" reaction to yield the PE-based graft terpolymers was also confirmed by the disappearance of the azide and alkyne peaks at 2104 and 3300 cm^{-1} in the FTIR spectra (**Figure 3.7**).

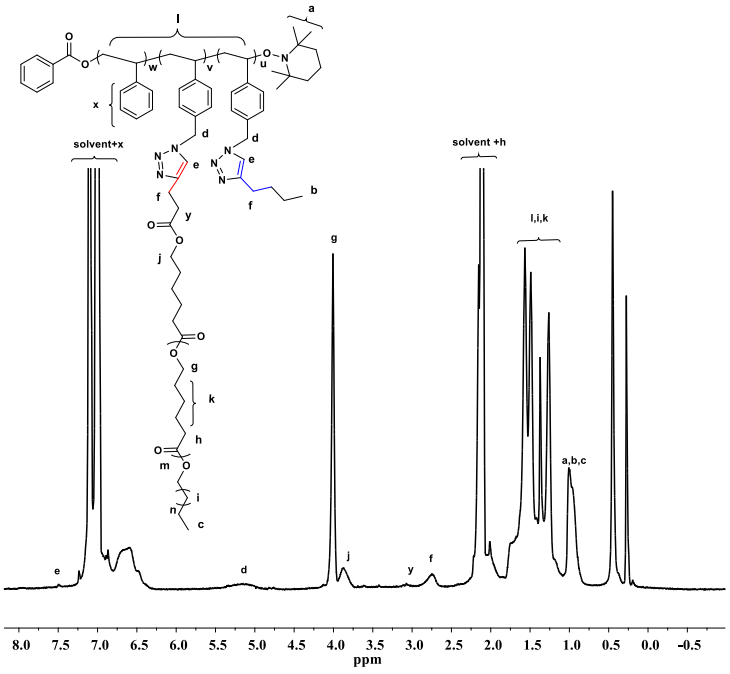

Figure 3.9 ^{1}H NMR spectrum of PSt-*g*-(PCL-*b*-PE) in toluene-d_8 at 80 ^{o}C (600 MHz).

Table 3.3 Molecular characterization data of graft terpolymers PSt-*g*-(PCL-*b*-PE)

No.	Polymers	$M_{n,\,SEC}$[a] (g·mol^{-1})	PDI[a]	$M_{n,\,NMR}$[b] (g·mol^{-1})	$Y_{grafting}$[c]
1	PSt-*g*-(PCL-*b*-PE)-1	55800	1.12	32900	5
2	PSt-*g*-(PCL-*b*-PE)-2	73100	1.18	56600	9

[a] High-temperature SEC, PSt standards. [b] $M_{n,\,NMR}$ of graft terpolymer was calculated from ^{1}H NMR spectrum using the area ratio of protons in PSt backbone to the ones on the side chains. [c] Number of branches ($Y_{grafting}$), was calculated from ^{1}H NMR by taking into account the $M_{n,\,NMR}$ of graft, the $M_{n,\,NMR}$ of backbone and the $M_{n,\,NMR}$ of branch.

3.3.4 Thermal properties of poly (St-*co*-4-CMS), poly (St-*co*-4-AMS) and PSt-*g*-(PCL-*b*-PE)

The poly (St-*co*-4-CMS), poly (St-*co*-4-AMS) and PSt-*g*-(PCL-*b*-PE) with different molecular weights were analyzed by DSC under a nitrogen atmosphere. As shown in **Figure 3.10**, the T_g of Poly (St-*co*-4-CMS) copolymers increases with functionality. It was noticed that the T_g values gradually decreased when the azide groups increased. The crystallinity of the PE-based grafts was also measured by DSC (**Figure 3.10**). After the CuAAC "click" reaction, the lack of chain movements, due to the PE, prevents the PCL chains from crystallizing as indicated by the presence of only one melting points corresponding to PE. This behavior was also observed in the PE-based bilayered molecular cobrushes.[42] The T_g of PSt block in PSt-*g*-(PCL-*b*-PE)-1 was observed but not in the case of PSt-*g*-(PCL-*b*-PE)-2 due to the increased graft concentration.

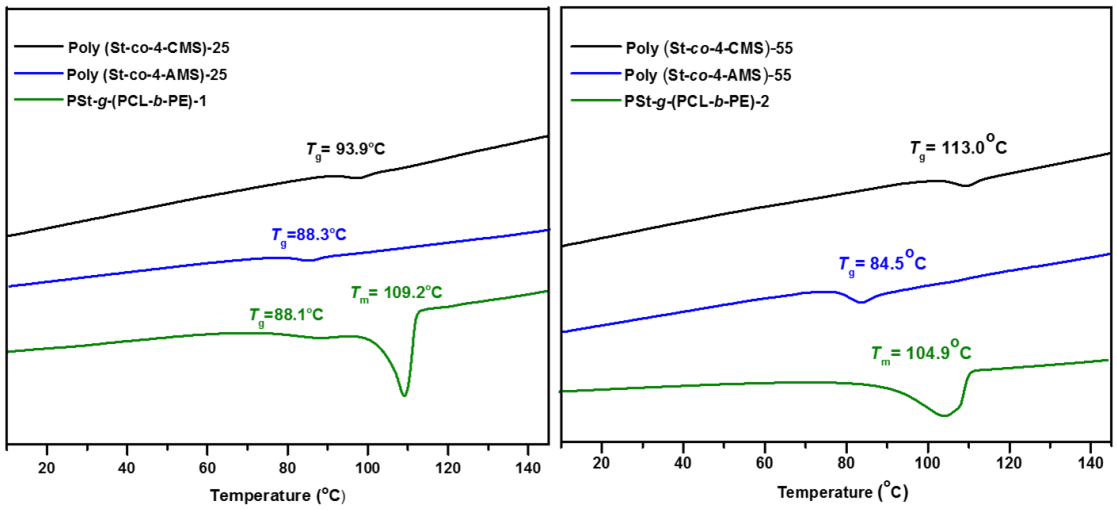

Figure 3.10 DSC curves of poly (St-*co*-4-CMS), poly (St-*co*-4-AMS) and PSt-*g*-(PCL-*b*-PE) at various stages (N_2 atmosphere, 10 °C/ min, second heating cycle).

3.4 Conclusions

Novel well–defined polyethylene–based graft terpolymers were synthesized *via* the "grafting onto" strategy by combining nitroxide-mediated radical polymerization (NMP), polyhomologation and copper (I)-catalyzed azide-alkyne cycloaddition (CuAAC) "click" chemistry. The well-defined characteristics were proved by HT-SEC, IR and ^{1}H NMR characterization. This general strategy allows the synthesis of various PE-based graft polymers with different structures. DSC studies on the graft terpolymers showed that due to the presence of PE the mobility of the attached PCL chains decreases resulting in the disappearing of the PCL melting point.

3.5 References

(1) Hadjichristidis, N., Pitsikalis, M., Pispas, S.; Iatrou, H. *Chem. Rev.***2001**, *101*, 3747.
(2) Hadjichristidis, N.; Iatrou, H.; Pitsikalis, M.; Mays, J. *Prog. Polym. Sci.* **2006**, *31*, 1068.
(3) Pakula, T.; Zhang, Y.; Matyjaszewski, K.; Lee, H.; Boerner, H.; Qin, S.; Berry, G. C. *Polymer* **2006**, *47*, 7198.
(4) Neugebauer, D.; Zhang, Y.; Pakula, T.; Sheiko, S. S.; Matyjaszewski, K. *Macromolecules* **2003**, *36*, 6746.
(5) Velichkova, R. S.; Christova, D. C. *Prog. Polym. Sci.* **1995**, *20*, 819.
(6) Neugerbauer, D.; Zhang, Y.; Pakula, T.; Matyjaszewski, K. *Polymer* **2003**, *44*, 6863.
(7) Iha, R. I.; Wooley, K. L.; Nystrom, A. M.; Burke, D. J.; Kade, M. J.; Hawker, C. J. *Chem. Rev*. **2009**, *109*, 5620.
(8) Gacal, B.; Durmaz, H.; Tasdelen, M. A.; Hizal, G.; Tunca, U.; Yagci, Y.; Demirel, A. L. *Macromolecules* **2006**, *39*, 5330.
(9) Durmaz, H.; Dag, A.; Cerit, N.; Sirkecioglu, Hizal, G.; Tunca, U.*; J. Polym. Sci., Part A: Polym. Chem.* **2010**, *48*, 5982.
(10) Tsarevsky, N. V.; Bencherif, S. A.; Matyjaszewski, K. *Macromolecules* **2007**, *40*, 4439.
(11) (a) Meldal, M.; *Macromol. Rapid Commun.* **2008**, *29*, 1016; (b) Tunca, U, *Macromol. Rapid Commun*. **2013**, *34*, 38.
(12) Binder, W.H.; Sachsenhofer, R. *Macromol. Rapid Commun*. **2007**, **28**, 15.
(13) Gungor, E.; Hizal, G.; Tunca, U. *J. Polym. Sci., Part A: Polym. Chem.* **2009**, *47*, 3409.
(14) Parrish, B.; R. B. Breitenkamp, R. B.; and T. Emrick, T. *J. Am. Chem. Soc.* **2005**, *127*, 7404.
(15) Li, H.; Riva, R.; Jerome, R.; Lecomte, P. *Macromolecules* **2007**, *40*, 824.
(16) Gao, H.; Matyjaszewski, K. *J. Am. Chem. Soc.* **2007**, *129*, 6633.
(17) Yuan, Y-Y; Du, Q.; Wang, Y-C; Wang, J. *Macromolecules* **2010**, *43*, 1739.
(18) Ladmiral, V.; Mantovani, G.; Clarkson, G. J.; Cauet, S.; Irwin, Haddleton, D. M. *J. Am. Chem. Soc.* **2006**, *128*, 4823.
(19) Quemener, D.; Hellaye, M. L.; Bissett, C.; Davis, T.P.; Kowollik, C. B.; Stenzel, M. H. *J. Polym. Sci., Part A: Polym. Chem.* **2008**, *46*, 155.
(20) Dag, H. Durmaz, E. Demir, G. Hizal, U. Tunca, *J. Polym. Sci., Part A: Polym. Chem*. **2008**, *46*, 6969.
(21) Fleischmann, S.; Komber, H.; Appelhans, D.; Voit, B. I. *Macromol. Chem. Phys*. **2007**, *208,* 1050.
(22) Boffa, L. S. *Chem. Rev*. **2000**, *100*, 1479.
(23) Dong, J. Y.; Hu, Y. *Coord. Chem. Rev*. **2006**, *250*, 47.
(24) Xu, T.; Zhu, J.; Yuan, C.; Yang, Q.; Cui, K.; Li, C.; Wei, L.; Ma, Z. *Eur. Polym. J.* **2014**, *54*, 109.

(25) Park, E. S.; Yoon, J. S. *J. App. Polym. Sci.* **2003**, *88*, 2434.
(26) Chung, T. C.; Lu, H. L.; Ding, R. D. *Macromolecules* **1997**, *30*, 1272.
(27) Park, E. S.; Kim, M. N.; Yoon, J. S. *J. Polym. Sci., Part B: Polym. Phys*. **2002**, *40*, 2561.
(28) Liu, S.; Sen, A. *Macromolecules* **2001**, *34*, 1529.
(29) Kashiwa, N.; Matsugi, T.; Kojoh, S. I.; Kaneko, H.; Kawahara, N. *J. Polym. Sci., Part A: Polym. Chem.* **2003**, *41*, 3657.
(30) Shea, K. J.; Busch, B. B.; Paz, M. M. *Angew. Chem., Int. Ed*. **1998**, *37*, 1391.
(31) Wagner, C. E.; Kim, J. S.; Shea, K. J. *J. Am. Chem. Soc.* **2003**, *125*, 12179.
(32) Shea, K. J.; Lee, S. Y.; Busch, B. B. *J. Org. Chem*. **1998**, *63*, 5746.
(33) Busch, B. B.; Paz, M. M.; Shea, K. J.; Staiger, C. L.; Stoddard, J. M.; Walker, J. R.; Zhou, X.; Zhu, H. *J. Am. Chem. Soc*. **2002**, *124*, 3636.
(34) Yuan, C.; H. Lu, H.; Q. Li, Q.; S. Yang, S.; Q. Zhao, Q.; J. Huang, J.; L. Wei, L. and Z. Ma, Z. *J. Polym. Sci., Part A: Polym. Chem.* **2012**, *50*, 2398.
(35) Alkayal, N.; Hadjichristidis, N. *Polym. Chem.* **2015**, *6*, 4921.
(36) Chen, J.; Zhao, Q.; Shi, L.; Huang, J.; Li, G.; Zhang, S.; Ma, Z. J. *Polym. Sci., Part A: Polym. Chem.* **2009**, *47*, 5671.
(37) Chen, J.; Cui, K.; Zhang, S.; Xie, P.; Zhao, Q.; Huang, J.; Shi, L.; Li, G.; Ma, Z. *Macromol. Rapid Commun* **2009**, *30*, 532.
(38) Xue, Y.; Lu, H.; Zhao, Q.; Huang, J.; Xu, S.; Cao, S.; Ma, Z. *Polym. Chem.* **2013**, *4*, 307.
(39) Lu, H.; Xue, Y.; Zhao, Q.; Huang, J; Xu, S.; Cao, S.; Ma, Z. *J. Polym. Sci., Part A: Polym. Chem.* **2012**, *50*, 3641.
(40) Wang, X.; Gao, J.; Zhao, Q.; Huang, J.; Mao, G.; Wu, W.; Ning, Y.; Ma, Z. J. *Polym. Sci., Part A: Polym. Chem.* **2013**, *51*, 2892.
(41) Zhang, H.; Y. Gnanou, Y.; and Hadjichristidis, N. *Polym. Chem.* **2014**, *5*, 6431.
(42) Zhang, H.; Zhang, Z.; Gnanou, Y; Hadjichristidis, N. *Macromolecules* **2015**, *48*, 3556-3562.
(43) Zhang, H.; Alkayal, N.; Gnanou, Y.; Hadjichristidis, N. *Macromol. Rapid Commun.* **2014**, *35*, 378.
(44) Gungor, E.; Durmaz, H.; Hizal, G.; Tunca, U. *J. Polym. Sci., Part A: Polym. Chem*. **2008**, *46*, 4459.

Chapter 4 Synthesis of Polyethylene-Based Tadpole Copolymer with a Polyethylene (PE) Ring and a Polystyrene (PSt) Tail by the Combination of Polyhomologation, ATRP and Glaser Coupling Reaction

4.1 Introduction

In recent years, polymer scientists have been focused on developing new synthetic routes for cyclic polymers because of the unique physical properties compared to their linear structures, including lower intrinsic viscosity, higher density, smaller hydrodynamic volume and higher glass transition temperature.[1-7] To date, cyclic polymers with different structures such as cyclic block,[8] eight-shaped,[9] tadpole copolymers[10-14] have been synthesized either by end-to-end linking process or ring-expansion process.[15-19] Among them, the tadpole copolymer is consisting of a ring polymer as a head and one or more linear polymer as tail. That structure can be used for theoretical and experimental studies as e.g. self-assembly in selective solvents and bulk.

Tadpole-shaped copolymers can be constructed by several strategies **(Scheme 4.1)**. The first approach depends on the intramolecular ring-closure reaction between two reactive groups placed in the middle and at the end of the chain.[13,14] The second one uses the linking reaction between cyclic and linear polymers or uses the cyclic polymer as a macroinitiator to initiate polymerization of another monomer.[20] The third one uses the intramolecular cyclization between the two end-functionalized arms of a three arm precursor via high efficient reaction. [10,21]

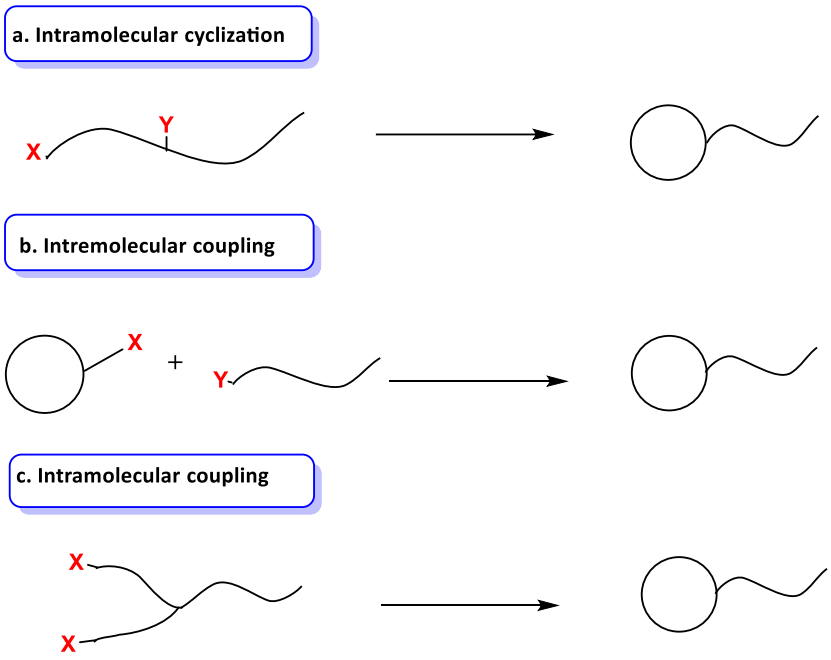

Scheme 4.1 Typical strategies to prepare tadpole-shaped copolymers.

Using some high-efficient coupling reaction such as Diels-Alder [22] and copper-catalyzed azide–alkyne cycloaddition (CuAAC),[10,14] the synthesis of tadpole-based polymers became more feasible. Lately, the Glaser coupling, involving the reaction between alkyne groups, has been widely used in organic[23] and polymer synthesis.[24–26] The main advantage of this reaction is fast, efficient and mild reaction conditions without deoxygenated step. By using this coupling reaction, few examples of tadpole copolymers have been reported with different segments and constructions.[27-30]

Although a variety of polymer-based cyclic structure have been prepared, there are only limited research up to now dealing with cyclic polyethylene due to the challenge to control functionality of polyethylene and molecular weight. For example, Grubbs *et al* employed ring-opening metathesis polymerization to prepare cyclic polyethylene (ring expansion method) by using a cyclic Ru catalyst (**Scheme 4.2**) and cyclooctadiene as

monomer followed by hydrogenation reaction. High molecular weights afforded and the polydispersity values were around 2.0. [31-33]

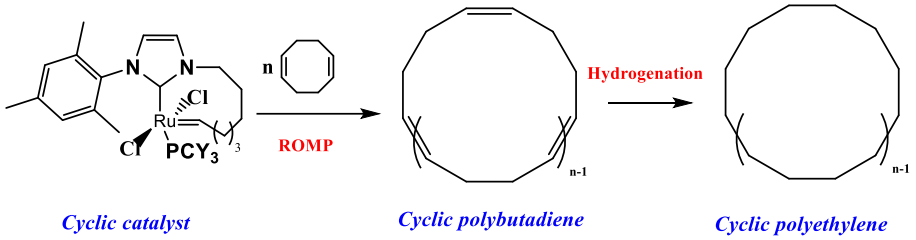

Scheme 4.2 ROMP to prepare cyclic polyethylene via a ring-expansion technique.

On the other hand, polyhomologation, a polymerization methodology leading to hydroxyl-terminated polyethylene, was developed by Shea[34-37] and is a particularly attractive method to make macrocyclic precursors by using designed organoborane initiators. Another approach followed for the synthesis of cyclic polyethylene with low molecular weight is using boracycles as initiator for polyhomologation. This method produced macrocyclic organoboranes via ring-expansion method followed by stitching reaction to obtain macrocyclic ketones (**Scheme 4.3**).[38]

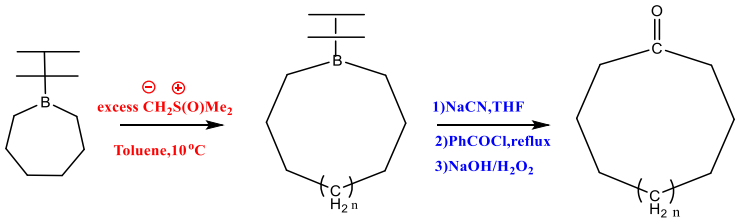

Scheme 4.3 Synthetic route to prepare cyclic polyethylene via polyhomologation

In our work, we provide a new strategy to synthesize PE-based macrocycles via ring-closure method. This new strategy was used to synthesize PE-based tadpole copolymers consisting from cyclic polyethylene (*c*-PE) and linear polystyrene (PSt) by combining of polyhomologation, ATRP and Glaser coupling reaction (**Scheme 4.4**).

4.2 Experimental section

4.2.1 Materials

Ethyl formate (97 %), vinyl magnesium chloride solution (1.6 M in THF), copper(I) bromide (CuBr, 99.999%), 2,3-dimethylbut-2-ene (≥ 99%), borane dimethyl sulfide complex solution (5.0 M in diethyl ether), 2-bromoisobutyryl bromide (BIBB, 98%), propiolic acid (95%), *p*-toluene sulfonic acid monohydrate (98%), *N*,*N*,*N*′,*N*′′,*N*′′-pentamethyldiethylenetriamine (PMDETA, 99%), NaOH (98%), Merrifield's resin (1% cross-linked chloromethylated PSt) and pyridine (99.8%) were obtained from Aldrich and used as received. Styrene (St, ≥99%) were distilled over calcium (I) hydride (CaH) under reduced pressure. Tetrahydrofuran (THF) and toluene were refluxed over sodium/ benzophenone and distilled under a nitrogen atmosphere just before use. Thexylborane was prepared by adding 2,3-dimethylbut-2-ene to the borane dimethyl sulfide complex solution (5.0 M in diethyl ether) in THF at 0 °C.[39] Dimethylsulfoxonium methylide was prepared as described previously in Chapter 2.

4.2.2 Measurements.

High-temperature-size exclusion chromatography (HT-SEC) measurements were carried out with the Agilent PL-SEC 220 with one PLgel 10 µm MIXED-B column. 1,2,4-Trichlorobenzene (TCB) was used as eluent at a flow rate of 1.0 mL/min at 150 °C. The system was calibrated with PSt standards. The ^{1}H NMR spectra were recorded with a Bruker AVANCE III 600 spectrometer. Differential scanning calorimetry (DSC) measurements were performed using a Mettler Toledo DSC1/TC100 system under inert

atmosphere (nitrogen). The sample was heated from room temperature to 150 °C, cooled to -10 °C and finally heated again to 150 °C with a heating/cooling rate of 10 °C/min.

4.2.3 Nomenclature

To simplify the identification of compounds the following terminology was applied: As a prefix, *c*- was assigned to cyclic polymers and the subscript number means the degree of polymerization. A suffix was added to indicate the functionality at the end of the polymer chain: -*alkyne,* for alkyne terminated polymer.

4.2.4 Synthetic procedures

4.2.4.1 Synthesis of 1, 4-pentadiene-3-yl 2-bromo-2-methylpropanoate (1) [40]

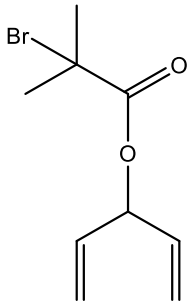

Ethyl formate (4.0 mL, 50 mmol) was added dropwise to a solution of vinyl magnesium chloride (63 mL, 100 mmol, 1.6 M in THF) in dry THF (30 mL) at 0 ^{o}C under argon (Ar). After completion of the addition, the mixture was stirred for one more hour at room temperature. Then the reaction was quenched with saturated NH_4Cl solution (30 mL), and the mixture was extracted with ethyl acetate (20 mL × 3). The obtained organic extracts were washed with brine, dried over $MgSO_4$, filtered and concentrated to give the crude 1,4-pentadiene-3-ol as a yellow oil.

2-bromoisobutyryl bromide (3.4 mL, 28 mmol) and pyridine (2.2 mL, 28 mmol) were added to a solution of crude penta-1, 4-dien-3-ol (2.1 g, 25 mmol) in THF (50 mL) at 0 ^{o}C under Ar. The mixture was stirred for 10 h at room temperature followed by dilution with hexane (20 mL) and washing with brine. The organic extracts were dried over $MgSO_4$, filtered and concentrated. The crude product was purified by distillation under vacuum to give the colorless oil (**1**) as a product (3.4 g, 58% yield). ^{1}H NMR (600 MHz, $CDCl_3$) included results: 1.94 ppm (6H, s), 5.27 (2H, d) 5.38 (2H, d), 5.70-5.73 (1H, m), 5.82-5.89 (2H, m).

4.2.4.2 Synthesis of initiator [40]

To a solution of 1,4-pentadiene-3-yl 2-bromo-2-methylpropanoate (1) (0.23 g, 1.0 mmol) in THF (4.0 mL) fresh prepared thexylborane (0.50 mL, 0.73 M) was added dropwise at 0 ^{o}C under Ar, and the mixture was stirred for 4 h at room temperature to give the organoborane solution.

4.2.4.3 Synthesis of macroinitiator (PE_{540}-OH)$_2$-Br

A 100 mL Schlenk flask, charged with methylide solution (10 mL, 1.7 M in toluene) and toluene (20 mL), was heated to 60 ^{o}C with stirring under Ar. Then 1.0 mL of the above-prepared organoborane solution was added. After stirring at 60 ^{o}C for 10 min, 0.10 mL of the reaction solution was taken out and added to water containing phenolphthalein. A neutral solution (pH indicator) indicated the complete consumption of the ylide. Then TAO·2H_2O (0.40 g) was added, and the mixture was stirred for 4 h at 80 ^{o}C. The mixture was precipitated in methanol, and the white solids were filtered, dried under vacuum.

(0.23 g, $M_{n,\ NMR}$= 15100 g·mol^{-1}) ^{1}H NMR (600 MHz, toluene-d_8, 90 ^{o}C) included results: 3.38 ppm (t, 2H, CH_2-OH), 1.36 ppm (m, 2H, -CH_2-, the backbone of PE).

4.2.4.5 Synthesis of macroinitiator (PE_{813}-OH)$_2$-Br.

A 100 mL Schlenk flask, charged with methylide solution (10 mL, 1.7 M in toluene) and toluene (20 mL), was heated to 60 ^{o}C with stirring under Ar. Then 1.5 mL of the above-prepared organoborane solution was added. After stirring at 60 ^{o}C for 10 min, 0.10 mL of the reaction solution was taken out and added to water containing phenolphthalein. A neutral solution (pH indicator) indicated the complete consumption of the ylide. Then TAO·2H_2O (0.40 g) was added, and the mixture was stirred for 4 h at 80 ^{o}C. The mixture was precipitated in methanol, and the white solids were filtered, dried under vacuum (0.22 g, $M_{n,\ NMR}$= 22700 g·mol^{-1}). ^{1}H NMR (600 MHz, toluene-d_8, 90 ^{o}C) included results: 3.38 ppm (t, 2H, CH_2-OH), 1.36 ppm (m, 2H, -CH_2-, the backbone of PE).

4.2.4.6 Synthesis of functionalized 3-miktoarm star copolymer (PE_{540}-OH)$_2$-*b*-PSt_{32}.

CuBr (0.003 g, 0.018 mmol), styrene (0.45 mL, 3.9 mmol), and toluene (5.0 mL) were placed into a 100 mL Schlenk flask. The mixture was subjected to two freeze-pump-thaw cycles and then PMDETA (8.0 μL, 0.036 mmol) was added and the mixture was stirred for 20 h at room temperature under Ar. Then the macroinitiator (PE_{540}-OH)$_2$-Br (0.20 g, 0.013 mmol) was added and the mixture was subjected to another two freeze-pump-thaw cycles. The solution was immediately immersed into an oil bath set at 100 ^{o}C to start the polymerization under stirring. After 24 h, the polymerization was quenched by cooling in a liquid nitrogen bath. The reaction mixture was precipitated in methanol, filtered and dried under vacuum (0.25 g, $M_{n,\ NMR}$= 19300 g·mol^{-1}). ^{1}H NMR (600 MHz,

toluene-d_8, 90 ^{o}C) included results: 6.60 ppm (m, 2H, Ar*H* of PSt), 3.38 ppm (t, 2H, CH_2-OH), 1.60 (m, 2H, aliphatic protons CH_2 of PSt) 1.36 ppm (m, 2H, -CH_2-, the backbone of PE).

4.2.4.7 Synthesis of functionalized 3-miktoarm star copolymer (PE_{813}-OH)$_2$-*b*-PSt_{19}.

CuBr (0.004 g, 0.025 mmol), styrene (0.51 mL, 4.9 mmol), and toluene (5.0 mL) were placed into a 100 mL Schlenk flask. The mixture was subjected to two freeze-pump-thaw cycles and then PMDETA (9.4 μL, 0.045 mmol) was added and the mixture was kept stirring at room temperature for 20 min under Ar. Then the macroinitiator (PE_{813}-OH)$_2$-Br (0.20 g, 0.008 mmol) was added and the mixture was subjected to another two freeze-pump-thaw cycles. The solution was immediately immersed into an oil bath set at 100 ^{o}C to start the polymerization under stirring. After 24 h, the polymerization was quenched by cooling in a liquid nitrogen bath. The reaction mixture was precipitated in methanol, filtered and dried under vacuum (0.24 g, $M_{n,\ NMR}$= 24200 g·mol^{-1}). ^{1}H NMR (600 MHz, toluene-d_8, 90 ^{o}C) included results: 6.60 ppm (m, 2H, Ar*H* of PSt), 3.38 ppm (t, 2H, CH_2-OH), 1.60 (m, 2H, aliphatic protons CH_2 of PSt) 1.36 ppm (m, 2H, -CH_2-, the backbone of PE).

4.2.4.8 Synthesis of (PE_{540}-alkyne)$_2$-*b*-PSt_{32}.

A mixture of (PE_{540}-OH)$_2$-*b*-PSt_{32} (0.23 g, 0.012 mmol), propiolic acid (0.02 mL, 0.24 mmol) and p-toluene sulfonic acid (0.005 g, 0.024 mmol) in toluene was heated to reflux by using Dean Stack apparatus 48-96 h and keep it for two days. Then, the solvent was removed under reduced pressure and the polymer was precipitated in methanol and dried under vacuum (0.22 g, $M_{n,\ NMR}$= 18400 g·mol^{-1}). ^{1}H NMR (600 MHz, toluene-d_8, 90

^{o}C) included results: 6.60 ppm (m, 2H, Ar*H* of PSt), 3.90 ppm (t, 2H, -CH_2-O-CO-alkyne), 1.60 (m, 2H, aliphatic protons CH_2 of PSt) 1.36 ppm (m, 2H, -CH_2-, the backbone of PE).

4.2.4.9 Synthesis of (PE_{813}-alkyne)$_2$-*b*-PSt_{19}.

A mixture of (PE_{813}-OH)$_2$-*b*-PSt_{19} (0.22 g, 0.010 mmol), propiolic acid (0.01 mL, 0.20 mmol) and *p*-toluene sulfonic acid (0.004 g, 0.020 mmol) in toluene was heated to reflux by using Dean Stack apparatus 48-96 h and keep it for two days. Then, the solvent was removed under reduced pressure and the polymer was precipitated in methanol and dried under vacuum (0.21 g, $M_{n,\,NMR}$= 24700 g·mol^{-1}). ^{1}H NMR (600 MHz, toluene-d_8, 90 ^{o}C) included results: 6.60 ppm (m, 2H, Ar*H* of PSt), 3.90 ppm (t, 2H, -CH_2-O-CO-alkyne), 1.60 (m, 2H, aliphatic protons CH_2 of PSt) 1.36 ppm (m, 2H, -CH_2-, the backbone of PE).

4.2.4.10 Synthesis of (cyclic polyethylene) block polystyrene (c-PE_{540})-*b*-PSt_{32}.

Toluene (400 mL), CuBr (0.047 g, 0.33 mmol), and PMDETA (0.07 mL, 0.33 mmol) were added to a 1000 mL round-bottomed flask and the solution was stirred for 1 h. In a separate flask, (PE_{540}-alkyne)$_2$-*b*-PSt_{32} was dissolved ($M_{n,NMR}$= 18400 g·mol^{-1}, 0.2 g, 0.011 mmol) in toluene (200 mL). The solution of polymer was then added to the CuBr/ PMDETA reaction solution via a peristaltic pump at a rate of 2 mL/h. After completion of the addition, the reaction solution was concentrated. Then the products were purified by passing through a neutral alumina column using toluene as eluent to remove the copper and precipitated in methanol. The crude product was dried overnight in a vacuum oven for 24 h. ^{1}H NMR (600 MHz, toluene-d_8, 90 ^{o}C) included results: 6.6 ppm (m, 2H, Ar*H* of PSt), 3.90 ppm (t, 2H, -CH_2-O-CO-alkyne), 1.6 (m, 2H, aliphatic protons CH_2 of PSt) 1.36 ppm (m, 2H, -CH_2-, the backbone of PE).

4.2.4.11 Synthesis of (cyclic polyethylene) block polystyrene (c-PE_{813})-*b*-PSt_{19}.

Toluene (400 mL), CuBr (0. 035 g, 0.24 mmol), and PMDETA (0.05 mL, 0.24 mmol) were added to a 1000 mL round-bottomed flask and the solution was stirred for 1 h. In a separate flask, (PE_{813}-alkyne)$_2$-*b*-PSt_{19} was dissolved ($M_{n,\,NMR}$= 24700 g·mol^{-1}, 0.2 g, 0.0081 mmol) in toluene (200 mL). The solution of polymer was then added to the CuBr/ PMDETA reaction solution via a peristaltic pump at a rate of 2 mL/h. After completion of the addition, the reaction solution was concentrated. Then the products were purified by passing through a neutral alumina column using toluene as eluent to remove the copper and precipitated in methanol. The obtained product was dried overnight in a vacuum oven for 24 h. ^{1}H NMR (600 MHz, toluene-d_8, 90 ^{o}C) included results: 6.6 ppm (m, 2H, Ar*H* of PSt), 3.90 ppm (t, 2H, -CH_2-O-CO-alkyne), 1.60 (m, 2H, aliphatic protons CH_2 of PSt) 1.36 ppm (m, 2H, -CH_2-, the backbone of PE).

4.2.4.12 General procedure to remove the unreacted (PE-alkyne)$_2$–*b*-PSt with Merrifield's resin-azide [41]

The crude polymers were dissolved in toluene in a Schlenk tube. 20 eq. of CuBr and PMDETA were added to the solution followed by addition of 0.1 g of Merrifield's resin-azide. The mixture was degassed by three freeze-pump-thaw (FTP) cycles and stirred under argon at 80 ^{o}C for two days. The obtained polymers were passed through a neutral alumina column to remove the copper and then precipitated in methanol and dried under vacuum at room temperature.

4.2.4.13 Polymer cleavage *via* hydrolysis [42]

A general hydrolysis procedure is as follows: (0.1 g) of the polymer sample was dissolved in 10 mL of toluene in a 250 mL round-bottomed flask fitted with a condenser at 90 ^{o}C. A solution of NaOH in methanol (5 mL of 1 M solution) was added to the polymer solution and the mixture was refluxed for 24 h. The cleaved polymer was precipitated in methanol, followed by washing with acetone and drying *in vacuum* overnight. ^{1}H NMR (600 MHz, toluene-d_8, 90 ^{o}C) included results: 3.38 ppm (t, 2H, -CH_2-O-CO-alkyne), 1.36 ppm (m, 2H, -CH_2-, the backbone of PE).

4.3 Results and discussion

Polyethylene-based tadpole copolymer (*c*-PE)-*b*-PSt was obtained according to the synthetics steps presented in **Scheme 4.4**. The α, ω-dihydroxy-polyethylene with bromide group at the middle of the chain was prepared by polyhomologation of ylide using functionalize initiator followed by ATRP of styrene monomer. The α, ω-dialkyne-poly ethylene block polystyrene was synthesized by esterification reaction. Then, the cyclization of the two of the three arm star by Glaser coupling led to the tadpole-shaped copolymers with PE ring and PSt tail.

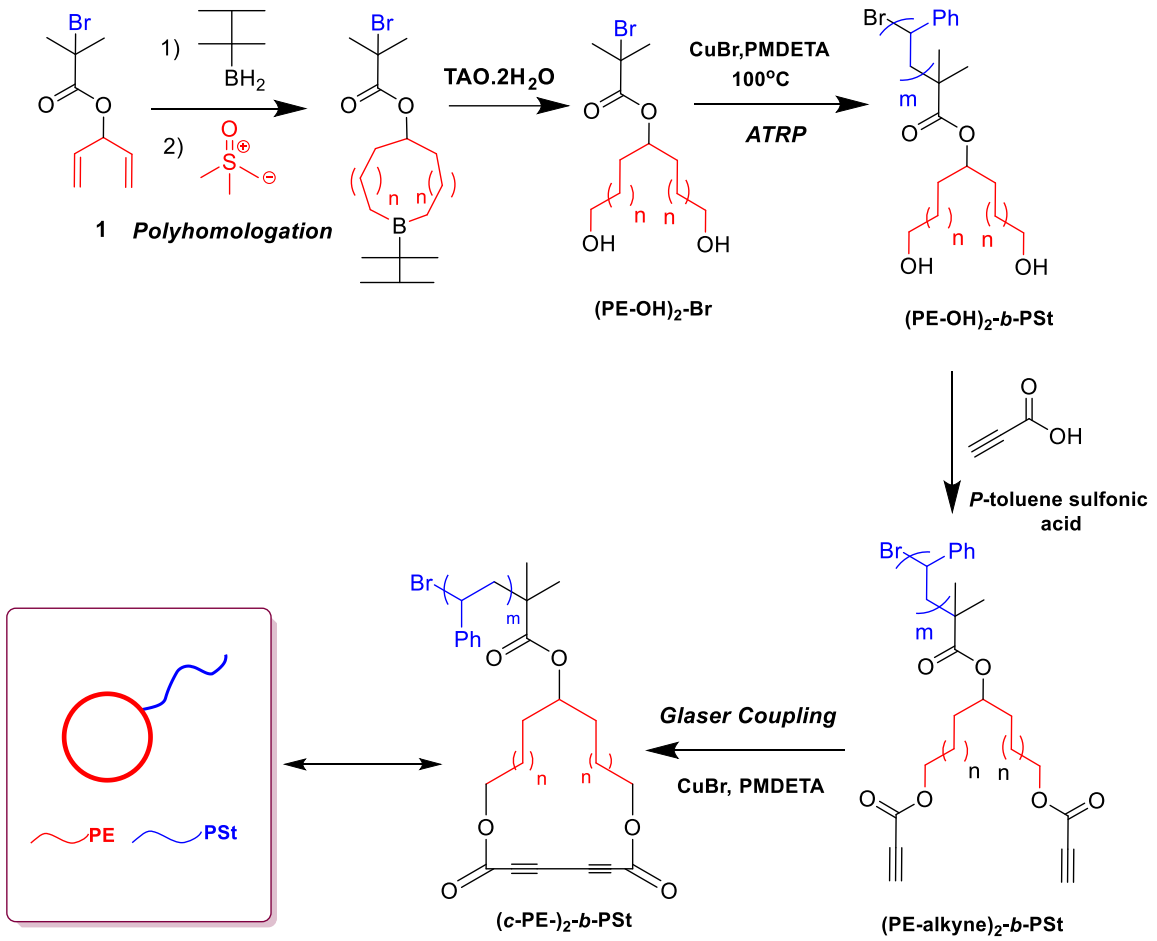

Scheme 4.4 Synthetics strategy for the preparation of PE-based tadpole copolymer (*c*-PE)-*b*-PSt.

4.3.1 Synthesis of PE-based macroinitiator $(PE\text{-}OH)_2$-Br.

The synthesis of the 1, 4-pentadiene-3-yl 2-bromo-2-methylpropanoate (**1**) was firstly reported by Hadjichristidis *et al* [40] by reaction of vinyl magnesium chloride with ethyl formate, followed by esterification with 2-bromoisobutyryl bromide to obtain (**1**). The diene group in the initiator 1,4-pentadiene- 3-yl 2-bromo-2-methylpropanoate was transformed to B-thexylboracycle then used to initiate the polyhomologation of ylide at 60 °C. The mixture became neutral in 10 min, indicating that the ylide was rapidly and quantitatively consumed. After the oxidation/hydrolysis with TAO·$2H_2O$, a bromo-

functionalized α, ω-dihydroxyl polyethylene (PE−OH)$_2$-Br was obtained. The proof of the successful synthesis of (PE-OH)$_2$-Br was derived from ^{1}H NMR and HT-SEC results. As shown in **Figures 4.1**, the characteristic peaks of polyethylene at δ = 1.1−1.5 ppm and δ = 3.4 ppm for the methylene protons connected to hydroxyl groups appeared after hydroboration /polyhomologation /oxidation reaction, indicating the successful polymerization of ylide. The degree of polymerization (DP$_n$) of each PE chain (n) was calculated from ^{1}H NMR by integration area ratio of the aliphatic protons at δ = 1.1−1.5 ppm (two protons for each methylene unit, two PE chains) to that of protons assigned to methylene connected to hydroxyl group (−*CH$_2$*−OH) at δ = 3.4 ppm (two protons for each PE arm, two end groups). The number-average molecular weight of the macroinitiator (PE-OH)$_2$-Br was calculated by $M_{n,\,NMR}$ = (n (DP of PE) × MW_{CH2} (14) × 2). HT-SEC curves of the obtained two PE samples (**Figure 4.2**, blue and red lines) illustrate the monomodal distribution that showed the high efficiency of polymerization of ylide using Bthexylboracycle initiator. Two samples with different molecular weights were synthesized and the data shown in **Table 4.1**.

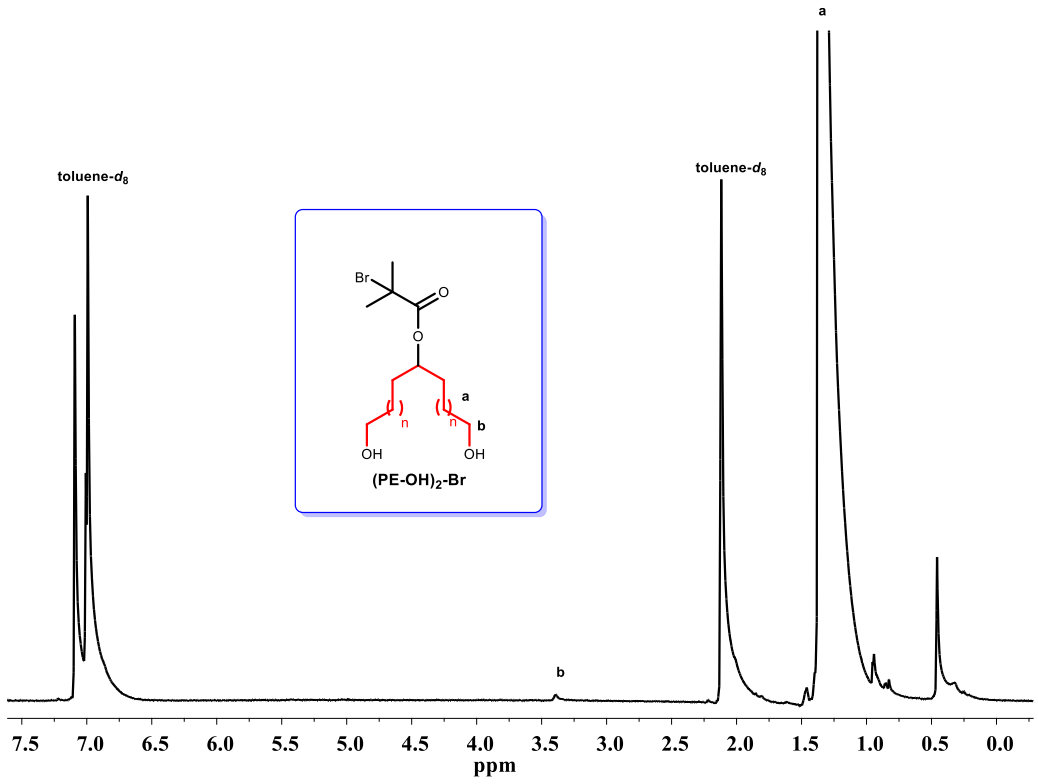

Figure 4.1 ^{1}H NMR spectrum of (PE-OH)$_2$-Br in toluene-d_8 at 90 ^{o}C (600 MHz).

Table 4.1 Molecular characteristics of (PE-OH)$_2$-Br synthesized by polyhomologation of ylide.

Entry	Sample	$M_{n,NMR}$[a] (g·mol^{-1})	DP$_{PE}$[a]	$M_{n,SEC}$[b] (g·mol^{-1})	PDI[b]
1	(PE$_{540}$-OH)$_2$-Br	15100	540	19600	1.25
2	(PE$_{813}$-OH)$_2$-Br	22700	813	30000	1.44

[a]$M_{n,NMR}$ and DP [degree of polymerization of one polymethylene (PE) chain] were calculated from ^{1}H NMR spectrum (toluene-d_8) using the integrated ratio of protons in terminal CH_2OH at δ = 3.4 ppm to the ones on the backbone. [b]$M_{n,SEC}$, PDI = M_w/M_n, determined by HT-SEC (TCB, 150 °C, PSt standards).

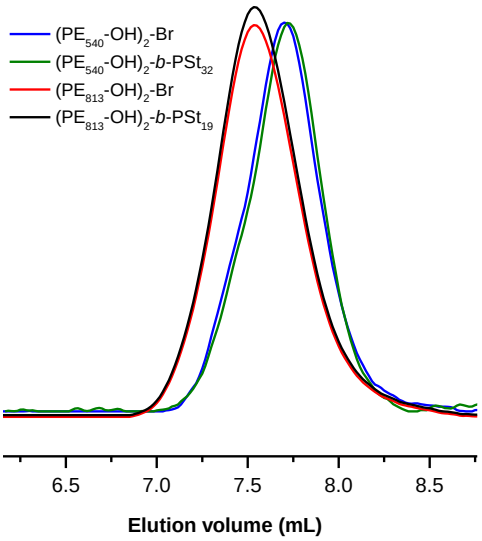

Figure 4.2 HT-SEC chromatograms of linear PEs (PE-OH)$_2$-Br and the corresponding miktoarm star polymers (PE-OH)$_2$-*b*-PSt.

4.3.2 Synthesis of A_2B star copolymers (PE-OH)$_2$-*b*-PSt.

ATRP of styrene was carried out using (PE-OH)$_2$-Br as macroinitiator and (CuBr)/(PMDETA) as catalyst/ligand in toluene at 100 °C to synthesize A_2B miktoarm star copolymers (PE-OH)2-b-PSt. The ratio [St]/[Br] was 600; the reaction was terminated after 24 h, followed by precipitation in methanol to give the polymer. The fingerprints for PSt and PE blocks are evident in the ^{1}H NMR spectrum (toluene-d_8, 90 °C) (**Figure 4.3**). The degree of polymerization of PSt chain (m) can be calculated from the integration area ratio of the aromatic protons at δ = 6.6 ppm (two protons for PSt unit) to that of protons assigned to the methylene protons connected to hydroxyl group (-*CH*$_2$-OH) at δ = 3.4 ppm (two protons for each PE arm, total four protons). The degree of polymerization of PE arm (n) was calculated as above and the number-average molecular weight of the A_2B star is $M_{n,NMR}$ = m (DP of PSt)×MW_{St} (104) + n (DP of PE)×MW_{CH2} (14) × 2. Two A_2B star samples

were synthesized, and the corresponding molecular characteristics are shown in **Table 4.2**.

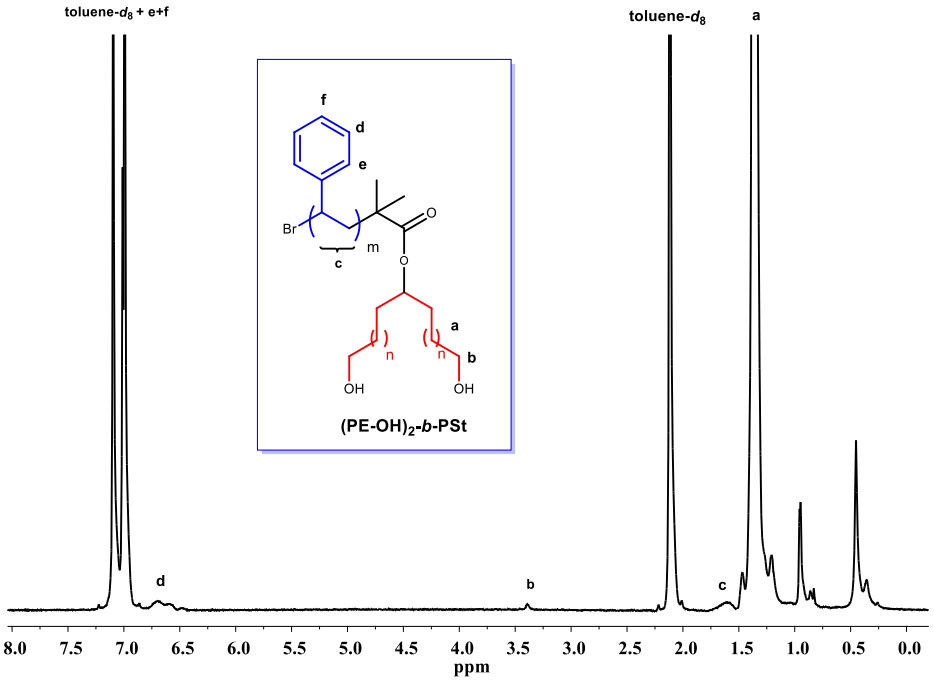

Figure 4.3 ^{1}H NMR spectrum of (PE-OH)$_2$-*b*-PSt in toluene-d_8 at 90 ^{o}C (600 MHz)**.**

The HT-SEC traces in **Figure 4.2** show a slight shift to low molecular weight of the star polymers (PE-OH)$_2$-*b*-PSt as compared with the linear PEs macroinitiators (PE-OH)$_2$-Br due to small hydrodynamic volume of star polymer as compared with linear precursor. All peaks are monomodal, symmetric and have narrow distributions (**Table 4.2**), indicating the highly efficient initiating of ATRP using (PE-OH)$_2$-Br as macroinitiators.

Table 4.2 Molecular characteristics of $(PE\text{-}OH)_2$-*b*-PSt synthesized by ATRP of styrene.

Star copolymer	macroinitiator	$M_{n,\,NMR}$[a] (g·mol^{-1})	$M_{n,\,SEC}$[b] (g·mol^{-1})	PDI[b]	PE (wt%)[c]
$(PE_{540}\text{-}OH)_2$-*b*-PSt_{32}	$(PE_{540}\text{-}OH)_2$-Br	19300	17500	1.29	80
$(PE_{813}\text{-}OH)_2$-*b*-PSt_{19}	$(PE_{813}\text{-}OH)_2$-Br	24200	27000	1.41	94

[a] $M_{n,NMR}$ and PE content were calculated from ^{1}H NMR spectra (toluene-d_8 ,90 °C). [b] $M_{n,\,SEC}$, PDI = M_w/M_n, determined by HT-SEC (TCB, 150 °C, PSt standards).

4.3.3 Synthesis of star-shaped $(PE\text{-alkyne})_2$-*b*-PSt and tadpole-shaped (*c*-PE)-*b*-PSt.

The α, ω-dialkyne-polyethylene block polystyrene $(PE\text{-alkyne})_2$-*b*-PSt was prepared via the esterification reaction between hydroxyl groups and propiolic acid in the presence of *p*-toluene sulfonic acid. The successful synthesis of $(PE\text{-alkyne})_2$-*b*-PSt was confirmed by ^{1}H NMR (**Figure 4.4**) by the presence of the typical signals of polyethylene and polystyrene. The quantitative esterification of $(PE\text{-}OH)_2$-*b*-PSt was confirmed by ^{1}H NMR spectroscopy (**Figure 4.4**) of the resulting product $(PE\text{-alkyne})_2$-*b*-PSt by the completely disappeared peak δ = 3.4 ppm attributed to methylene protons close to hydroxyl groups (–CH_2-OH) and appeared a new signal at δ = 3.90 ppm assigned to methylene protons close to ester groups (-CH_2-O-CO-alkyne).

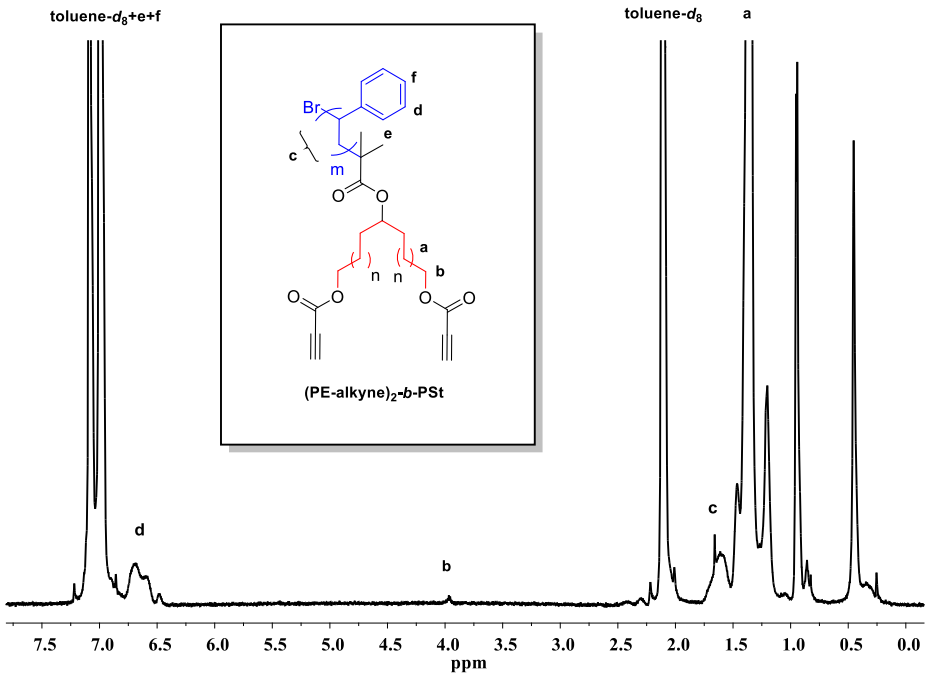

Figure 4.4 ^{1}H NMR spectrum of (PE-alkyne)$_2$-*b*-PSt in toluene-d_8 at 90 °C (600 MHz)**.**

Table 4.3 Data of tadpole copolymers (*c*-PE)-*b*-PSt and three arm star polymers (PE-alkyne)$_2$-*b*-PSt.

Copolymer	$M_{n,NMR}$ [a] (g·mol^{-1})	$M_{n,SEC}$ [b] (g·mol^{-1})	PDI [b]	T_m [c]
(PE$_{540}$-alkyne)$_2$-*b*-PSt$_{32}$	18400	18000	1.25	123.0
(*c*-PE$_{540}$)-*b*-PSt$_{32}$	19200	6800	1.43	123.3
(PE$_{813}$-alkyne)$_2$-*b*-PS$_{19}$	24700	26900	1.41	126.7
(*c*-PE$_{813}$)-*b*-PSt$_{19}$	24500	6300	1.43	127.5

[a] $M_{n,NMR}$ were calculated from ^{1}H NMR spectra (toluene-d_8 ,90 °C). [b] $M_{n,SEC}$ and PDI = M_w/M_n were determined using HT-SEC (TCB, 150 °C, PSt standards).[c] Melting points (T_m) were determined by DSC (N_2, 10 °C/min, second heating cycle)

The intramolecular cyclization was accomplished between two alkynes at the end groups of the star polymers precursor (PE-alkyne)$_2$-*b*-PSt using Glaser linking reaction in high diluted solution (**Scheme 4.4**). Quite stringent coupling reaction conditions (90 °C,

toluene, PMDETA/CuBr were utilized to achieve the Glaser coupling reaction. HT-SEC analysis of the crude polymer shows the bimodal peak meaning that a mixture of star and tadpole polymer was produced after the cyclization process (**Figure 4.5**, dotted curves).

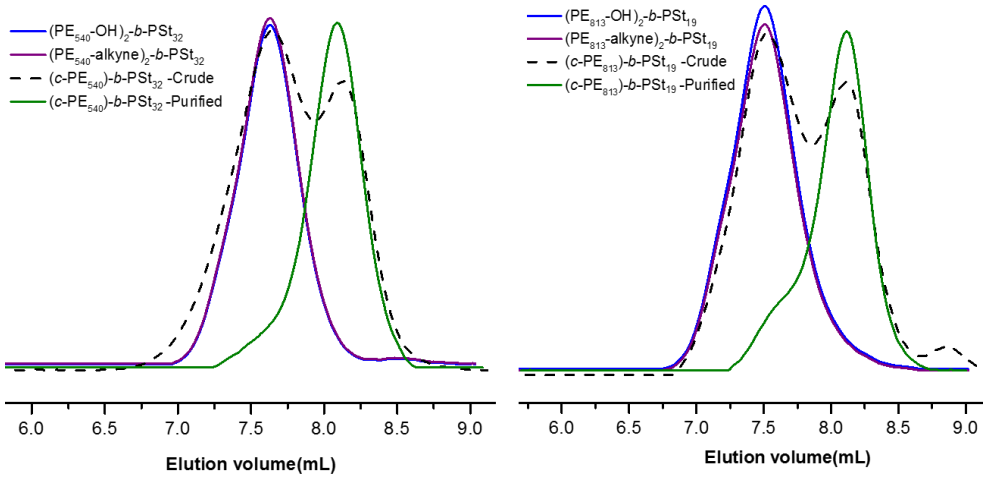

Figure 4.5 HT-SEC chromatograms of linear (PE-alkyne)$_2$-*b*-PSt and (*c*-PE)-*b*-PSt.

Effective purification step was utilized for the crude polymers by removing the unreacted (PE-alkyne)$_2$–*b*-PSt with azido Merrifield's resin in the presence of PMDETA/CuBr. Most importantly, the peak of the tadpole copolymers after purification (*c*-PE)-*b*-PSt clearly shifts to lower molecular weight as compared with the star polymer precursor (PE-alkyne)$_2$-*b*-PSt. As a result, the change to low molecular weight direction of PE-based tadpole copolymers can be attributed to the reduced hydrodynamic volume due to the more compact structure of tadpole copolymers as compared to that of star polymers. From the ^{1}H NMR spectrum in **Figure 4.6**, it can be seen that the fingerprints of PE and PSt segments are apparent in synthesis of (*c*-PE)-*b*-PSt. The molecular weight of the tadpole-shaped products was derived by ^{1}H NMR according to this formula: $M_{n,NMR}$ = m (DP of PSt) × MW_{St} (104) + n (DP of PE) × MW_{CH2} (14) × 2.

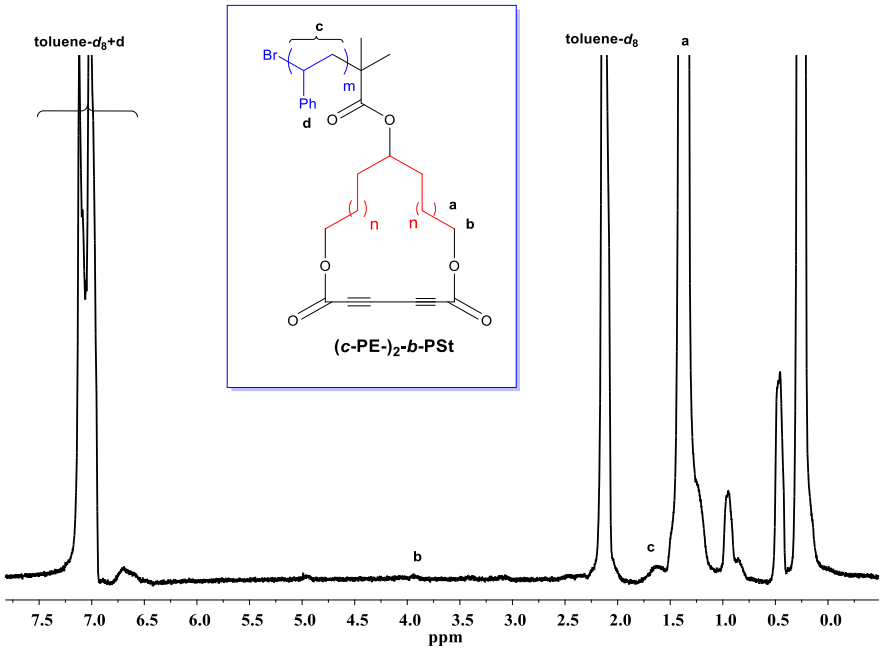

Figure 4.6 ^{1}H NMR spectrum of (*c*-PE)-*b*-PSt in toluene-d_8 at 90 °C (600 MHz)**.**

4.3.4 Degradation behavior by alkaline hydrolysis

After the synthesis and purification steps, the tadpole copolymers (*c*-PE)-*b*-PSt were cleaved via alkaline hydrolysis of the ester groups (**Scheme 4.5**). In particular, the resultant cleaved polymers represent the polyethylene blocks after washing with acetone to remove the polystyrene segments.

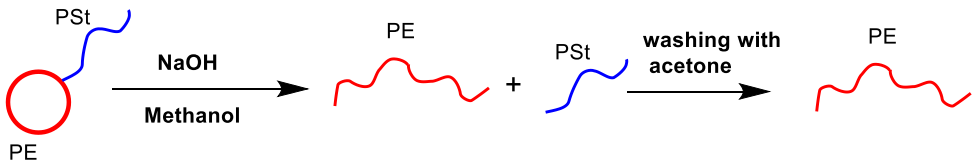

Scheme 4.5 Schematic representation of the alkaline hydrolysis of the polyethylene-based tadpole copolymer

Figure 4.7 illustrates the HT-SEC chromatograms of the linear, cyclic and cleaved polymers and their corresponding $M_{n,\,SEC}$. The higher apparent molecular weight of the

cleaved polymers was attributed to the higher hydrodynamics volume of the linear analogs as compared with the cyclic.

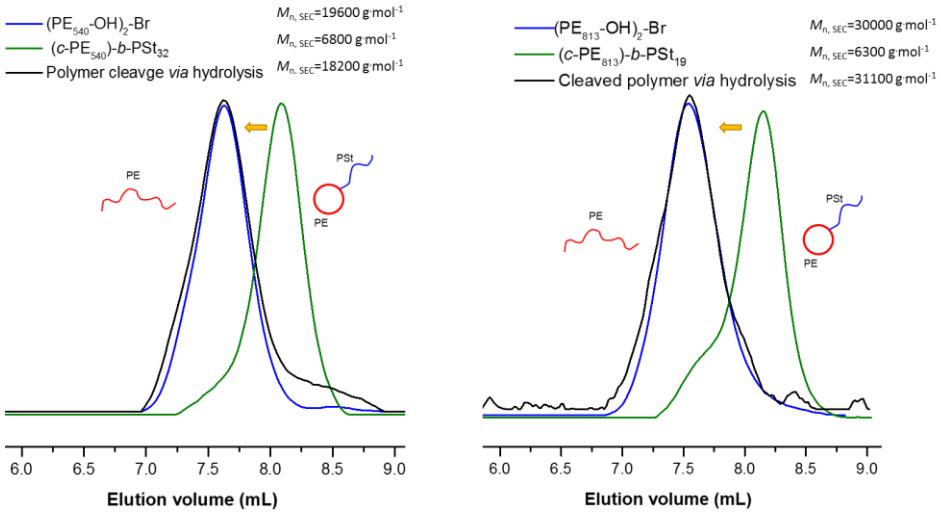

Figure 4.7 HT-SEC chromatograms of linear (PE-OH)$_2$-Br, (*c*-PE)-*b*-PSt and cleaved polymers.

4.3.5 Thermal properties of three arm star (PE-alkyne)$_2$-*b*-PSt and tadpole copolymer (*c*-PE)-*b*-PSt.

The melting behavior of star-shaped and tadpole-shaped copolymers was studied using DSC as shown in **Figure 4.8**. The melting temperature (T_m) was determined from the second heating cycle. Noticeably, only a single peak was observed assigned to the melting temperature of the PE blocks. The results show that T_m of tadpole copolymer (*c*-PE)-*b*-PSt are slightly higher than that of star polymer (PE-alkyne)$_2$-*b*-PSt because of reduced mobility and compact structure of tadpole-shaped.

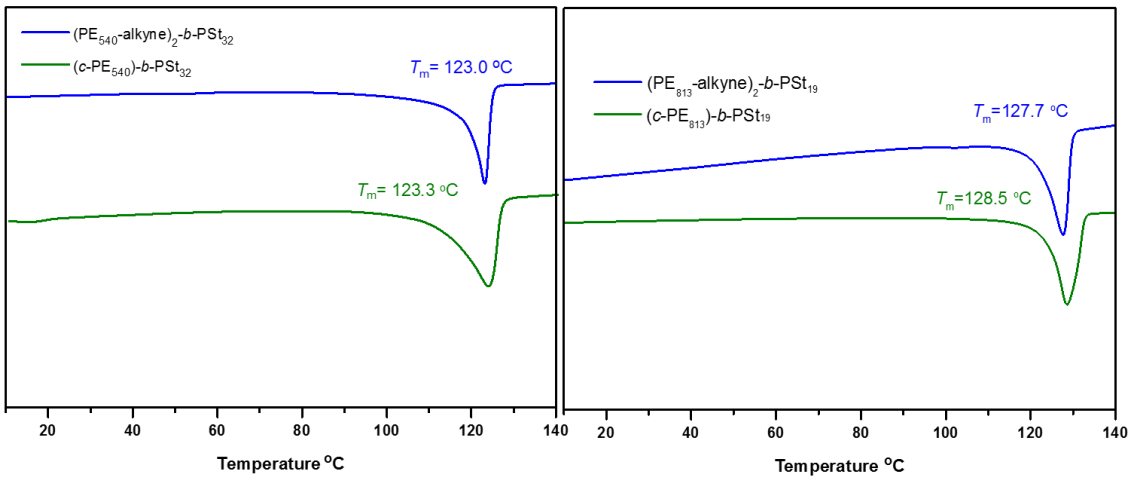

Figure 4.8 DSC curves of star-shaped (PE-alkyne)$_2$-*b*-PSt and tadpole-shaped (*c*-PE)-*b*-PSt (N_2 atmosphere, 10 °C/ min, second heating cycle).

4.4. Conclusions

In this study, novel polyethylene-based tadpole copolymers were synthesized by combining polyhomologation, ATRP and Glaser coupling. The synthetic strategy includes the following three steps: a) preparation of linear precursor of hydroxyl-telechelic polyethylene (PE-OH)$_2$-Br with controlled molecular weight and low PDI via polyhomologation followed by ATRP of styrene to afford (PE-OH)$_2$-*b*-PSt. b) Highly efficient esterification to produce (PE-alkyne)$_2$-*b*-PSt and c) cyclization by Glaser coupling conducted in PMDETA/CuBr system followed by purification with Merrifield's resin-azide to obtain the pure tadpole-shaped copolymer (*c*-PE)-*b*-PSt. The obtained polymers and intermediates were characterized by HT-SEC, DSC and ^{1}H NMR in detail. The HT-SEC traces of the resulting tadpole copolymers exhibited a strong shift to lower molecular weight region than their precursors. This approach presents a general method to prepare polyethylene-based tadpole copolymers with defined architecture and compositions.

4.5 References

(1) Endo, K. *Adv. Polym. Sci*. **2008**, *217*, 121.
(2) Kricheldorf, H.R. *J. Polym. Sci., Part A: Polym. Chem*. **2010**, *48,* 251.
(3) Minatti, E.; Borsali, R.; Schappacher, M.; Deffieux, A.; Soldi, V.; Narayanan, T.; Putaux, J. L. *Macromol. Rapid Commun*. **2002**, *23*, 978.
(4) Schappacher, M.; Deffieux, A. *J. Am. Chem. Soc.* **2008**, *130*, 14684.
(5) Hadjichristidis, N.; Hirao, A.; Tezuka, Y.; Prez, F. Du, Eds, *Complex Macromolecular Architectures,* Wiley, Singapore: 2011.
(6) Laurent, B. A.; Grayson, S. M. *Chem. Soc. Rev*. **2009**, *38*, 2202.
(7) Nasongkla, N.; Chen, B.; Macaraeg, N.; Fox, M. E.; Frechet, J. M.; Szoka, F. C. *J. Am. Chem. Soc.* **2009**, *131*, 3842.
(8) Honda, S.; Yamamoto, T.; Tezuka, Y. *J. Am. Chem. Soc.* **2010**, *132*, 10251.
(9) Shi, G. Y.; Sun, J. T.; Pan, C. Y. *Macromol. Chem. Phys*. **2011**, *212*, 1305.
(10) Kubo, M.; Hayashi, T.; Kobayashi, H.; Itoh, T. *Macromolecules* **1998**, *31*, 1053.
(11) Wan, X. J.; Liu, T.; Liu, S. Y. *Bio macromolecules* **2011**, *12*, 1146.
(12) Fu, G. D.; Phua, S. J.; Kang, E. T.; Neoh, K. G. *Macromolecules* **2005**, *38*, 2612
(13) Ohno, S.; Nese, A.; Cusick, B.; Kowalewski, T.; Matyjaszewski, K. *Polym. Sci. Ser. A* **2009**, *51*, 1210.
(14) Shi, G. Y.; Tang, X. Z.; Pan, C. Y. *J. Polym. Sci. Part A: Polym. Chem*. **2008**, *46*, 2390.
(15) Kubo, M.; Hibino, T; Tamura, M., Uno T.; Itoh, T. *Macromolecules* **2002**, *3*5, 5816.
(16) Voter, A. F.; Tillman, E. S. *Macromolecules* **2010**, *43*, 10304.
(17) Wang, S. S.; Zhang, K.; Chen, Y. M.; Xi, F. *Macromolecules* **2014**, *47*, 1993.
(18) Laurent, B. A.; Grayson, S. M. *J. Am. Chem. Soc.* **2006**, *128*, 4238.
(19) Touris, A.; Hadjichristidis, N. *Macromolecules* **2011**, *44*, 1969.
(20) Adachi, K.; Irie, H.; Sato, T.; Uchibori, A.; Shiozawa, M.; Tezuka, Y. *Macromolecules* **2005**, *38*, 10210.
(21) Ge, Z. S.; Liu, S. Y. *Macromol. Rapid. Commun*. **2009**, *30*, 1523.
(22) Dedeoglu, T.; Durmaz, H.; Hizal, G.; Tunca, U. *J. Polym. Sci. Part A: Polym. Chem.* **2012**, *50*, 1917.
(23) Siemsen, P.; Livingston, R. C.; Diederich, F. *Angew. Chem. Int. Ed*. **2000**, *39*, 2632.
(24) Zhang, Y.; Wang, G.; Huang, J. *J. Polym. Sci. Part A: Polym. Chem*. **2011**, *49*, 4766.
(25) Zhang, Y.; Wang, G.; Huang, J. *Macromolecules* **2010**, *43*, 10343.
(26) Wang, G.; Fan, X.; Hu, B.; Zhang, Y.; Huang, J. *Macromol. Rapid Commun.* **2011**, *32*, 1658.
(27) Wang, G.; Hu, B.; Fan, X.; Zhang, Y.; Huang, J. *J. Polym. Sci. Part A: Polym. Chem.* **2012,** *50,* 2227.
(28) Fan, X.; Huang, B.; Wang, G.; Huang, J.; Fan, X. Polymer **2012**, *53*, 2890.

(29) Fan, X.; Tang, T.; Huang, K.; Wang, G.; Huang, J. *J. Polym. Sci. Part A: Polym. Chem*. **2012**, *50*, 3095.
(30) Huang, B.; Fan, X.; Wang, G.; Zhang, Y.; Huang, J. *J. Polym. Sci. Part A: Polym. Chem*. **2012**, *50*, 2444.
(31) Bielawski, C. W.; Benitez, D; Grubbs, R. H. *J. Am. Chem. Soc*. **2003**, *125*, 8424.
(32) Bielawski, C. W.; Benitez, D; Grubbs, R. H. Science **2002**, *297*, 2041.

(33) Dong, J. Y.; Hu, Y. *Coord. Chem. Rev*. **2006**, *250*, 47.
(34) Shea, K, J.; Busch, B. B.; Paz, M. M. *Angew. Chem., Int. Ed*. **1998**, *37*, 1391.
(35) Wagner, C.E.; Kim, J. S.; Shea, K. J. *J. Am. Chem. Soc.* **2003**, *125*, 12179.
(36) Shea, k. J.; Lee, S. Y.; Busch, B. B. *J. Org. Chem*. **1998**, *63*, 5746.
(37) Busch, B. B.; Paz, M. M.; Shea, K. J.; Staiger, C. L.; Stoddard, J. M.; Walker, J. R.; Zhou, X.; Zhu, H. *J. Am. Chem. Soc*. **2002***, 124*, 3636.
(38) Shea, K. J.; Walker, H. D.; Greaves, J. *J. Am. Chem. Soc*. **1997**, *119*, 9049.
(39) (a) Negishi, E.; Brown, H. C. *Synthesis* **1974**, 77. (b) Brown, H. C.; Negishi, E. *J. Am. Chem. Soc.* **1972**, *94*, 3567. (c) Brown, H. C.; Mandal, A. K. *J. Org. Chem*. **1992**, *57*, 4970.
(40) Zhang, Z.; Altaher, M.; Zhang, H.; Wang, D.; Hadjichristidis, N. *Macromolecules* **2016**, *49*, 2630.
(41) Gungor, E.; Durmaz, H.; Hizal, G.; Tunca, U. *J. Polym. Sci., Part A: Polym. Chem.* **2008**, *46*, 4459.
(42) Zhang, K.; Ye, Z.; Subramanian, R. *Macromolecules* **2009***, 42*, 2313.

Chapter 5 Self-Assembly Behavior of Linear Polymethylene-Block-Polyethylene Glycol Copolymer in Aqueous Solution

5.1 Introduction

Recently, fundamental interest has been focused on self-assembly behavior of block copolymers because of their ability to form different aggregation structures,[1,2] such as spheres, vesicles and lamellae, depending on the molecular weight, architecture, composition and the compatibility of various polymer segments. In particular, the self-assembly of amphiphilic molecules in nanoscale has been applied in drug delivery, separation techniques, emulsion stabilization and oil applications.[3-15]

The fact that the impressive results of the self-organized aggregation of double crystalline diblock copolymers, such as poly (ethylene oxide) (PEO), polyethylene (PE) and poly (ε-caprolactone) (PCL) have received more attention in order to use for potential applications.[16–18] According to chain symmetry and high incompatibility, PE-*b*-PEG copolymer was considered the best typical model to study the crystallinity and self-assembled structures in aqueous solutions.[19,20]

However, very few reports have studied the self-assembled structures of PE-*b*-PEO in selective solvents. Most importantly, the nonlinear polyethylene block in PE-*b*-PEO was usually synthesized from metallocene catalysts with high molecular weight and polydispersity,[21,22,19,20] or via hydrogenation of the poly (1,4-butadiene) with 7% alkyl branches.[23,24] Furthermore, prior reports have concentrated on homogeneous oligomeric PE–*b*-PEO copolymers, which can be prepared via organic synthesis.[25-27]

There is only one report regarding the self-assembly of linear polyethylene-based micelles in water, in which linear polyethylene or polymethylene was prepared via polyhomologation. Specifically, polymethylene-*b*-poly (acrylic acid) copolymers (PM-*b*-PAA) were prepared by combining polyhomologation and ATRP.[28] Two series of narrowly dispersed PM-*b*-PAA copolymers (PDI less than 1.09) with molecular weight ranging from 9600 to 15800 g·mol^{-1} were synthesized in order to study the micelle formation in aqueous solution. The critical micelle concentrations (CMC) were determined by fluorescence spectroscopy using pyrene as probe (**Figure 5.1**). As the molecular weight of the block copolymer was increased, the CMC decreased from 2.10×10^{-6} to 1.60×10^{-6} g mL^{-1}, while the micelle diameter increased from 175 to 290 nm as determined by DLS. The micelles were visualized by TEM, which revealed diameters of 120 to 500 nm (**Figure 5.2**).

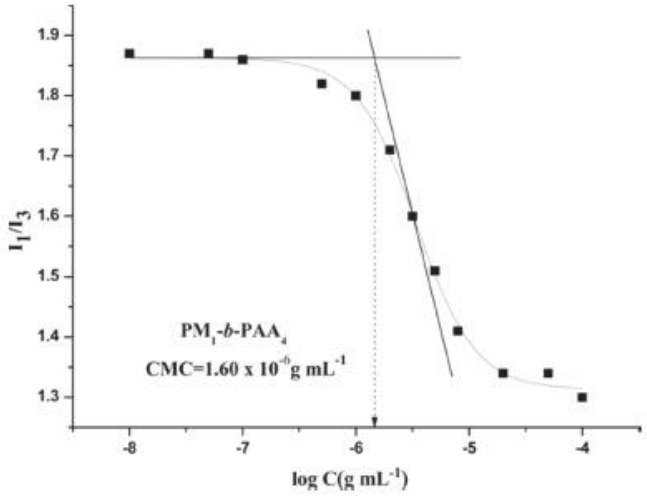

Figure 5.1 Dependence of fluorescence intensity ratios of pyrene emission bands on the concentrations of PM-*b*-PAA (M_n= 15800 g·mol^{-1}).[28]

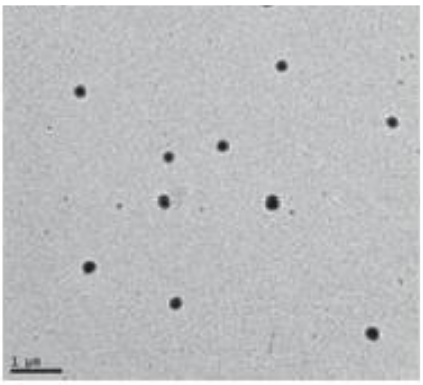

Figure 5.2 TEM images of PM-*b*-PAA (M_n=15800 g·mol^{-1}) aggregates in water.[28]

In this work, the self-assembly of the block copolymer PM-*b*-PEG in aqueous solution was studied. First, three samples of PM-*b*-PEG copolymer with different PM block lengths were synthesized, as previously described in chapter 2, by combining polyhomologation and Diels-Alder reaction. Subsequently, the self-assembled structure of PM-*b*-PEG in water was investigated by DLS, Cryo-TEM and AFM. The critical micelle concentration (CMC) was estimated from the intensity of the pyrene emissions in the fluorescence spectrum.

5.2 Experimental section

5.2.1 Synthesis

Block copolymers polymethylene-*b*-polyethylene glycol (PM-*b*-PEG) were prepared as previously described in chapter 2.

Synthesis of PM$_{80}$-*b*-PEG$_{100}$: Ant-PM$_{80}$-OH (0.1 g, 0.091 mmol, $M_{n,\ NMR}$=1100 g·mol^{-1}, 1 equiv.) and PEG$_{100}$-MI (0.61 g, 0.140 mmol, $M_{n,\ NMR}$= 4500 g·mol^{-1}, 1.5 equiv.) were dissolved in 25 mL of toluene under Ar. The mixture was refluxed at 110 ^{o}C and kept in the dark for 48 h. The solvent was then evaporated to dryness, the product was dissolved

in THF, precipitated in hexane, and dried in vacuum oven at 40 ^{o}C overnight (0.4 g, 57% yield, $M_{n,\ NMR}$=5380 g·mol^{-1}, PDI=1.14).

Synthesis of PM$_{175}$-*b*-PEG$_{100}$: Ant-PM$_{175}$-OH (0.1 g, 0.040 mmol, $M_{n,\ NMR}$=2500 g·mol^{-1}, 1 equiv.) and PEG$_{100}$-MI (0.27 g, 0.060 mmol, $M_{n,\ NMR}$=4500 g·mol^{-1}, 1.5 equiv.) were dissolved in 25 mL of toluene under Ar. The mixture was refluxed at 110 ^{o}C and kept in the dark for 48 h. The solvent was then evaporated to dryness, the product was dissolved in THF, precipitated in hexane, and dried in vacuum oven at 40 ^{o}C overnight (0.25 g, 68% yield, $M_{n,\ NMR}$= 5800 g·mol^{-1}, PDI=1.32).

Synthesis of PM$_{360}$-*b*-PEG$_{100}$: Ant-PM$_{360}$-OH (0.1 g, 0.020mmol, $M_{n,\ NMR}$=5000 g·mol^{-1}, 1 equiv.) and PEG$_{100}$-MI (0.14 g, 0.030 mmol, $M_{n,\ NMR}$= 4500 g·mol^{-1}, 1.5 equiv.) were dissolved in 25 mL of toluene under Ar. The mixture was refluxed at 110 ^{o}C and kept in the dark for 48 h. The solvent was then evaporated to dryness, the product was dissolved in THF, precipitated in hexane, and dried in vacuum oven at 40 ^{o}C overnight (0.1 g, 42% yield, $M_{n,\ NMR}$= 8980 g·mol^{-1}, PDI=1.24). A typical ^{1}H NMR of the copolymer PM-*b*-PEG (600 MHz, toluene-d_8, 80 ^{o}C) included results: 3.54 ppm (m, 4H, *CH$_2$CH$_2$O* of PEG), 1.40 ppm (m, -*CH$_2$*- of PM).

5.2.2 Preparation of micellar solution

The typical procedure to form the aqueous micellar solution was as follow: 4 mg from (PM-*b*-PEG) sample was dissolved in 4 mL toluene at 70 ^{o}C and the solution was stirred at 70 ^{o}C for 24 h. Then, deionized water (4mL) was added dropwise and stirred at 70 ^{o}C for another 24 h. Next, the toluene was evaporated under stirring at 25 ^{o}C. Finally,

the micelle solution with a concentration of 1 mg/mL was obtained followed by passing through a 0.45 μm PTFE membrane filter for analyzing.

5.2.3 Dynamic Light Scattering (DLS) Measurement

The DLS measurements were conducted using Zetasizer nano HT system from Malvern at a wavelength of 633nm with 173^{o} angle and performed at 25 ^{o}C in all experiments. The particle size distribution was determined by using the correlation function.

5.2.4 Cryo-transmission electron microscopic (cryo-TEM) observation

Samples for cryo-TEM were measured in TEM machine of type Titan 80-300 Krios from FEI Company (Hillsboro, OR) using accelerating voltage of 300 keV. By using an automated plunge-freezing instrument of model Vitrobot mark-IV, a few drops of the aqueous solutions were placed onto the carbon coated copper grids followed by freezing the grids in liquid ethane cryogen. Then, the samples of the thin frozen layer were moved to the autoloader of Titan Krios for imaging.

5.2.5 Atomic force microscope (AFM)

Silicon wafer was utilized as a substrate for atomic force microscopy (AFM). Before use, the silicon wafer was washed with dichloromethane, DI water (5 min) and piranha solution (3:1 v/v H_2SO_4/H_2O_2, 30 min) in sequence. Followed by rinsing with DI water and dried under vacuum. The aqueous micellar solution (1 mg/mL) was slowly added on a silicon wafer then dried at 25 ^{o}C for 24 h before use. AFM was accomplished on Agilent 5500 SPM with AAC mode and K (spring constant) probe model.

5.2.6 Determination of critical micelle concentration (CMC)[29]

The CMC of the block copolymer was determined by fluorescence spectroscopy. First, 0.1 mL of pyrene solution (1.0×10^{-4} mmol/mL) was added into different vials and acetone was evaporated. Different amount of the aqueous micellar solution of the block copolymer (1 mg/mL) was added to the vial containing pyrene. The total volume was adjusted with water to give series of solutions with varying polymer concentrations (10^{-2} mg/mL to 10^{-5} mg/mL) followed by sonicating for 10 min. The emission spectrum was documented by a varian cary eclipse (λ_{ex} = 337 nm and emission bandwidth 5.0 nm).

5.3 Results and discussion

5.3.1 Synthesis results

Three samples of copolymers PM-*b*-PEG with different polymethylene lengths were synthesized by combining Diels-Alder reaction with polyhomologation, as previously described in chapter 2. The successful synthesis of PM-*b*-PEG was confirmed by ^{1}H NMR and HT-SEC (**Figure 5.3**). The number-average molecular weight M_n, polydispersity and melting temperature for all samples are recorded in **Table 5.1**.

Table 5.1: Characteristic molecular weight data of PM-*b*-PEG.

Entry	Polymer	PDI [a]	$M_{n,\ NMR}$ [b] g·mol^{-1}	$M_{n,\ theo}$ [c] g·mol^{-1}	PE [d] (wt %)	T_m(PE)[e]	T_m(PEG)[e]
1	PM_{80}-*b*-PEG_{100}	1.14	5380	5800	21	97.2 °C	57.0 °C
2	PM_{175}-*b*-PEG_{100}	1.32	5800	6800	43	118.5 °C	56.9 °C
3	PM_{360}-*b*-PEG_{100}	1.24	8980	9400	56	122.9 °C	54.5 °C

[a] SEC in THF, PSt standards. [b, d] $M_{n,\ NMR}$ of copolymers and PM (wt%) were calculated from ^{1}H NMR spectrum. [c] $M_{n,\ theo}$ = sum of $M_{n,\ NMR}$ of homopolymers of PM and PEG. [e] Melting points (T_m) were determined by DSC (N_2, 10 °C/min, second heating cycle)

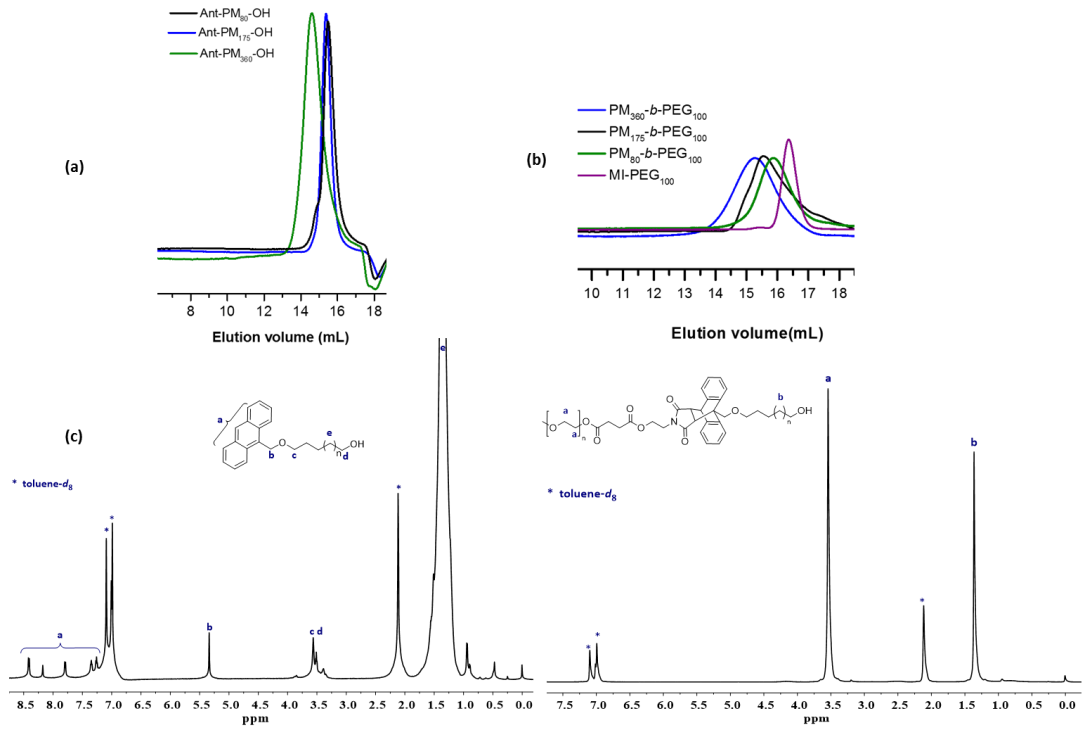

Figure 5.3 HT-SEC traces for ant-PM-OH (a), THF-SEC traces for PM-*b*-PEG (b) and ^{1}H NMR spectra (c) in toluene-d_8 at 90 ^{o}C (600 MHz) of three samples of ant-PM-OH and three samples of PM-*b*-PEG copolymers.

5.3.2 Self-assembly properties of PM-*b*-PEG diblock copolymer in water

The self-organized behavior of block copolymers containing PM should be studied at high temperature. The polymer was dissolved in toluene at 70^{o}C and kept for 24 h. Then, the water, which is a selective solvent for polyethylene glycol, was added slowly at 70^{o}C under stirring. Upon heating, the dispersion appeared which referred to micelle solution and the toluene was evaporated. The amphiphilic copolymer PM-*b*-PEG was self-assembled into micelles with polymethylene as core and polyethylene glycol as shell as shown in **Figure 5.4**.

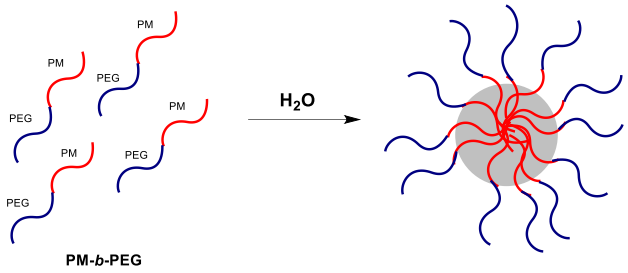

Figure 5.4 Self-assembly behavior of PM-*b*-PEG in aqueous water at 25 ^{o}C.

As shown in **Figure 5.5**, the average hydrodynamic diameter (d in nm) was determined by DLS at 25 ^{o}C with concentration equal to 1 mg/mL for the three micelle solutions. The polydispersity values were in the range from (0.23 to 0.37) and the hydrodynamic diameters (d nm) were 25.54 nm, 36.16 nm and 49.42 nm (**Table 5.2** and **Figure 5.5**) for PM_{80}-*b*-PEG_{100}, PM_{175}-*b*-PEG_{100} and PM_{360}-*b*-PEG_{100}, respectively.

Table 5.2 The hydrodynamic diameter (d), polydispersity and critical micelle concentrations (CMC) of the micelle solution.

Micelle from polymer solution	**Temp.**	**d (nm)[a]**	**PdI[b]**	**Kcps[c]**	**CMC (mg/mL) [d]**
PM_{80}-*b*-PEG_{100}	25 ^{o}C	25.54	0.269	133.7	3.9×10^{-3}
PM_{175}-*b*-PEG_{100}	25 ^{o}C	36.16	0.378	275.7	2.5×10^{-3}
PM_{360}-*b*-PEG_{100}	25 ^{o}C	49.42	0.236	293.9	2×10^{-3}

[a,b,c] Determined by DLS measurements (concentration, 1mg/mL; temperature 25°C). [d] Estimated by fluorescence method at 25 °C.

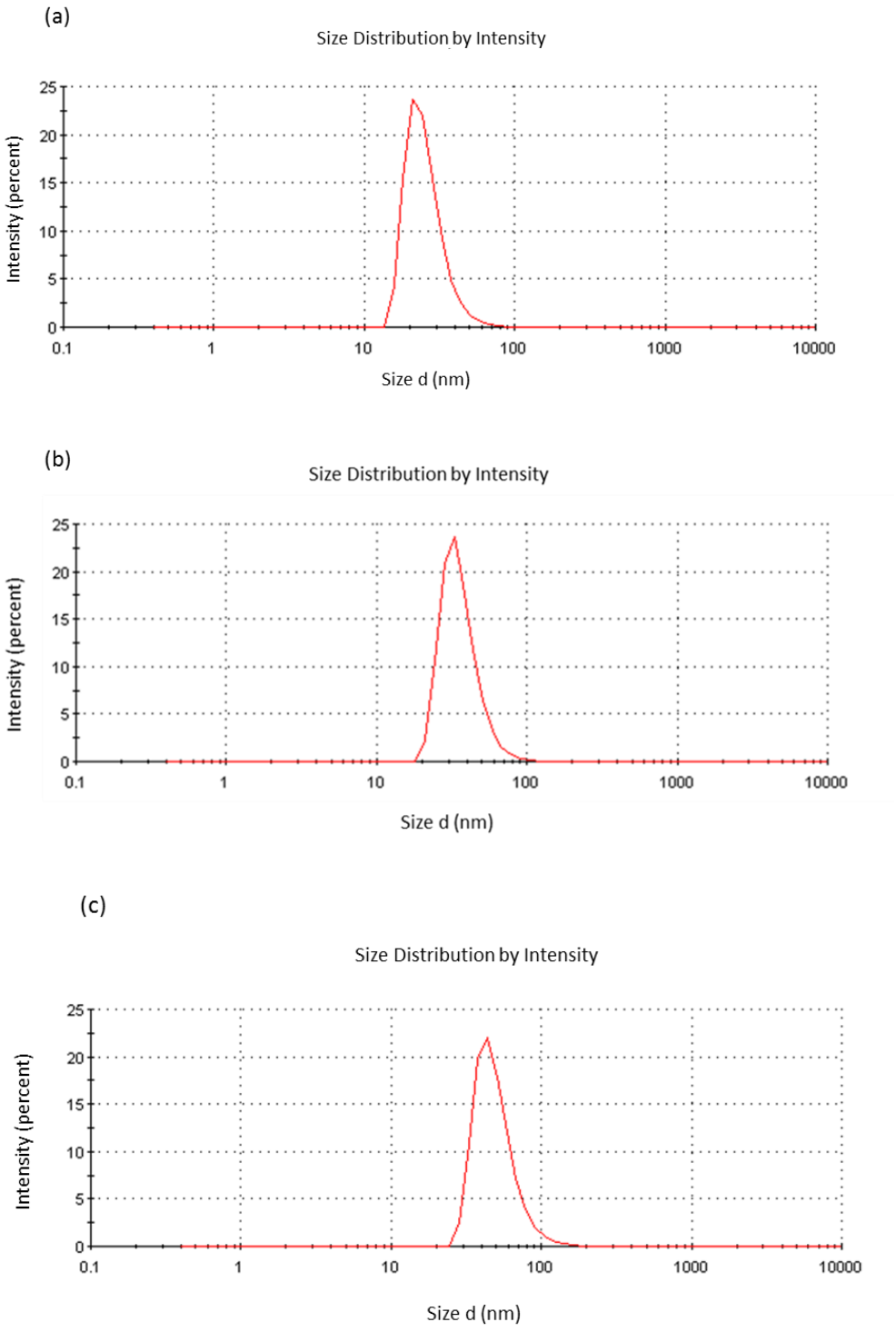

Figure 5.5 DLS measurements of the aqueous solution of (a) PM_{80}-*b*-PEG_{100}(b) PM_{175}-*b*-PEG_{100}(c) PM_{360}-*b*-PEG_{100}.block copolymer with concentration 1 mg/mL.

The actual morphology of the nanoparticle was evaluated by cryo-TEM microscopy, which revealed the presence of spherical nanoparticles or agglomerates for every block copolymer sample (**Figure 5.6**) with the average diameters about 16, 25 and 33 nm (estimated by calculating the average size of 15 micelles) for PM_{80}-*b*-PEG_{100}, PM_{175}-*b*-PEG_{100} and PM_{360}-*b*-PEG_{100}, respectively. Frequently, due to low contrast in TEM images, the size measurement of the micelles could be underestimated resulting in this size difference between the two characterization methods.

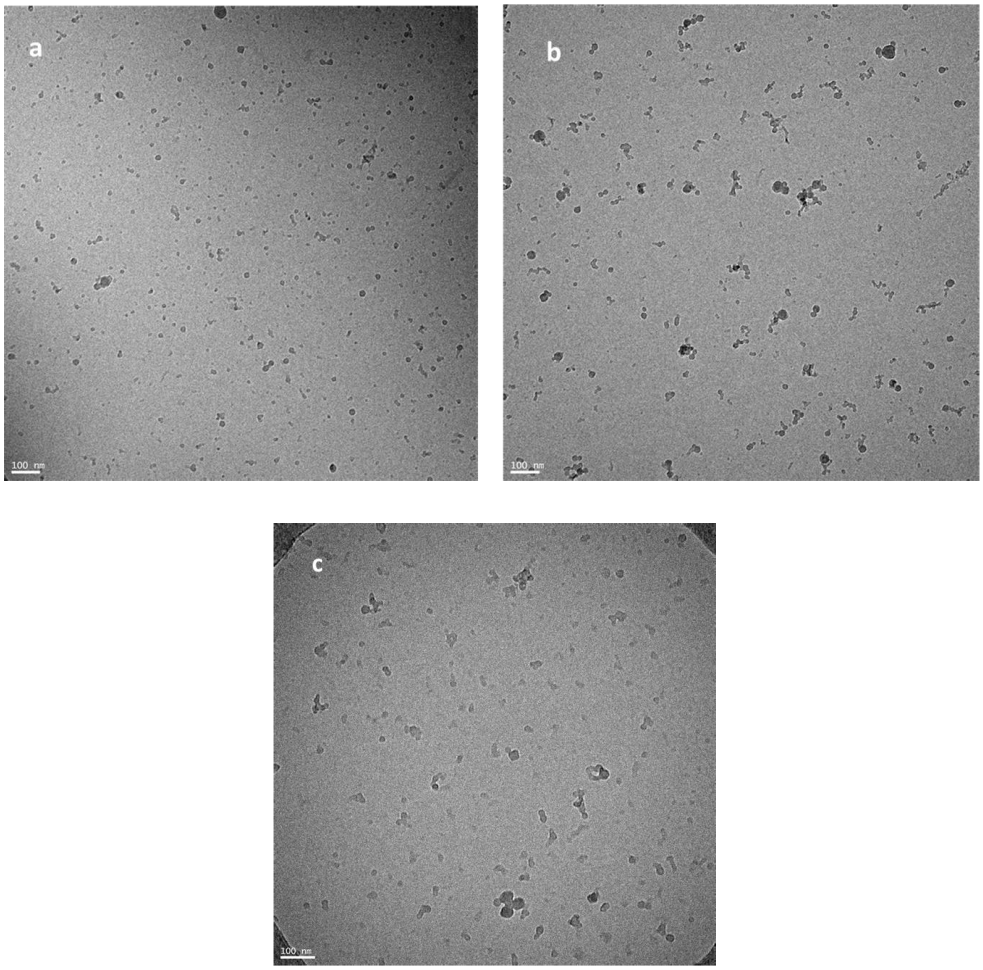

Figure 5.6 Cryo-TEM images of PM-*b*-PEG micelles (a) PM_{80}-*b*-PEG_{100}(b) PM_{175}-*b*-PEG_{100}(c) PM_{360}-*b*-PEG_{100}.

The spherical structure of micelle was confirmed by atomic force microscopy (AFM) and spin coating method was followed in order to perform block copolymers thin films on silica wafer. The sample was prepared by dropping the aqueous micelle solution on the silica wafer for AFM and directly imaged in tapping mode (**Figure 5.7**). AFM height images indicate that the average diameters corresponding to the micelles were 32, 40 and 55 nm, respectively.

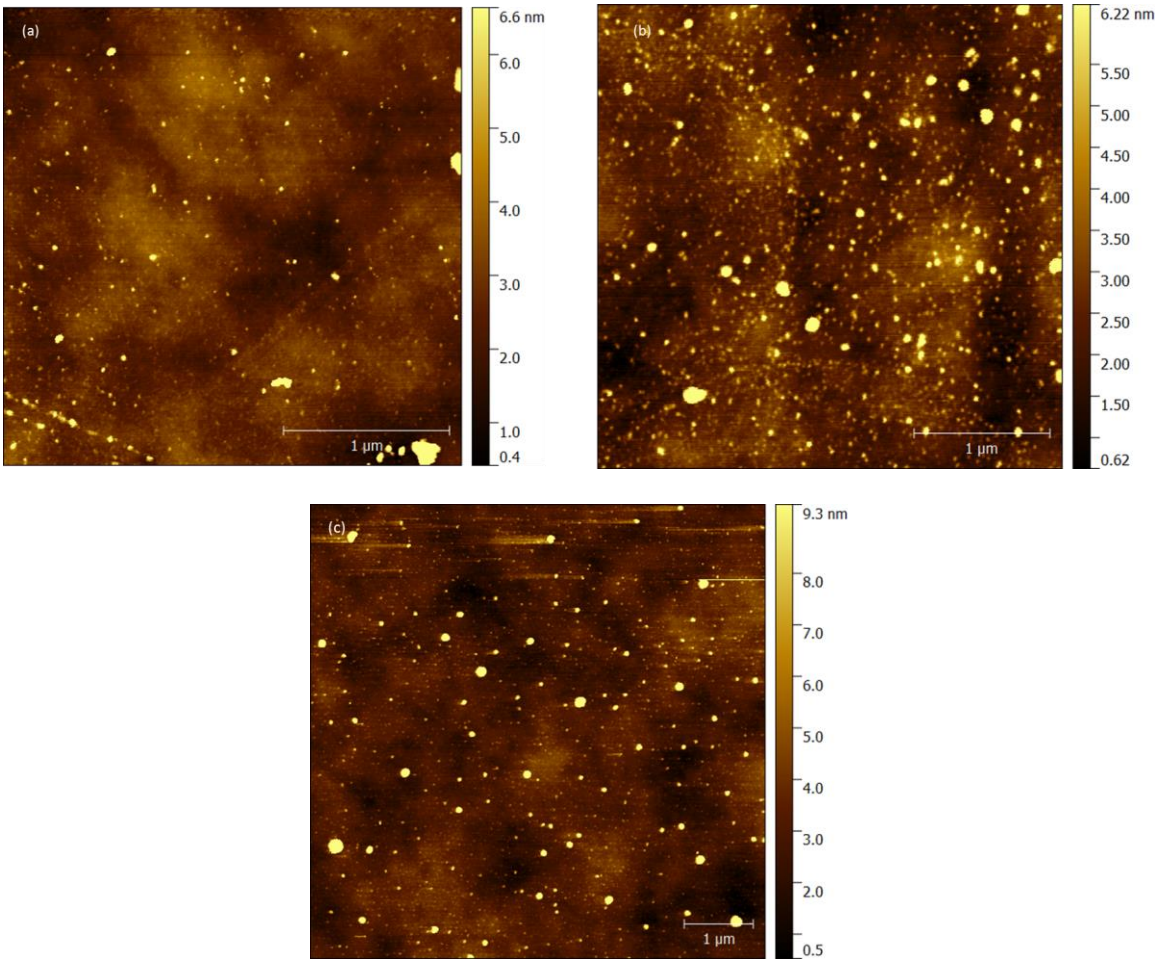

Figure 5.7 AFM height images of (a) PM_{80}-*b*-PEG_{100} (b) PM_{175}-*b*-PEG_{100} (c) PM_{360}-*b*-PEG_{100}.

5.3.3 Determination of critical micelle concentration (CMC)

The CMC can be defined as the concentration below which only single chains are present but above which both single chains and micellar aggregates can be found. The CMC of PM-*b*-PEG copolymers in aqueous solution was estimated via fluorescence method in the presence of pyrene at room temperature. In the case of pyrene which shows fluorescence intensity peaks at λ_{max} = 373 and 384 nm, denoted as I_{373} and I_{384} respectively, the ratio of I_{373}/I_{384} is a sensitive parameter to any changes in the polarity of the probe environment. As shown in **Figure 5.8**, the ratios of the emission intensities (I_{373}/I_{384}) were plotted versus the concentration of the polymer. The CMC can be calculated from the inflection point in the graph. The graph in **Figure 5.8** shows the ratio of the emission intensities I_{373}/I_{384} remains constant below the CMC and decreases sharply above the CMC in all samples. This decrease can be attributed to the encapsulation of pyrene in the hydrophobic core. Thus, the CMC values of the polymer solution were in the range of (2.0−4.0) $\times 10^{-3}$ mg/mL (**Table 5.2**and **Figure 5.8**), implying a minimal effect of the hydrophobic lengths on the CMC values.

5.3.4 Effect of the molecular weight of PM on the self-assembled behavior of PM-*b*-PEO in aqueous solution

At a constant PEG length, the hydrodynamic radius of the spherical micelle slightly increased from 25 to 49 nm when the molecular weight of the copolymer PM-*b*-PEG increased (**Figure 5.9**). Also, the size of the micelle is dependent on the length of PM block that making the core of the micelle.

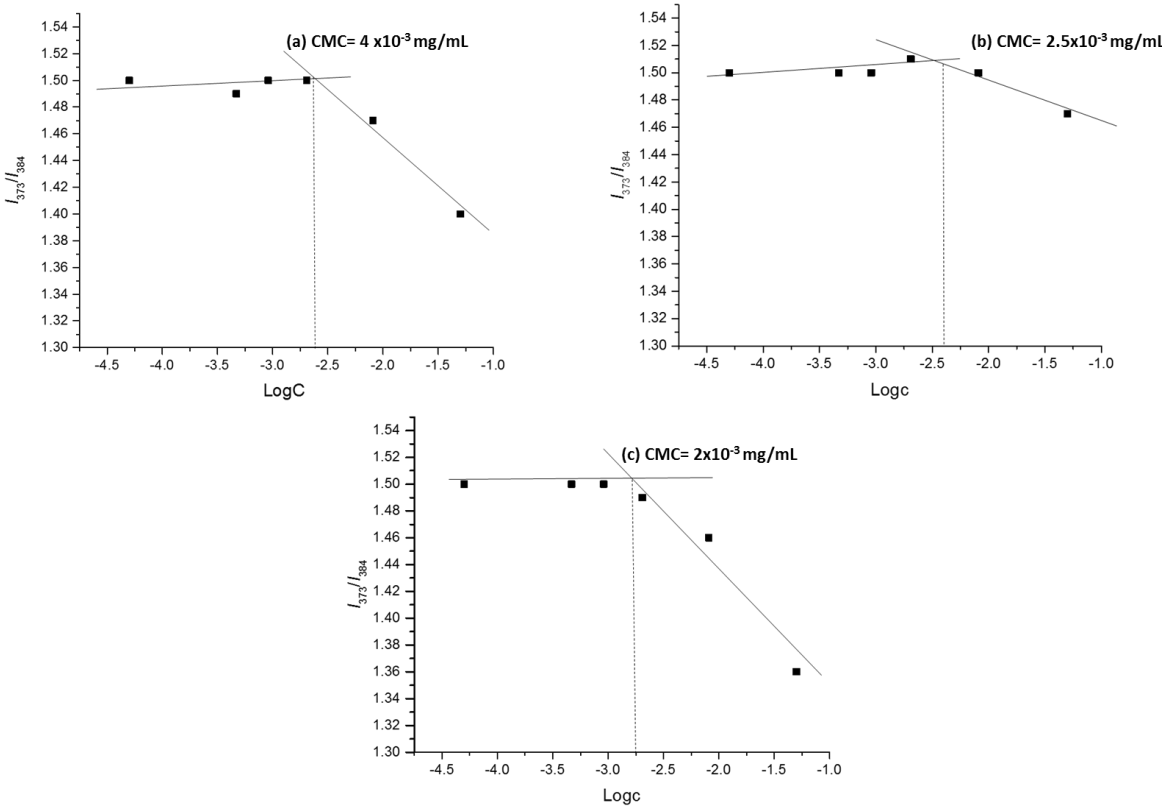

Figure 5.8 Three ratio of pyrene emission spectra I_{373}/I_{384} for (a) PM_{80}-*b*-PEG_{100}(b) PM_{175}-*b*-PEG_{100}(c) PM_{360}-*b*-PEG_{100}against of polymer concentrations.

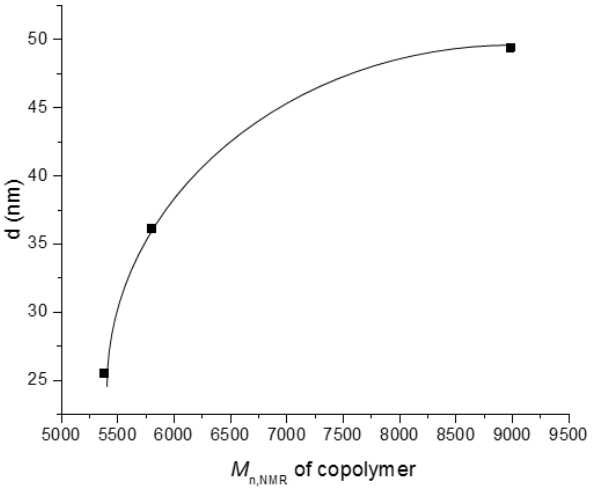

Figure 5.9 Relationship between the molecular weight of PM-*b*-PEG copolymer and diameter of the micelle.

The molecular weight of the polymethylene block in PM-*b*-PEG copolymer can influence not only the hydrodynamic radius of the micelle but also the critical micelle concentration. As depicted in **Figure 5.10**, the critical micelle concentrations (CMC) decreases as the molecular weight of PM-*b*-PEG copolymer increases at the constant PEG length, indicating that the PM-*b*-PEG copolymer with larger PM block formed micelles at lower concentration.

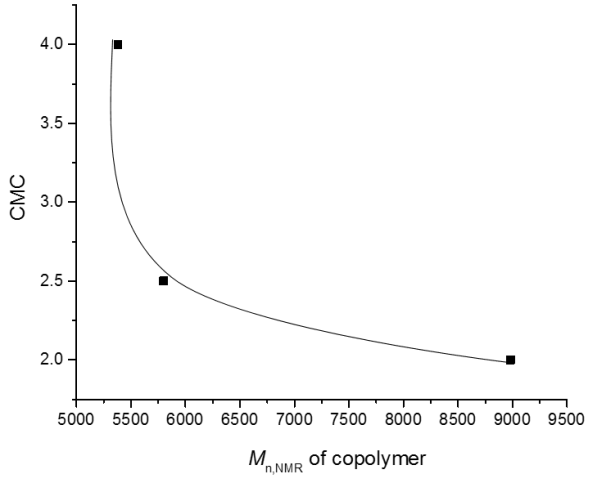

Figure 5.10 Relationship between the molecular weight of PM-*b*-PEG copolymer and the CMC of the micelles.

5.4 Conclusions

Amphiphilic PM-*b*-PEG block copolymers, with a constant length of PEG and different length of PM, were prepared via a combination of polyhomologation and Diels-Alder reaction. The obtained amphiphilic block copolymers can self-assemble to form spherical micelles in water, a selective solvent for PEG block, with PM core and PEG block as the shell. The average size and morphology of micelles were characterized using DLS, AFM and cryo-TEM. The CMC of the micelle solution was determined using fluorescence

method in the presence of pyrene. All the measurements revealed that there is a direct association between the CMC and the size of micelles with the molecular weight of the PM block.

5.5 References

(1) Hadjichristidis, N.; Hirao, A.; Tezuka, Y.; Prez, F. Du, Eds, *Complex Macromolecular Architectures,* Wiley, Singapore: 2011.
(2) Schacher, F. H.; Rupar, P. A.; Manners, I. *Angew. Chem., Int. Ed*. **2012**, *51*, 7898.
(3) Ryan, A. J.; Hamley, I. W.; Bras, W.; Bates, F. S. *Macromolecules* **1995**, *28*, 3860.**J.**
(4) Bilalis, P.; Zorba, G.; Pitskalis, N.; Hadjichristidis, N. *Polym. Sci. Part A: Polym. Chem*. **2006**, *44*, 5719.
(5) Manaure, A. C.; Morales, R. A.; Sanchez, J. J.; Muller, A. J. *J. Appl. Polym. Sci.* **1997**, *66*, 2481.
(6) Polymeropoulos, G.; Zapsas, G.; Hadjichristidis, N.; Avgeropoulos, A. *ACS Macro Lett*. **2015**, *4*, 1392.
(7) Albuerne, J.; Marquez, L.; Muller, A. J. *Macromolecules* **2003**, *36*, 1633.
(8) Chuang, V. P.; Ross, C. A.; Bilalis, P.; Hadjichristidis, N. *ACS Nano.* **2008***, 2,* 2007.
(9) Chen, H. L.; Hsiao, S. C.; Lin, T. L.; Yamauchi, K.; Hasegawa, H.; Hashimoto, T. *Macromolecules* **2001**, *34*, 671.
(10) Yueh, L. L.; Richard, A. R.; Anthony, J. R. *Macromolecules* **2002**, *35*, 2365.
(11) Hadjichristidisa, N.; Iatrou, H.; Pitsikalis, M.; Pispas, S.; Avgeropoulos, A. *Prog. Polym. Sci.* **2005**, *30*, 725.
(12) Hiroki, T.; Katsuhiko, F.; Takeshi, O.; Takayuki, O.; Masamitsu, M.; Katsuhiko, T.; Tomoo, S. *Polymer* **2006**, *47*, 8210.
(13) Hamley, I. W. Block Copolymers in Solution: Fundamentals and Applications; John Wiley & Sons, Ltd.: New York, 2005.
(14) Choi, Y. K; Bae, Y. H.; Kim, S. W. *Macromolecules* **1998**, *31*, 8766.
(15) Alexandridis, P.; Lindman, B. Amphiphilic Block Copolymers: Self- Assembly and Applications, 1st ed.; Elsevier: Amsterdam, 2000.
(16) Bogdanov, B.; Vidts, A.; Schacht, E.; Berghmans, H. *Macromolecules* **1999**, *32*, 726.
(17) Li, Z. Y.; Liu, R.; Mai, B. Y.; Wang, W. J.; Wu, Q.; Liang, G. D.; Gao, H. Y.; Zhu, F. M. *Polymer* **2013**, *54*, 1663.
(18) Fujiwara, T.; Miyamoto, M.; Kimura, Y.; Iwata, T.; Doi, Y. *Macromolecules* **2001**, *34*, 4043.
(19) Li, T.; Wang, W. J.; Liu, R.; Liang, W. H.; Zhao, G. F.; Li, Z.; Zhu, F. M. *Macromolecules* **2009**, 42, 3804.
(20) Lu, Y. Y.; Hu, Y. L.; Wang, Z. M.; Manias, E.; Chung, T. C. *J. Polym. Sci., Part A: Polym. Chem.* **2002**, *40*, 3416.
(21) Li, P.; Fu, Z.; Fan, Z. *J. Appl. Polym. Sci.* **2015**, 42236.
(22) Suna, L.; Liua, Y.; Zhua, L.; Hsiaob, B. S.; Avila-Orta, C*. Polymer* **2004**, *45*, 8181.
(23) Hillmyer, M. A.; Frank, S. B. *Macromolecules* **1996**, *29*, 6994.

(24) Hillmyer, M. A.; Frank, S. B. *Macromol. Symp.* **1997**, *117*, 121.
(25) Ding, Y.; Rabolt, J.F.; Chen, Y.; Olson, K. L.; Baker, G. L.; *Macromolecules* **2002**, *35*, 3914.
(26) Yeates, S. G.; Booth, C. *Eur. Polym. J*. **1985**, 21, 217.
(27) Matsuura, H.; Fukuhara, K.; Masatoki, S.; Sakakibara, M. *J. Am. Chem. Soc.* **1991**, 113, 1193.
(28) Lu, H.; Xue, Y.; Zhao, Q.; Huang, J.; Xu, S.; Cao, S.; Ma, Z. *J. Polym. Sci., Part A: Polym. Chem.* **2012**, *50*, 3641.
(29) Kalyanasundaram, K.; Thomas, J. K. *J. Am. Chem. Soc*. **1977**, *99*, 2039

Future Research Directions

The findings presented in this dissertation may provide fundamental insights for design polyethylene-based complex macromolecular architectures by combining the powerful coupling reactions with polyhomologation. This allows for good control over their molecular weight and low polydispersity of the polymers. The fundamental synthetic methods developed can be used to prepare a variety of new materials, and continued investigation of them can lead to new potential applications.

The following topics are identified as areas for future work based on the findings of this dissertation.

In Chapter 2, work of combining anthracene-terminated polyethylene with maleimide-terminated polymer via Diels Alder reaction is needed to broaden the applicability to use a wider range of other segment such as peptide classes, which will require the design and tailored synthesis of novel polyethylene block polypeptide co/terpolymers. The simplistic approach presented here should also be expanded to study the properties and self-assembly behavior.

The continuation of the work described in Chapter 3 can be extended by using different backbone such as poly (glycidylmethacrylate-*co*-methylmethacrylate) followed by opening the epoxide ring using NaN_3 and NH_4Cl to generate azido and hydroxyl group. By using one pot strategy of ''CuAAC click'' reaction and ROP, synthesis of polyethylene-based double graft polymer can be obtained

The work that described in Chapter 4 on the preparation of polyethylene-based cyclic polymers shows great promise to investigate the self-assembly behavior and study

the morphology of tadpole and three arm polymer. The scope of this project should be expanded to include other polymer segments like polyethylene oxide or PAA.

APPENDICES

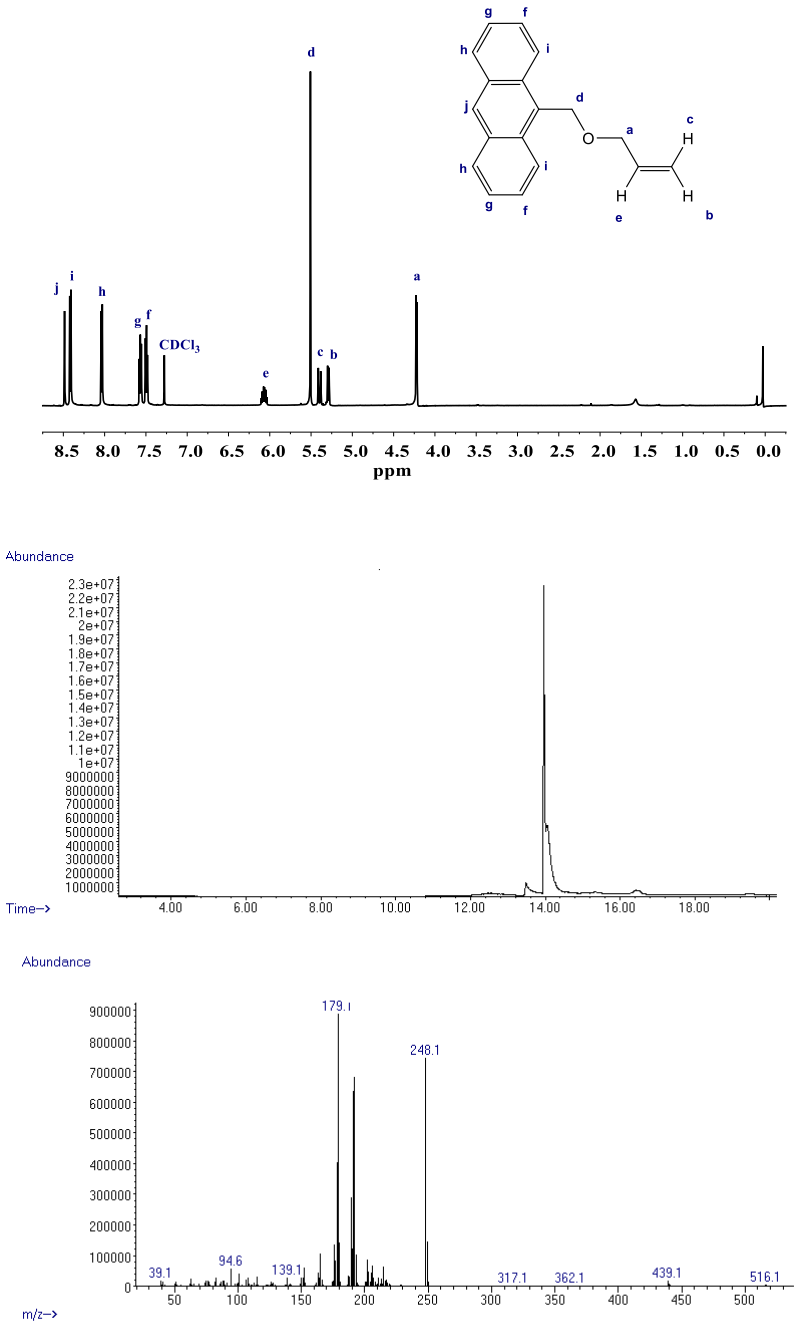

Figure A.1 ^{1}H NMR and GC-MS of 9-anthracenemethyl allyl ether in $CDCl_3$ (600 MHz).

.

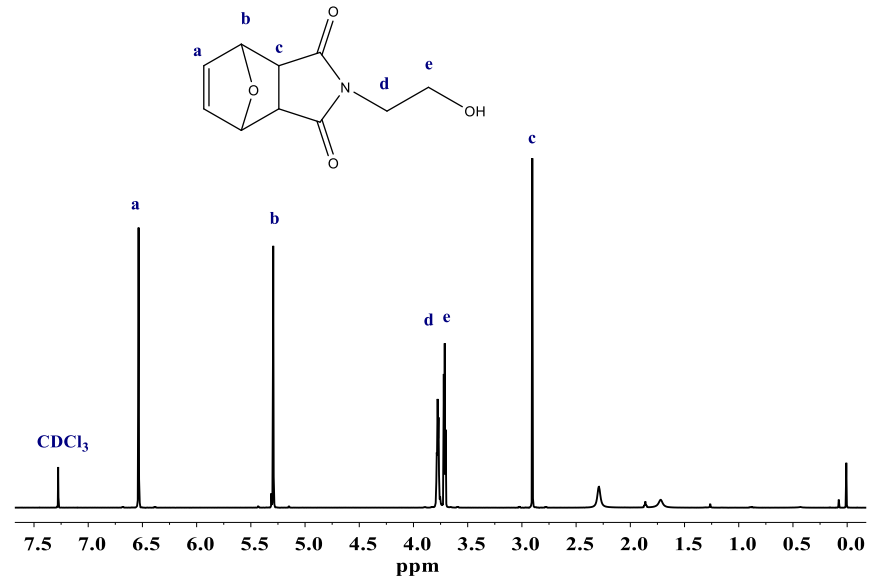

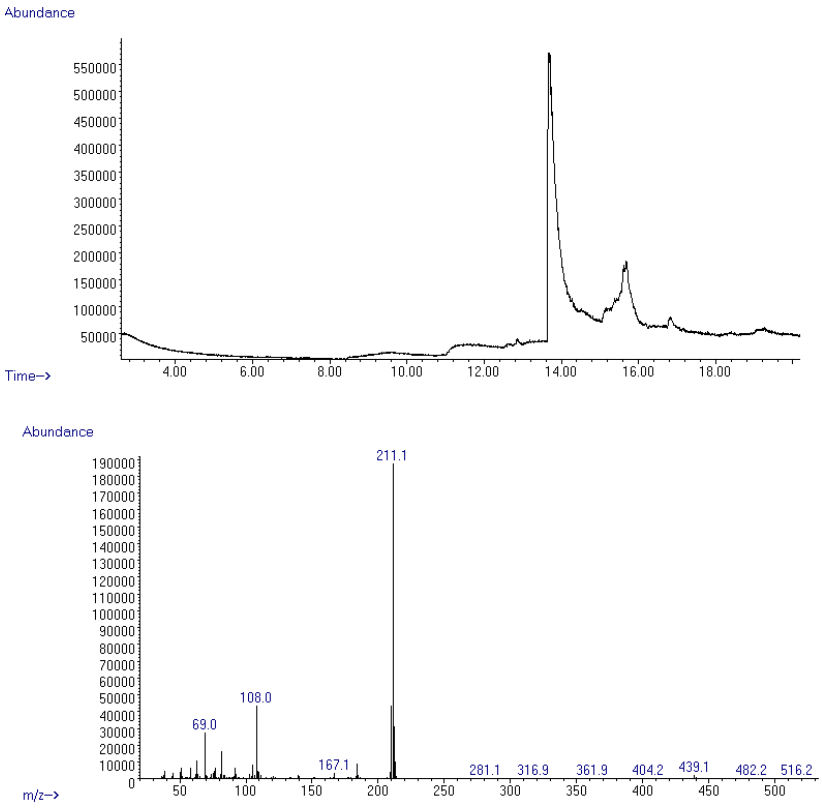

Figure A.2 ^{1}H NMR in $CDCl_3$ (600 MHz) and GC-MS of (2-Hydroxyethyl)-10-oxa-4-azatricyclo [5.2.1.02, 6] dec-8-ene-3, 5-dione.

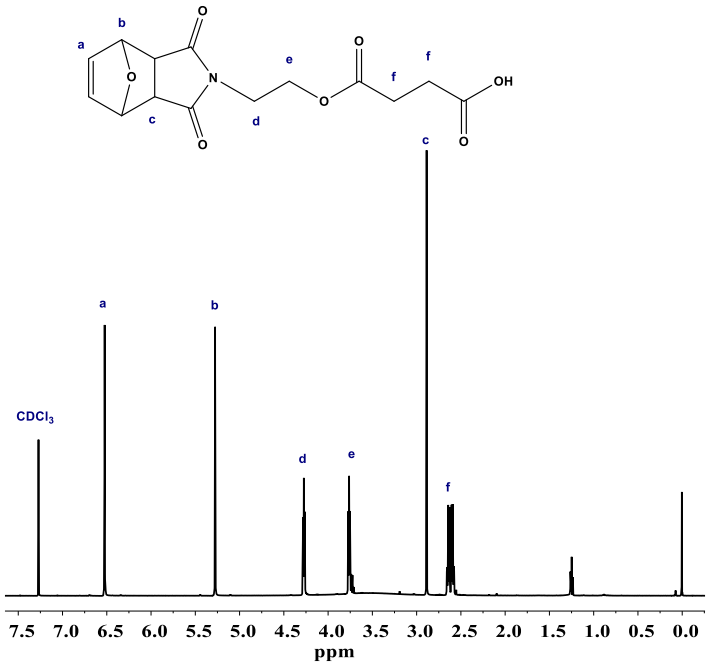

Figure A.3 ^{1}H NMR of maliemide adduct acid in $CDCl_3$ (600 MHz).

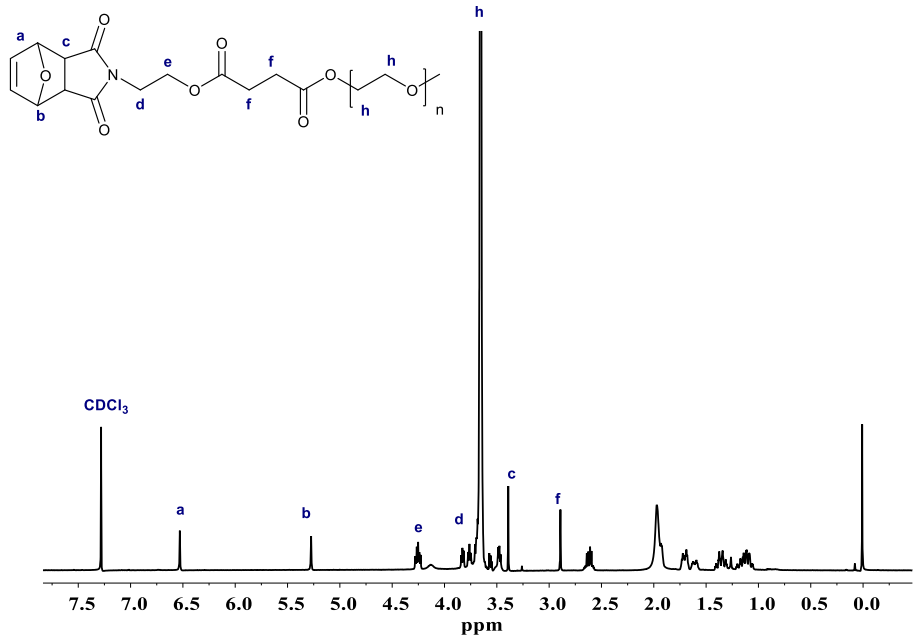

Figure A.4. ^{1}H NMR of PEG_{100}-MI in $CDCl_3$ (600 MHz).

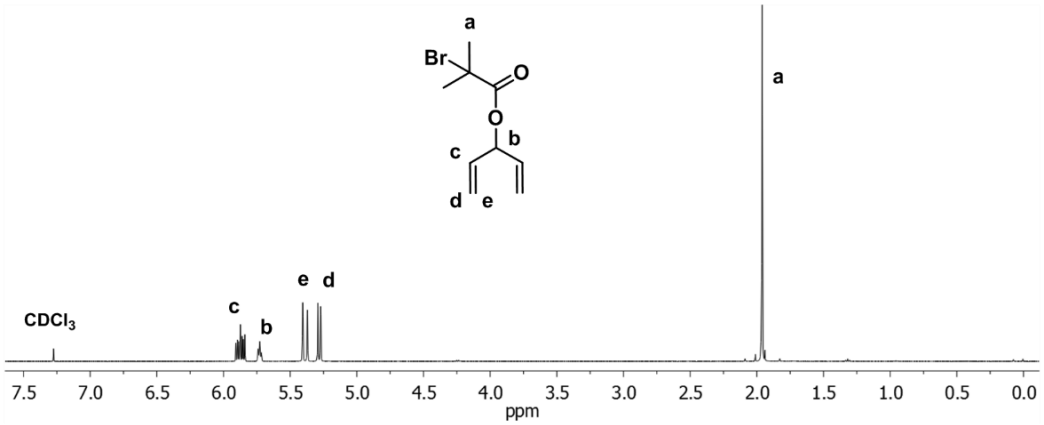

Figure A.5 ^{1}H NMR of 1,4-pentadiene-3-yl 2-bromo-2-methylpropanoate in $CDCl_3$ (600 MHz).

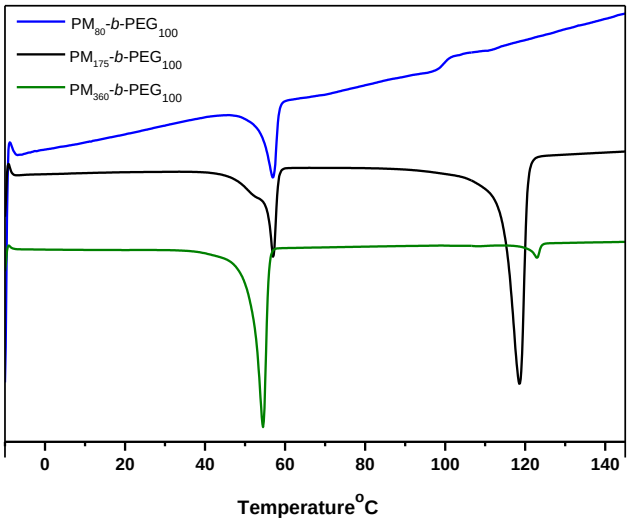

Figure A.6 DSC curves of three samples of PM-*b*-PEG (N_2 atmosphere, 10 ^{o}C/ min, second heating cycle)

LIST OF PUBLICATION

1-Zhang, H.; Alkayal, N.; Gnanou, Y.; Hadjichristidis, N. *Chem. Commun.* **2013**, *49*, 8952.
2-Zhang, H.; Alkayal, N.; Gnanou, Y.; Hadjichristidis, N. *Macromol. Rapid Commun.* **2014**, *35*, 378.
3- Alkayal, N.; Hadjichristidis, N. *Polym. Chem.* **2015**, *6*, 4921.
4- Alkayal, N.; Durmaz, H.; Tunca, U.; Hadjichristidis, N. *Polym. Chem*. **2016**, *7*,2986.
5-Alkayal, N.; Zhang, Z.; Bilalis, P.; Hadjichristidis, P. *Macromolecules*. Synthesis of polyethylene-based tadpole copolymer with a polyethylene (PE) ring and a polystyrene (PSt) tail by the combination of polyhomologation, ATRP and Glaser coupling reaction, *to be submitted*.
6-Alkayal, N.; Zapsas, G.; Bilalis, P.; Hadjichristidis, N. *Polymer*. Self-assembly behavior of linear polymethylene-block-polyethylene glycol copolymer in aqueous solution, *Accepted.*